Polymer Testing 160 (2026) 109234

Contents lists available at ScienceDirect

Polymer Testing

journal homepage: www.elsevier.com/locate/polytest

A comprehensive review of recent advances in the fabrication and applications of polyacrylamide-based hydrogels for water treatment

AbdElAziz A. Nayl [a,*], Ismail M. Ahmed [a], Sultan A. Alsahli [a], Wael A.A. Arafa [a], Abdullah A. AlShammari [a], Ahmed Hamad Alanazi [a], Meshari D. Alanazi [b], Mohammed Ezzeldien [c], Stefan Bräse [d,**], Ahmed I. Abd-Elhamid [e]

[a] Department of Chemistry, College of Science, Jouf University, Sakaka, Al Jouf, 72341, Saudi Arabia
[b] Department of Electrical Engineering, College of Engineering, Jouf University, Sakakah, 72388, Saudi Arabia
[c] Department of Physcis, College of Science, Jouf University, Sakaka, Al Jouf, 72341, Saudi Arabia
[d] Institute of Biological and Chemical Systems – Functional Molecular Systems (IBCS-FMS), Kaiserstrasse 12, Karlsruhe, 76131, Germany
[e] Composites and Nanostructured Materials Research Department, Advanced Technology and New Materials Research Institute, City of Scientific Research and Technological Applications (SRTA-City), New Borg Al-Arab, Alexandria, 21934, Egypt

ARTICLE INFO

Keywords:
Polyacrylamide hydrogels
Nanocomposite hydrogels
Water treatment
Heavy metal adsorption
Dye removal
Functional polymeric materials
Hydrogel fabrication
Environmental remediation

ABSTRACT

Today, global freshwater resources are increasingly threatened by rapid population growth and intensified industrial activity, which contribute significantly to the discharge of untreated wastewater into surrounding environments. Rapid urbanization and large-scale industrial expansion have markedly reduced the availability of clean freshwater, elevating water pollution to a major global challenge and further aggravating water scarcity. Polyacrylamide-based hydrogels have attracted significant attention from the scientific community as versatile materials for wastewater treatment, thanks to their promising properties. This review presents a comprehensive overview of recent progress in the synthesis, modification, and environmental applications of polyacrylamide-based hydrogels for the elimination of toxic metal ions and dyes from aquatic systems. Various synthesis approaches, including free radical polymerization & crosslinking, controlled/"living" polymerizations (CRP), (RAFT, ATRP), and grafting techniques, in-situ formation of nanocomposite hydrogels, electrospinning and fiber fabrication, and post-polymer modification (functionalization, anchoring), are critically examined. Also, recently published works on incorporated polyacrylamide-based hydrogels with functional materials, as an effective strategy to improve selectivity, sorption capacity, and reusability, are highlighted. Finally, current challenges and future perspectives related to mechanical and structural, selectivity, reusability and regeneration, environmental risks, and production and scalability are discussed. Overall, this review provides critical insights to direct the rational design of high-performance polyacrylamide-based materials hydrogel adsorbents for sustainable water treatment and environmental remediation.

1. Introduction

Recently, the employment of polymeric materials across various industrial fields has attracted significant attention [1]. Various types of polymeric materials, e.g., conducting polymers, microgels, magnetic hyperbranched polymers, cryogels, and hydrogels, have been utilized on a large scale for different applications [2]. Recently, soft crosslinked polymeric networks with a hydrophilic nature, known as hydrogels (HG), have attracted attention and become of high interest owing to their unique characteristics. Hydrogels are three-dimensional (3D) porous matrices containing a variety of functional groups and exhibit excellent water-swelling capabilities, durability without dissolving in different solutes, good mechanical strength, biomimetic design, and remarkable cyclic performance [3–7]. In general, hydrogel materials have advanced significantly, moving from first-generation chemically crosslinked networks to third-generation hydrogels, distinguished by

* Corresponding author.
** Corresponding author.
E-mail addresses: aanayel@ju.edu.sa, aanayl@yahoo.com (A.A. Nayl), mdalsayer@ju.edu.sa (M.D. Alanazi), meabas@ju.edu.sa (M. Ezzeldien), braese@kit.edu (S. Bräse), ahm_ch_ibr@yahoo.com (A.I. Abd-Elhamid).

https://doi.org/10.1016/j.polymertesting.2026.109234
Received 14 February 2026; Received in revised form 20 April 2026; Accepted 25 May 2026
Available online 26 May 2026

multifunctional integration [7]. In recent years, the promising properties of hydrogels have attracted considerable attention from researchers worldwide, leading to the publication of numerous review articles highlighting the significance of hydrogels and functionalized hydrogel-based materials across a wide range of applications, notably in the fields of energy and water sustainability [8,9]. Therefore, hydrogels can be considered among the most important polymeric materials. These hydrophilic material chains are characterized by multifunctional integration groups, such as hydroxyl (-OH), amide (–CONH), sulfate (SO_3H-), carboxyl (-COOH), and amino (-NH_2), which can be used in various applications [6]. Generally, hydrogels are classified as synthetic and natural categories [1]. Raw organic materials are the main source of natural hydrogels, while synthetic hydrogel materials are fabricated in chemical and polymer laboratories [1]. On the other hand, they can be classified into biopolymer and copolymer groups [1]. Remarkably, the advent of third-generation hydrogels, driven by nanotechnologies, 3D printing, and biomimetic strategies, has overcome the mechanical limitations of earlier generations and introduced sophisticated functions including self-healing, adaptive responsiveness, and anisotropic behavior [7]. Scheme 1 represents the most important applications of hydrogels. PAm is one of the most interesting polymers discussed in this field, a synthetic polymer with an amide side group, a water-soluble linear macromolecule, and one that can be functionalized or copolymerized. PAm-based hydrogels are highly cross-linked polymeric networks comprising 2.5%–5% PAm and 95%–97.5% intermolecular water. Also, they are biocompatible, non-toxic, exhibit considerable mechanical properties, and widely used in various applications [10–12]. Polyacrylamide polymers are swellable and high molecular weight water-soluble polymers synthesized from acrylamide or by a combination of acrylamide with acrylic acid monomers [12–16]. Its structural flexibility permits chemical modifications, including hydrolysis or copolymerization with various functional monomers [12,16].

Scheme 2 represented the two mainstream composite synthesis-routes and the role of PAm which is strongly dependent on the composite fabrication route. In copolymerization systems, PAm is incorporated into the hydrogel network through covalent bonds and dominates structural stability. In contrast, in physical mixing systems, PAm provides functional sites through non-covalent interactions and primarily contributes accessible amide functionalities and interfacial compatibility. Consequently, PAm serves as a network-forming structural component in copolymerized composites and acts as a functional/adsorptive modifier that enhances adsorption performance in physically mixed systems.

With its remarkable flocculation, adhesion, and thickening properties, PAm has emerged as a material of great interest for diverse applications, including papermaking, food processing, textiles, and petroleum [15]. The inherent shortcomings of conventional Polyacrylamide (PAm), particularly its insufficient stability in extreme reservoir environments, have driven the development of new, multifunctional materials. Nanomaterial–polymer hybrids have emerged as a promising strategy, exploiting the distinctive properties of nanoparticles to markedly enhance the perf

Ormance of PAm-based systems [12]. Therefore, PAm-based nanomaterials have gained significant importance in various applications, such as water treatment, and have attracted scientists' interest due to their low-cost fabrication, eco-friendliness, tunability, high water-holding capacity, chemical infusion with compounds and elements, and biocompatibility [16]. Among various hydrogel types, polyacrylamide (PAm)-based hydrogels are widely used across a range of potential applications [17].

1.1. *Biopolymers and copolymers*

Establishing and scientifically grounded distinction between biopolymers and copolymers is important in the fabrication of advanced hydrogel-based adsorbents for water treatment. Biopolymers, including cellulose, alginate, and chitosan, are naturally abundant derived macromolecules and characterized by a high density of functional groups (e.g., –NH_2, –OH, and –COOH) in addition to ability to interact with different contaminants by H-bonding, coordination interactions, and other attraction mechanisms [1–5]. Despite these advantages, biopolymers suffer from inherent limitations which restrict their practical applicability [6–8]. On the other hand, copolymers, especially polyacrylamide (PAm)-based systems, are synthetically fabricated materials composed of two or more monomers, enabling greater control over polymer composition, functional group density, and network structure through well-established polymerization strategies such as free-radical polymerization, grafting, and crosslinking [9–12]. This level of structural tunability governs critical physicochemical properties such as swelling behavior, surface charge characteristics, and porosity, which are known to influence adsorption performance, kinetics, and reusability [13–15]. In advanced hydrogel systems, the integration of

Scheme 1. Common applications of hydrogels.

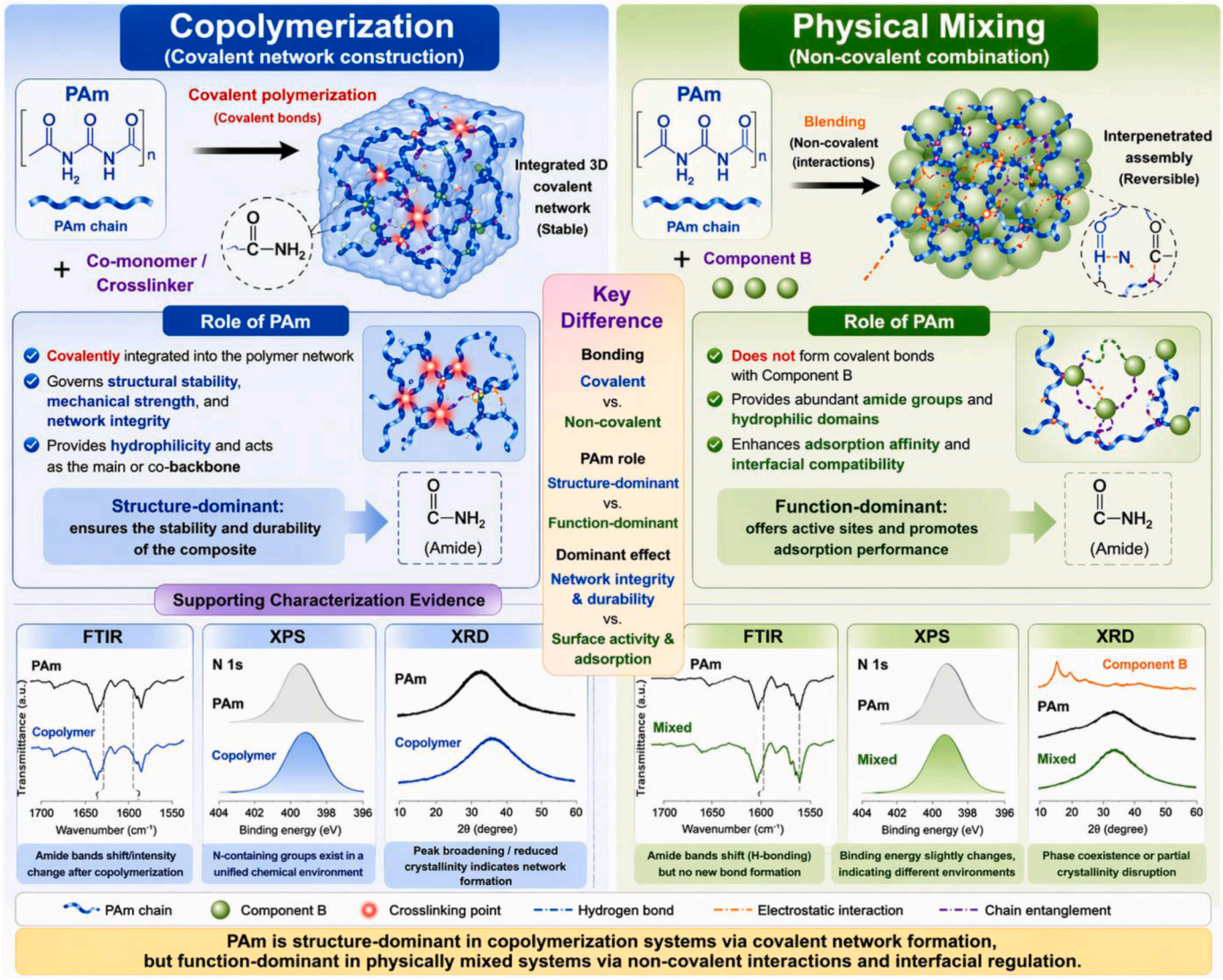

Scheme 2. Scientific comparison of copolymerization vs physical mixing methods.

biopolymers with copolymers (e.g., CTS/PAm and SA/PAm) was investigated to yield hydrogel systems, where the biopolymer act as sources of active binding sites and contribute functional adsorption sites, while the synthetic copolymer network (e.g., PAm backbone) provides mechanical integrity, structural stability, controllable physicochemical properties, and improve durability during repeated adsorption–desorption cycles [16,17]. Accordingly, the synergistic combination of biopolymer functionality with copolymer tunability represents an effective strategy for developing high-performance hydrogel-based adsorbents for water treatment applications.

1.2. Selection of PAm-based hydrogels in water/wastewater treatment applications

Due to the promising properties of hydrogels, various hydrogels-based materials have gained considerable attention in water/wastewater treatment. Owing to their tunable surface chemistry, rich functional groups, high water uptake capacities, and 3D-crosslinked structure, hydrogels based-materials can be utilized as effective adsorbent materials to eliminate different types of pollutants from aqueous media, including organic dyes and heavy metal ions. among hydrogels based-materials, such as chitosan (CTS)-, poly(vinyl alcohol) (PVA)-, poly(acrylic acid) (PAA)-, and natural polysaccharide-based hydrogels, have specific advantages in addition other disadvantages that reduce their practical applicability. Table (1) represents comparative analysis between PAm-based hydrogels and other widely investigated materials based-hydrogels systems utalized for water treatment, For example, CTS-based hydrogels, despite their abundant amino and hydroxyl functional groups which facilitate electrostatic interactions and H-bonding with contaminants but often suffer from their poor mechanical robustness, batch variability limit their performances adsorption–desorption recycles, which can be restrict their practical applications. Also, PVA-based hydrogels, although mechanically robust, typically require additional modification to achieve high adsorption efficiency. On the other hand, PAA-based hydrogels which characterized by rich –COOH functional groups that improve their affinities toward various types of pollutants, can exhibit excessive swelling due to their high ionization degree and strong ionic sensitivity may compromise structural integrity and reusability. Similarly, although the promising advantages of natural polysaccharide based-hydrogels, including biocompatibility and sustainability, they often suffer from limited structural controllability and reproducibility, which may hinder scale-up. In contrast, due to the well-established free-radical polymerization and controllable network architecture of PAm-based hydrogels, they can offer a uniquely balanced platform that integrates mechanical robustness, structural tunability, physicochemical and aqueous stabilities, as

well as their engineering scalability. Also, the existence of various functional active groups, such as amide groups (–$CONH_2$), can participate in H-bonding, coordination interactions, and chemical modification reactions and provides moderate polarity and enhance interactions with different types of contaminants, and enabling further functionalization via copolymerization. Moreover, PAm-based hydrogels exhibit considerable reproducibility, processability, and cost-effectiveness compared with other various hydrogels-based materials, making them more attractive for water treatment applications. Accordingly, PAm-based hydrogels systems are selected in this study and strategically justified as a versatile and robust platform for integrating multiple functional components and offering an optimal balance between scalability, structural stability, functional adaptability, and modifiability. These characteristics make PAm-based hydrogels particularly attractive candidates for advanced water treatment applications, thereby highlighting their distinct research value and practical applications in water treatment systems.

On the other hand, to the best of our knowledge, the recent reviews in this area are very limited and have not covered many relevant concepts. Few published reviews explain and summarize the synthesis, modifications, and applications of PAm-based hydrogel materials.

During the last years (2020-2025, with 2025 representing partial data), treatment of water by PAm-based hydrogels and other hydrogel-based materials has attracted rapidly increasing attention. A recent bibliometric analysis based on the Web of Science Core Collection and Scopus databases was collected and restricted to English-language articles and reviews using predefined keywords combination related to hydrogels, polyacrylamide, and water treatment applications, as represented in Scheme 3. In this Scheme bibliometric indicators, including annual publications output, citation frequency, and country-level contributions, were extracted and analyzed. The obtained data revealed a clear and continuous increase in both research activity output and citation impact of hydrogel-based materials for water treatment from 2020 to 2025, indicating that hydrogel-based materials have become a

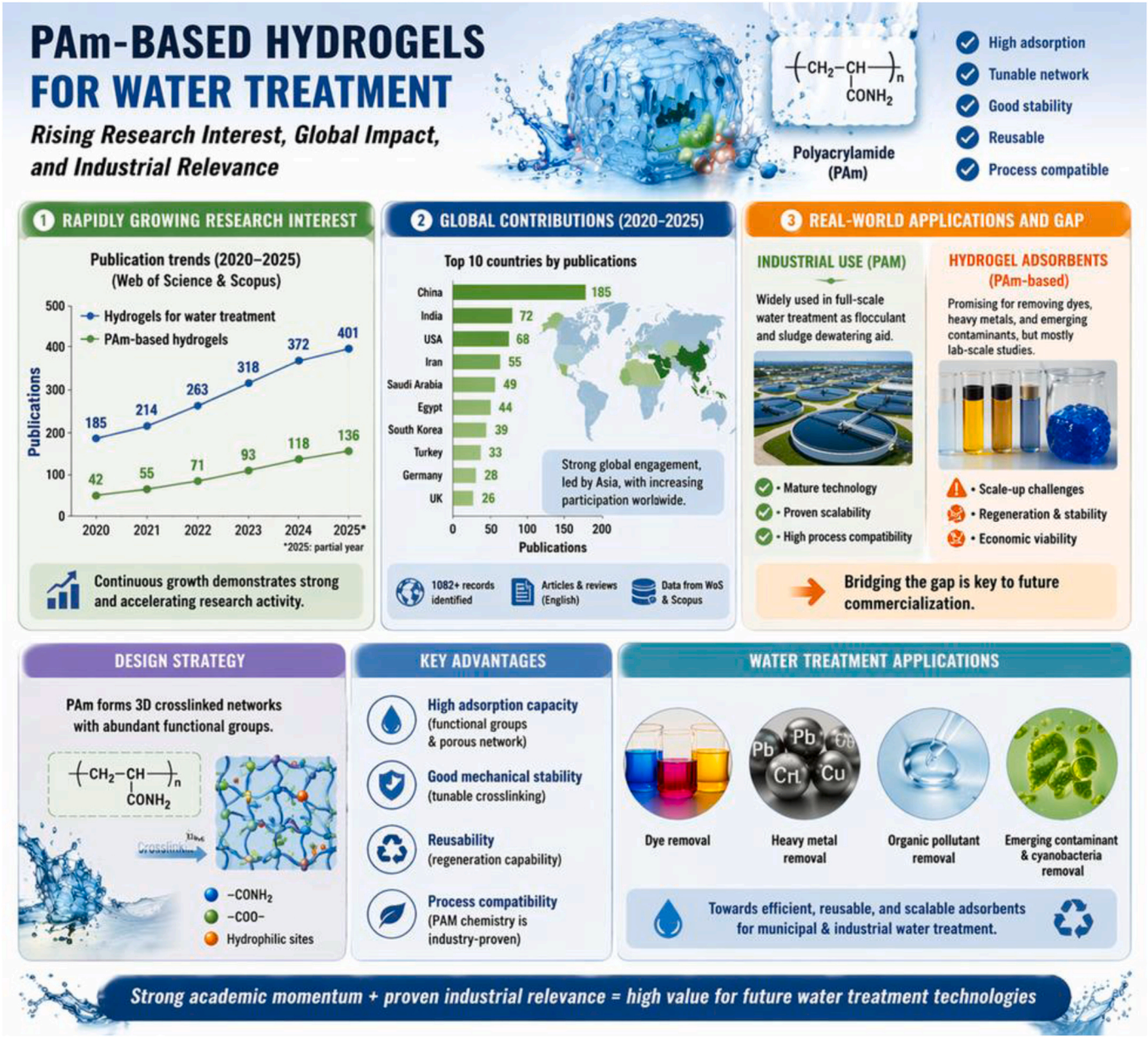

Scheme 3. Recent bibliometric analysis for treatment of water by hydrogel-based materials based on the Web of Science Core Collection and Scopus databases (2020-2025).

rapidly expanding research area within environmental and materials science. PAm-based hydrogels exhibited a similar growth trend, reflecting their emerging importance in advanced water treatment applications. The distribution of publications related to hydrogel-based materials for water treatment across multiple leading countries further highlights the widespread relevance of this research field. Despite these progresses, extensive academic development and practical implementation remain limited, and the predominance of laboratory-scale studies suggests a gap between research development and large-scale application, underscoring the need for further work on scalability and practical implementation.

Accordingly, this review highlights recent advances in fabrication techniques and functionalization methods, the advantages of PAm-based hydrogel materials, and their applications in various fields. Also, it aims to provide a roadmap for researchers and engineers.

Also, the perspectives and current challenges in the fabrication of PAm-based materials and hydrogels, and their applications for wastewater treatment, are emphasized. In addition, this review highlights the challenges associated with the application of these materials in water treatment and ways to overcome them.

2. Overview and recent advances of fabrication strategies of polyacrylamide-based hydrogel materials

Recently, hydrogels have gained geat attention and are widely recommended as adsorbent materials due to their considerable advantages over other adsorbents, include adjustable dimensions, cost-effectiveness, easy handling, high porosity, significant affinity for water, reusablilty and eco-friendly [3,4]. Hydrophilic groups, such as -COOH, -SO_3H, -NH_2 and -OH, in their polymeric chains allow them to capture huge amounts of water and various types of pollutants via different interactions, include chelation/coordination, ion exchange, surface complexation, π-π interactions, electrostatic, and H-bonding [3,4,18].

In recent years, several synthesis routes have been investigated to synthesize hydrogels. In this work, the fabrication techniques will be classified into commonly used categories and highlighted, with recent improvements. Hydrogels are fabricated through chemical and physical processes, and their properties and functionalities differ depending on the chosen fabrication approach.

In this section, the most common fabrication techniques of PAm-based hydrogel materials are summarized, including CRP, (RAFT, ATRP), and grafting techniques, in-situ formation of nanocomposite hydrogels, electrospinning and fiber fabrication, and post-polymer modification (functionalization, anchoring).

2.1. Free-radical polymerization & crosslinking of polyacrylamide-based hydrogel materials

Over the last few decades, PAm-based hydrogel materials have been successfully fabricated by classical free-radical polymerization [19]. It is one of the most common techniques for preparing PAm-based hydrogels due to its scalability and simplicity, and it involves three major steps: initiation, propagation, and termination [20,21]. PAm-based hydrogels are predominantly fabricated via free-radical polymerization, which can be initiated thermally with agents such as ammonium persulfate or photochemically with UV-responsive initiators. These initiators generate macroradicals, which are the nucleus of chain propagation, and then interact with crosslinkers, leading to the formation of a stable 3D network [22]. Photopolymerization provides precise spatial control, enabling complex patterning and the fabrication of microstructured hydrogels. Alternatively, ionic crosslinking exploits electrostatic forces between PAm derivatives and oppositely charged ions, yielding reversible gels with environmentally responsive swelling properties. Thermosensitive variants, created by grafting N-isopropylacrylamide (NIPAm) or similar responsive groups onto PAm, exhibit temperature-dependent sol–gel transitions. Advances in click chemistry, especially azide–alkyne cycloaddition, have introduced fast, selective, and biocompatible crosslinking pathways, greatly enhancing the versatility of PAm-based materials and hydrogel architectures [22–27]. Physically cross-linked PAm hydrogels can be efficiently optimized at both the molecular and microstructural levels through a simple thermal engineering approach. By applying thermal dehydration followed by rehydration, the PAm hydrogels demonstrated significant mechanical enhancements, with tensile strength increasing 11-fold and toughness improving 60-fold [28].

PAm-based hydrogels are widely recognized for their strong affinity for water and their capacity to retain more than 90 wt % of it, resulting in soft, elastic materials with mechanical properties resembling those of natural tissues. This high-water content supports molecular diffusion and nutrient transport. The mechanical behavior of PAm-based hydrogel materials, ranging from soft and pliable (<10 kPa) to rigid and strong (>100 kPa), is determined by the crosslinking degree and the length of the polymer chain. Their chemical inertness under physiological conditions, combined with resistance to protein adsorption, makes them stable and less prone to nonspecific biological interactions.

While pure PAm is not degradable, its chemical structure can be modified through copolymerization with degradable segments or by introducing enzymatically cleavable crosslinkers to achieve controlled biodegradation. Furthermore, surface modification with ionic or bioactive groups enables precise adjustment of the gel's swelling rate, charge characteristics, and cellular affinity, making PAm-based hydrogel materials adaptable to a broad spectrum of biomedical and technological applications [22–28].

Generally, crosslinkers, such as N,N′-methylene bisacrylamide, produce hydrogels whose pore structure is tuned by the monomer/crosslinker ratio, temperature, and initiator system. Inverse emulsion polymerization enables the dispersion of water-soluble PAm particles in oil (for beads/nanospheres). Improvements include control of particle size via surfactant templating and optimized emulsification processes to achieve narrower dispersity [29].

Overall, the investigated standardized chemical reaction equations for core reaction principles for free-radical polymerization & crosslinking approaches can be summarized as follows:

Initiation: $(NH_4)_2S_2O_8 \xrightarrow{\Delta} 2\ SO_4^{\bullet -}$

Primary radical attack: $SO_4^{\bullet -} + CH_2{=}CHCONH_2 \rightarrow CH_2^{\bullet}CHCONH_2$

Propagation: $CH_2^{\bullet}{-}CHCONH_2 + n(CH_2{=}CHCONH_2) \rightarrow [{-}CH_2{-}CH(CONH_2){-}]_n^{\bullet}$

Crosslinking (MBAA): $Poly^{\bullet} + CH_2{=}CH{-}CONH{-}CH_2{-}NHCO{-}CH{=}CH_2 \rightarrow$ covalent 3D network

Termination (combination): $Poly^{\bullet} + Poly^{\bullet} \rightarrow Poly{-}Poly$

Termination (disproportionation): $Poly^{\bullet} + Poly^{\bullet} \rightarrow$ saturated + unsaturated chains

(conditions: APS/TEMED redox system, aqueous medium, inert atmosphere, controlled temperature).

2.2. Controlled/"living" polymerizations (CRP), (RAFT, ATRP), and grafting techniques of polyacrylamide-based hydrogel materials

CRP has recently emerged as a useful strategy for modifying numerous nanomaterials [30,31]. Stimuli-responsive CRP methods, which can be activated by photochemical, thermal, or electrochemical cues, have attracted widespread interest for their ability to switch polymerization "ON" and "OFF reversibly. In particular, photo-radical polymerization approaches such as photoinduced electron transfer–atom transfer radical polymerization (PET-ATRP) and photoinduced

electron transfer–reversible addition–fragmentation chain transfer (PET-RAFT) [30–34] have received growing attention for offering exceptional spatial and temporal control over polymer growth.

RAFT and ATRP approaches provide precise molecular weight control, block architectures, and functional chain ends, enabling the formation of PAm brushes, block copolymers, and grafted architectures on nanoparticle surfaces. These methods allow fine-tuning of hydrophilicity, stimulus responsiveness, and anchor points for further conjugation (drugs, targeting moieties, or inorganic nanoparticles). Recent works have emphasized RAFT- and ATRP-derived multifunctional PAm-based hydrogel materials for biomedical and other applications [30,35–42].

Generalized chemical reaction equations for core reaction principles of the RAFT technique can be investigated as follows, in which RAFT involves reversible chain-transfer processes mediated by a thiocarbonylthio compound.

Initiation)initiator(AIBN → 2 $R^{\bullet}$ (heat, inert atmosphere)

Propagation: $R^{\bullet} + nM \rightarrow P^{n\bullet}$

Chain transfer: $P^{n\bullet} + Z\text{–}C(=S)\text{–}S\text{–}R \rightleftharpoons P^{n}\text{–}S\text{–}C(=S)\text{–}Z + R^{\bullet}$

Re-initiation: $R^{\bullet} + nM \rightarrow$ new poly chain

Equilibrium ensures uniform chain growth and narrow dispersity (conditions: RAFT agent (dithioester/trithiocarbonate), organic/aqueous solvent, heat).

On the other hand, standardized chemical reaction equations for core reaction principles of ATRP processes can be investigated as follows;

Activation: $R\text{–}X + Cu(I)/L \rightarrow R^{\bullet} + Cu(II)X/L$

Propagation: $R^{\bullet} + nM \rightarrow P^{n\bullet}$

Deactivation: $P^{n\bullet} + Cu(II)X/L \rightarrow P^{n}\text{–}X + Cu(I)/L$

Dynamic equilibrium maintains low radical concentration (conditions: CuBr/ligand (bipyridine/PMDETA), heat, oxygen-free environment).

Also, the standardized chemical equations for core reaction principles for graft polymerization approach can be investigated as follows,

Backbone activation: Substrate–H + initiator (APS/Ce^{4+}) → $Substrate^{\bullet}$

Graft growth: $Substrate^{\bullet} + CH_2{=}CHCONH_2 \rightarrow$ Substrate–g–PAm

Propagation continues to form side chains (conditions: aqueous medium, redox initiator, controlled temperature).

2.3. In-situ formation of polyacrylamide-based materials hydrogels

PAm-based hydrogel materials exhibit significant promise in numerous fields, especially with the development of metallohydrogels [43]. Over the last few years, various publications and reviews have demonstrated the remarkable potential of modified PAm-based materials during hydrogel polymerization by embedding nanoparticles (such as magnetic nanoparticles, metal oxides, MOFs, silica, GO, MWCNTs, and TiO_2) to enhance their unique properties for various applications.

Fabricated nanocomposite hydrogels exhibit various desirable properties, such as enhanced mechanical properties, additional adsorption sites, catalytic activity, and magnetic responsiveness [8,43–55]. In-situ reduction or nucleation within the PAm network results in stronger interfacial bonding and a more uniform dispersion than post-mixing.

Generally, one of the most important properties of nanocomposite hydrogel networks is their capacity to support both in situ and ex situ nanoparticle synthesis. The distinct nanoscale voids within the polymer framework, known as nanoscopic domains, enable nanoparticles to grow extensively while minimizing aggregation. Such hydrogel networks efficiently accommodate metal and metal oxide nanoparticles, thereby stabilizing them, shielding them from oxidation, and enhancing their toughness, conductivity, and adsorptive performance [49].

In summary, the standardized chemical equations for core reaction principles for the in-situ formation of polyacrylamide-based materials hydrogels approach can be investigated as follows,

Simultaneous polymerization: AAm + MBAA + initiator → crosslinked hydrogel network.

Occurs inside matrix/template (e.g., pores, membranes, nanoparticles).

(conditions: APS/TEMED, ambient–70 °C, confined environment).

Scheme 4(3) represents the proposed interaction mechanisms between nanofillers (GO, Fe_3O_4, MOFs, TiO_2) and the Polyacrylamide (PAm) matrix, resulting in enhanced dispersion, structural integrity, and functional performance. and reinforces the nanocomposite structure.

2.4. Electrospinning and fiber fabrication of polyacrylamide-based materials hydrogels

Over the years, various techniques, including electrospinning, have been developed to produce hydrogel-based materials with unique properties and functionalities to fulfill the needs of specific applications. Hydrogel–fiber composites fabricated by this technique combine the properties of electrospun nanofibers and hydrogels into a unified structure, forming a multifunctional system that leverages the strengths of both materials while mitigating their drawbacks [56]. It is also increasingly recognized as a straightforward technique for producing one-dimensional fibrous membranes [57]. On the other hand, the excellent properties of different polymer nanofibers render them suitable for diverse applications [58].

Overall, the standardized chemical equations of core reaction principles for electrospinning and fiber fabrication of polyacrylamide-based materials hydrogels approach can be investigated as follows,

Poly solution → nanofibers under high voltage

Jet stretching + solvent evaporation → fiber formation

Post-crosslinking: fibers + crosslinker/heat → stable hydrogel fibers

(conditions: controlled humidity, voltage, and flow rate).

2.5. Post-polymer modification (PPM) - strategies of polyacrylamide-based hydrogel materials

Recently, the incorporation of PAm hydrogel matrices with nanomaterials has led to a new generation of functional hybrid networks with promising physicochemical properties, suitable for applications such as catalysis, environmental science, sensing, and biomedicine. Therefore, post-polymer modification (PPM) strategies (defined as any chemical or physical modification approaches applied after hydrogel network formation) have emerged as key tools for tailoring PAm-based nanocomposite hydrogels, enabling structural and functional refinements that overcome the limitations of conventional polymerization routes and provide an efficient process to upgrade PAm hydrogels into multifunctional PAm-based nanocomposite materials. In addition to PPM-techniques provide several benefits such as (a) introducing reactive functional groups for further bioconjugation, (b) adjusting the ionic nature of the fabricated hydrogels (for adsorption or swelling control), (c) improving nanoparticle immobilization or interfacial compatibility, and (d) impart spatially defined functionality via surface-selective treatments (e.g., photopatterning or plasma) [59,60]. PPM approaches are especially attractive when the target functionality cannot withstand in-situ polymerization conditions, such as delicate biomolecules or

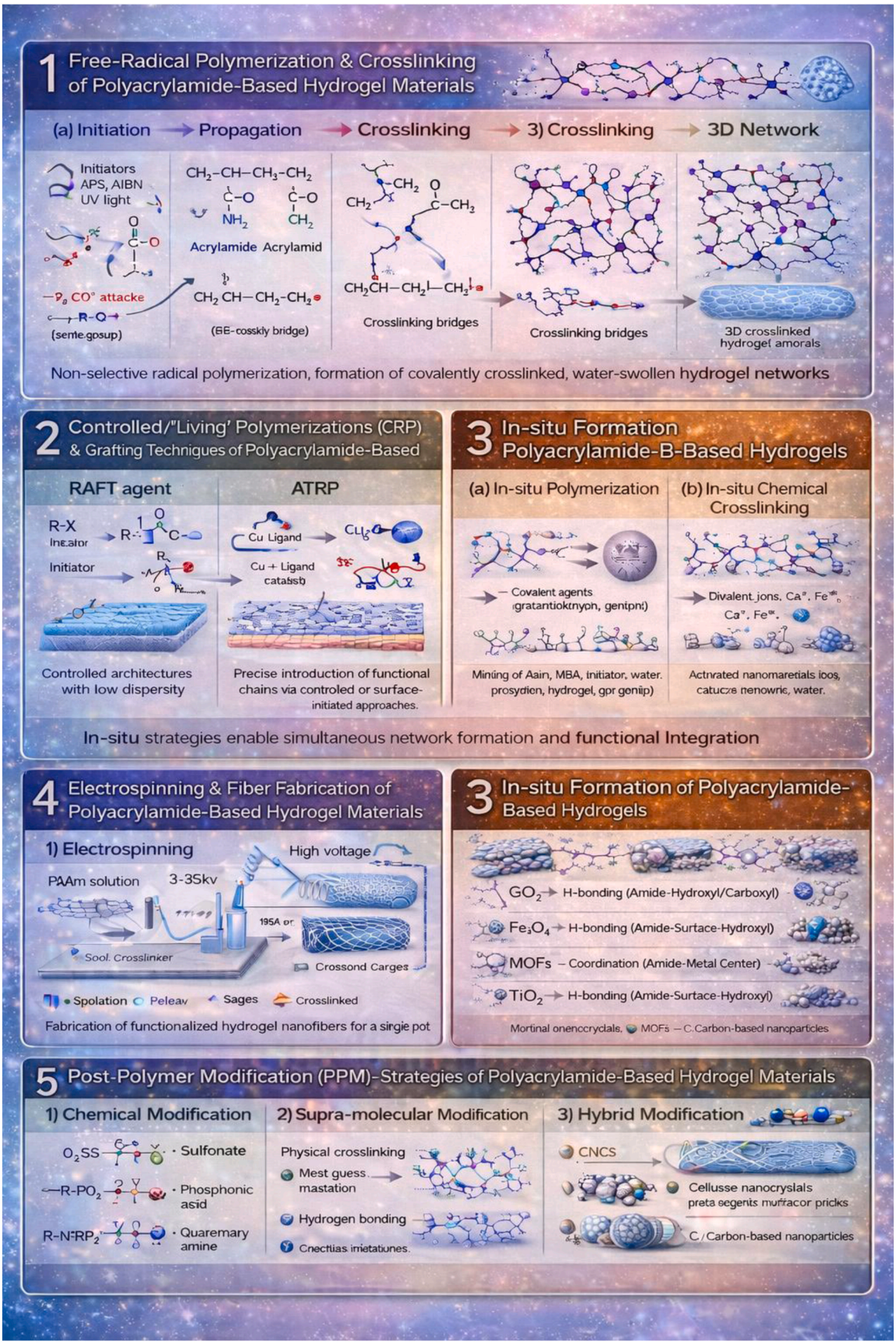

Scheme 4. Scientific infographic for mechanisms of Fabrication Strategies of polyacrylamide-based hydrogels, (1) Free-radical polymerization & crosslinking, (2) Controlled/"living" polymerizations (CRP), (RAFT, ATRP), and grafting techniques, (3) In-situ formation, (4) Electrospinning and fiber fabrication, and (5) Post-polymer modification (PPM).

fabricated nanoparticles, or when modification of surface selectivity is required [59,60]. In chemical modification techniques, partially hydrolyzed polyacrylamide (HPAm) can be produced by alkaline hydrolysis, which converts amide groups (–$CONH_2$) into carboxylate groups (–COOH/–COO^-). These modification approaches enhance the metal-binding capacities, ionic characters, and swelling behavior while providing reactive sites for further covalent coupling. Hydrolysis degree must be tightly controlled; excessive hydrolysis weakens the network. Studies on HPAm-based nanocomposite hydrogels have shown improved adsorption performance and enhanced nanoparticle interactions [8,12,45,51,60–63]. Also, transamidation and amide substitution are important strategies for introducing amine-based functionalities into pre-formed PAm systems to form HPAm-based nanocomposite hydrogels. Recently, publications reported that transamidation processes are feasible in aqueous solutions, though catalysts and temperature must be optimized to prevent gel degradation [64–66]. On the other hand, carbodiimide (EDC) and N-hydroxysuccinimide (NHS) mediated polymerization (EDC/NHS) coupling chemistry is widely used in the formation of an amide bond by linking carboxyl groups (from HPAm or acrylic-acid comonomers) to primary amines through an intermediate step involving carbodiimide activation to form stable amide bonds [37,67]. (EDC/NHS) Reactions are important processes for surface biofunctionalization of hydrogels and require careful purification, but are sometimes superseded by thiol-based or click approaches for biocompatibility [37,67,68]. Scheme 5 (a-c) illustrates stepwise post-polymer modification of amide groups in PAm hydrogels, which can be systematically modified through alkaline hydrolysis, transamidation, and click chemistry, generating –COO-, –NH_2, and tailored functional groups at specific sites along the polymer network, thereby governing the material's adsorption performance and structural properties.

Generally, the standardized chemical equations of core reaction principles for the PPM strategy can be investigated as follows,

Alkaline hydrolysis: $–CONH_2 + OH^- \rightarrow –COO^- + NH_3$

(conditions: NaOH solution, heat, time-dependent conversion)

For EDC/NHS Coupling (Amide Bond Formation),

EDC activation: R–COOH + EDC → O-acylisourea intermediate

NHS stabilization: intermediate + NHS → R–CO–NHS

Amide coupling: $R–CO–NHS + R'–NH_2 \rightarrow R–CO–NH–R' + NHS$

(conditions: pH 4.5–7.5 buffer, aqueous medium).

Overall, Scheme 4 summarizes a comprehensive, mechanism-oriented visualization of the four principal fabrication strategies employed in advanced design and engineering of functional polymer-based materials and nanocomposites (see Table 1). Also, Table 2 highlights the direct correlation between fabrication conditions, structural evolution, and adsorption mechanisms. The data obtained revealed that the adsorption behavior of the fabricated PAm-based hydrogels is controlled by the interplay between these parameters.

Click and bio-orthogonal chemistry, involving CuAAC, SPAAC, thiol-ene, thiol-yne, tetrazine–norbornene, and oxime/hydrazone ligations reactions, offers high selectivity, yield, and compatibility with aqueous conditions [69–74]. Recently published works emphasized click chemistry as an enabling technology for functionalized and injectable PAm hydrogels [69,71,75–77].

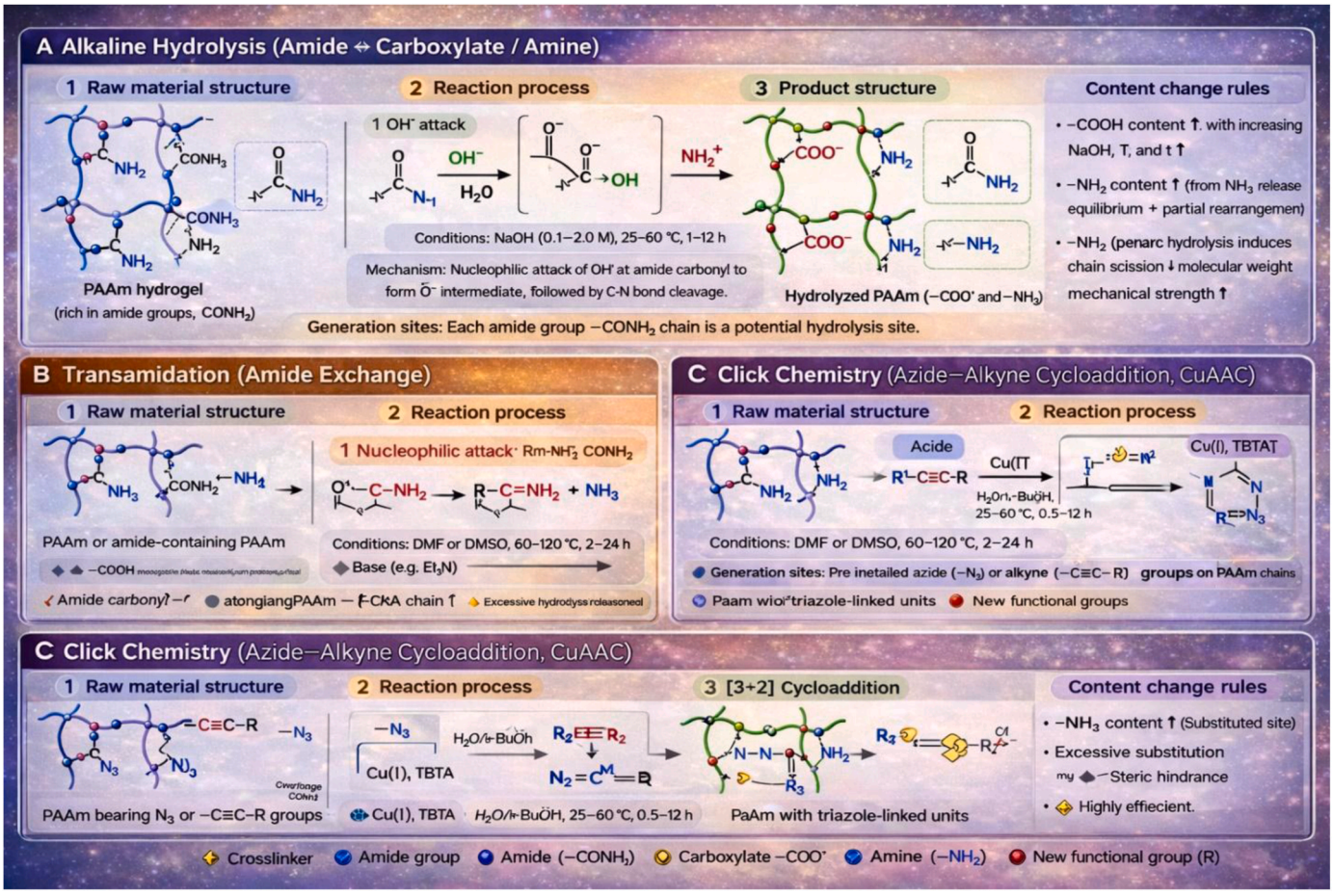

Scheme 5. Chemical reaction pathways for PAm modifications by a) alkaline hydrolysis, b) transamidation, and c) click chemistry.

Table 1
Comparative analysis of mainstream hydrogels systems for water treatment [1–16].

Hydrogel	Functional Groups	Adsorption Capacity	Mechanical Strength	Swelling Behavior	Reusability	Key Advantages	Limitations	Ref.
PAm-based hydrogels	$–CONH_2$ (modifiable to –COOH/$–NH_2$)	Moderate–High (tunable)	Good–High (adjustable via crosslinking)	High (controllable)	High	Tunable structure, balanced performance, high scalability	Requires functionalization for optimal adsorption	[7–16]
CTS-based hydrogels	$–NH_2$, –OH	Moderate–High	Low–Moderate	Moderate (pH-sensitive)	Moderate	Strong metal affinity (chelation), biocompatible	Poor mechanical stability, sensitive to acidic conditions	[1–10]
PVA-based hydrogels	–OH	Low–Moderate	High	Moderate	High	Excellent mechanical integrity, stable network	Low intrinsic adsorption capacity	[1–8]
PAA-based hydrogels	–COOH/$–COO^-$	High	Moderate	Very high (ionic swelling)	Moderate	High affinity for cationic pollutants	Excessive swelling, reduced structural stability	[6–12, 16]
Natural polysaccharide-based hydrogels	–OH, –COOH, $–NH_2$	Moderate	Low–Moderate	Moderate–High	Moderate	Renewable, eco-friendly materials	Limited reproducibility and structural control	[1–9]

Table 2
Influence of reaction conditions for the studied strategies on the fabrication of polyacrylamide-based hydrogel materials [22–60].

Fabrication Strategy	Key Reaction Variable	Structural Parameter	Structure Evolution (Condition → Structure)	Dominant Functional Groups/Features	Adsorption Mechanism	Effect on Adsorption Performance	Ref.
Free-radical polymerization & crosslinking	Crosslinker dosage	Crosslink density; pore size	↑ Crosslinker → ↑ network density → ↓ pore size	$–CONH_2$, –COOH	H-bonding; electrostatic	High density improves stability but may limit diffusion at excessive levels.	[22–26]
	Initiator concentration	Chain length between crosslinks (Mc)	↑ Initiator → ↑ radical flux → ↓ chain length (Mc)	$–CONH_2$	H-bonding; dipole interaction	Faster gelation but reduced flexibility and accessibility	[27–30]
	Reaction temperature	Network homogeneity	↑ Temperature → faster kinetics; excessive → heterogeneous network	Distributed functional groups	Indirect (affects all mechanisms)	Influences the uniformity of adsorption sites	[31,32]
CRP (RAFT/ATRP) & grafting	CTA/initiator ratio; catalyst system	Molecular weight; dispersity	Controlled radical concentration → uniform chain growth	Tailored –COOH, $–NH_2$, $–SO_3H$	Electrostatic; chelation; H-bonding	Improved selectivity and functional group accessibility	[33–36]
	Grafting conditions (time, monomer conc.)	Graft density; chain length	Grafting increases to an optimum, then is limited by termination	High-density pendant groups	Electrostatic; chelation; ion exchange	Increased active sites; excessive grafting causes steric hindrance	[37–40]
	Reaction temperature	Chain-end fidelity	↑ Temperature → reduced control	Functional end groups	Indirect	Affects the precision of functionalization	[41]
In-situ composite hydrogels	Filler loading and dispersion	Interfacial structure; pore morphology	↑ Filler → ↑ interfacial interaction; excessive → aggregation	–OH, –COOH, metal sites, aromatic domains	H-bonding; chelation; π–π; electrostatic	Synergistic adsorption; aggregation reduces accessibility	[42–46]
	Water content (porogen effect)	Pore size; porosity	↑ Water → larger pores and an open network	Exposed functional groups	Electrostatic; H-bonding	Improved diffusion; reduced strength if excessive	[47,48]
	Polymerization rate	Network homogeneity	Fast reaction → non-uniform filler distribution	Non-uniform sites	All mechanisms affected	Reduced adsorption efficiency	[49]
Electrospinning & fiber fabrication	Polymer concentration; viscosity	Fiber diameter; surface area	↑ Concentration → ↑ fiber diameter; low → bead formation	Surface $–CONH_2$, –COOH	Surface adsorption; H-bonding; electrostatic	High surface area improves adsorption kinetics	[50–53]
	Post-curing (crosslinking)	Internal crosslink density	↑ Curing → ↑ stability → ↓ swelling	Fixed functional groups	Electrostatic; H-bonding	Improved stability; reduced accessibility if excessive	[54,55]
Post-polymer modification (PPM)	Temperature; pH; time	Functional group conversion (hydrolysis degree)	↑ Temperature/pH/time → ↑ hydrolysis → $–CONH_2$ → $–COO^-$	$–COO^-$, $–NH_2$	Electrostatic; chelation; ion exchange	Increased charge density enhances the adsorption of cationic species	[56–60]
	Reagent concentration	Degree of functionalization	↑ Reagent → ↑ substitution up to saturation	Functionalized groups	Electrostatic; chelation; H-bonding	Increased active sites; excessive modification reduces stability	[61–63]

Symbols: ↑ increase; ↓ decrease; → indicates causal progression between reaction condition and resulting structural parameter.

Recently, other physical and surface-selective modification techniques have been investigated, such as post-loading of nanoparticles of PAm hydrogels [38,78–80], layer-by-layer (LbL) coatings onto PAm hydrogel surfaces [12,81–84], and double- and interpenetrating-network (DN/IPN) formation, which exhibit exceptional mechanical performance and functional integration [85–92].In addition to other important strategies, such as enzymatic and biocompatible conjugation approaches, nanoparticle surface modification for hydrogel integration, and photochemical and plasma-based surface engineering, nanoparticle surface modification for hydrogel integration was reported.

Scheme 6 summarizes the most common fabrication strategies widely employed in the design of advanced polyacrylamide-based hydrogels matrix. Where free-radical polymerization forms stable 3D crosslinked networks, In-situ nanocomposite formation integrates nanoparticles into the polymer frameworks, PPM introduces specific active functional groups into polymer chains, and IPNs combines two interlaced polymer frameworks, providing improved mechanical resilience, swelling control, and multifunctional performance for water purification applications.

Overall, Table 3 presents the principal fabrication strategies, their advantages and disadvantages, applicable systems, product performance, and potential scalability.

3. Applications for water treatment and pollutants removal

Over the last decades, industrial growth and the accelerating pace of urbanization have sharply reduced the supply of clean water, elevating water contamination to a pressing global challenge [48]. Daily, large amounts of various organic and inorganic contaminants resulting from human and industrial activities are discharged into surrounding water bodies and other water ecosystems. Such hazardous materials pose a serious threat to water security and water scarcity, as well as to human health and the ecological environment [93]. As reported recently, nearly half of the world's

Population lacks reliable access to safe, clean water. If existing patterns continue till 2050, when the global population is anticipated to reach 10 billion, these numbers may increase threefold [5].

Generally, real wastewaters are complex, variable mixtures of trace elements, minerals, vitamins, and organic compounds that can serve as carbon sources for biological processes, unlike synthetic wastewater, which has a limited, well-defined composition. Additionally, the properties of real wastewater, such as salinity, competing ions, and pH, vary depending on its source. Heavy metals and organic dye compounds are examples of toxic substances that pollute water and continue to pose a serious environmental challenge [11]. Therefore, scientists worldwide have extensively evaluated various eco-friendly materials and a range of chemical, physical, and biological techniques for treating wastewater contaminated by such pollutants. Numerous sectors, such as households

And industries (mining, paint, plastics, textiles, paper, food processing, fertilizers, pesticides, cosmetics, pharmaceuticals, electronics, plating, woodworking, and leather manufacturing), generate substantial wastewater. Scheme 7 represents the most common applications of hydrogels in the elimination of pollutants from water.

Conventional water treatment techniques, such as coagulation/flocculation, membrane filtration, and adsorption, were extensively examined to remove various pollutants, including heavy metal ions and dyes, from wastewater. Table 4 represents the advantages and

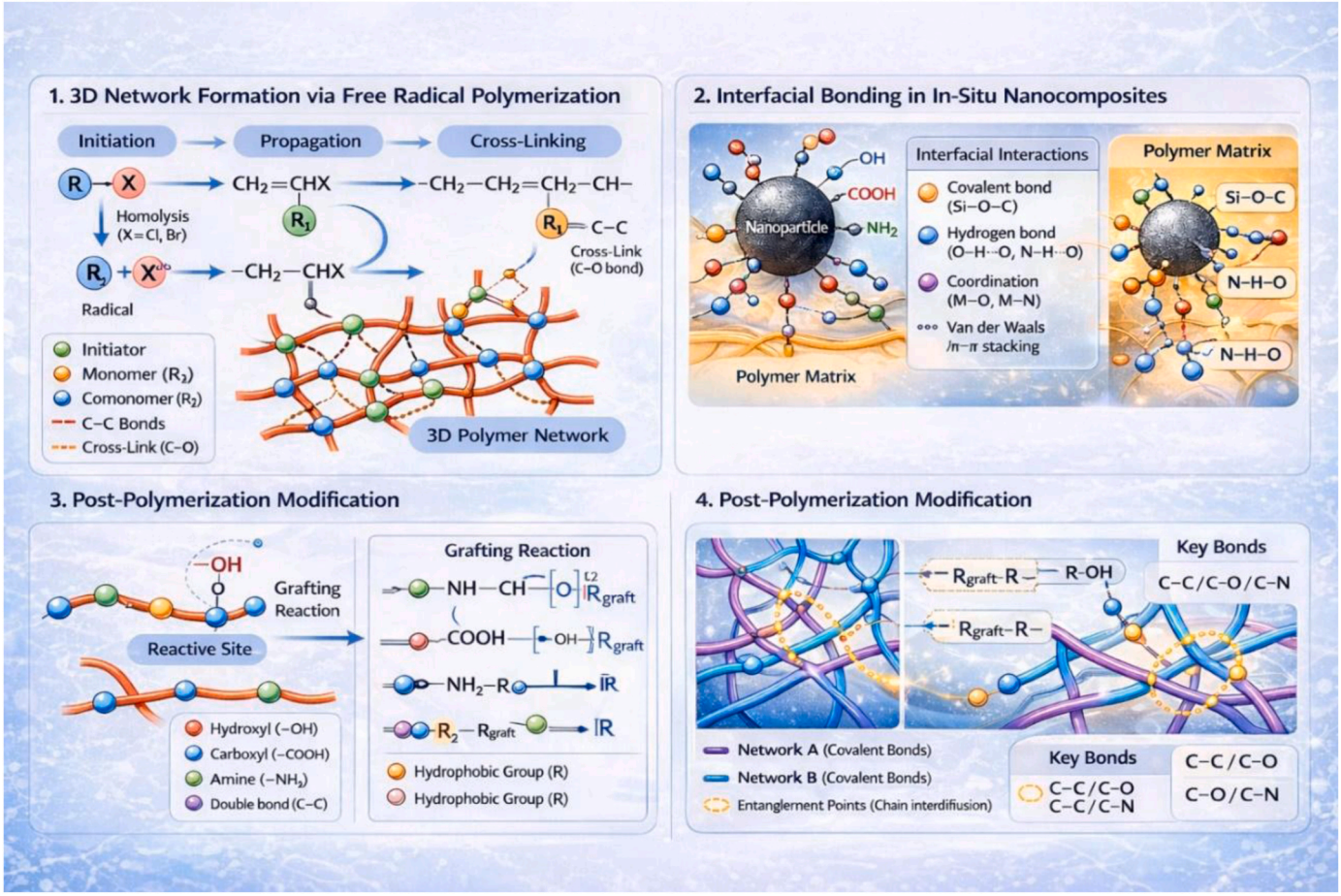

Scheme 6. The most common fabrication strategies for polyacrylamide-based hydrogels.

Table 3
Comparative Summary between the Fabrication Strategies studied 19–81.

Synthetic method	Advantages	Disadvantages	Applicable systems	Product performance	Scalability potential	References
Free radical polymerization (FRP)	Simple, low-cost, widely used; flexible formulation	Limited control over structure; possible heterogeneity	PAm hydrogels; lignin–PAm; bulk adsorbents	Good swelling, hydrophilicity, tunable composition	High	[19], [21], [42], [64], [72]
Controlled radical polymerization (CRP)	Precise control; advanced functional design	Complex synthesis; higher cost; catalysts required	Grafted PAm; surface-modified systems; CNT-based materials	Improved structural precision and tunability	Moderate	[31], [33], [34], [35], [36], [38], [39], [40], [41]
In-situ composite formation	Simultaneous network formation and filler incorporation	Dispersion and compatibility challenges	GO/PAm; clay/PAm; TiO_2/PAm; cellulose/PAm	Enhanced mechanical and adsorption properties	Moderate–High	[51], [52], [53], [54], [62], [63], [68], [74], [75], [80], [81]
Electrospinning/fiber fabrication	High surface area; porous structure; fast mass transfer	Low throughput; specialized equipment needed	Nanofiber membranes; fibrous adsorbents	Rapid adsorption kinetics; high accessibility	Low–Moderate	[45]
Post-polymerization modification (PPM)	Targeted functionalization; improved selectivity	Multi-step; possible structural alteration	Functionalized PAm; grafted systems	Improved adsorption selectivity	Moderate	[43], [46], [58], [61], [73]

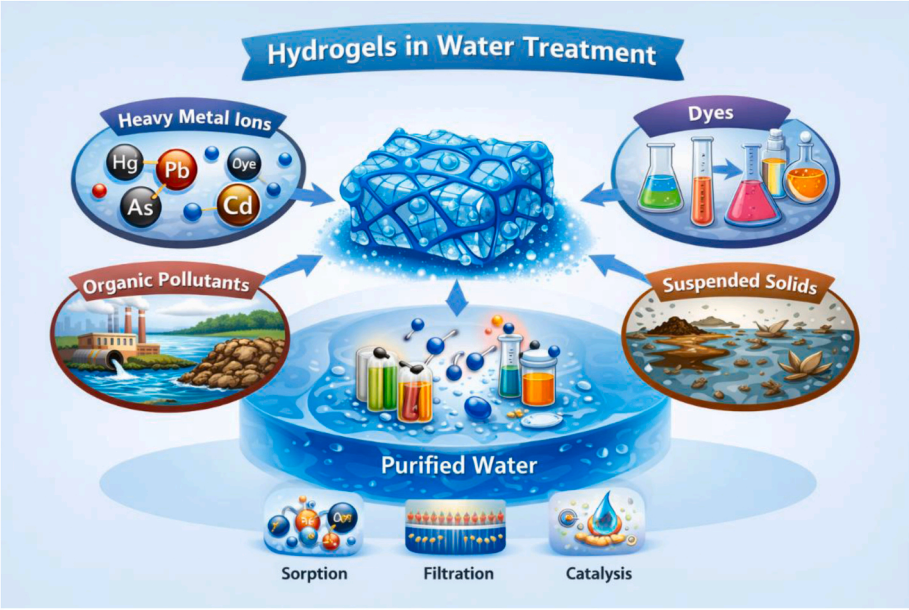

Scheme 7. Applications of hydrogels in wastewater treatment.

disadvantages of the most common techniques that are more commonly applied for wastewater treatment [1,3–8,16–18,93–95]. Among the innovative materials under intense investigation, polymers and polymer-based materials that help address limitations of conventional water treatment techniques, hydrogels represent a specialized class with structural and functional features. Polyacrylamide-based and PAm nanocomposite hydrogels provide a flexible platform that can be engineered for targeted removal of pollutants, including dyes and heavy metals, improved operational efficiency, reusability, and integration into advanced water treatment systems, highlighting PAm-based hydrogel materials as promising materials for next-generation sustainable water purification.

3.1. Removal of heavy metals

Heavy metal contamination from industrial activities, including chemical processing, textile production, battery manufacturing, smelting, and mining, has become a major global environmental challenge affecting aquatic ecosystems [95,96]. Recently, heavy metal pollution levels in surface and groundwater have continued to increase, posing extreme risks to aquatic organisms and human health [95,96]. Therefore, the researchers found that it is crucial to direct their work toward investigating and developing renewable, efficient, and environmentally friendly materials, such as (PAm)- and (PAm)-based nanomaterials and hydrogels, for the remediation of heavy metal ions from wastewater bodies. In this review, we will disscus a wide range of works published in this field over the past few years. In addition to highlighting emerging trends, unresolved challenges, and the overall progression of knowledge within the domain, it provides a comprehensive perspective on current advancements and future research directions. Table 5 summarizes the applications of polyacrylamide and polyacrylate-based nanohydrogel materials in the elimination of different metal ions from aqueous media 97–154.

The chemical behavior of anionic PAm hydrogel was investigated with respect to swelling, which was found to be related to the initial concentrations of Ni and Co ions [97].This work demonstrates that polyacrylamide is a promising and reliable adsorbent for removing metal ions from aqueous media and provides valuable insights into the governing mechanisms and key factors that influence its performance. [97]. On the other hand, a series of hydrogels (Radix Isatidis residue/-polyacrylic acid (RIR/PAA_4), Radix Isatidis residue/polyacrylamide (RIR/PAm), and Radix Isatidis residue/acrylic acid-co-acrylamide) as a

Table 4
Advantages and disadvantages of conventional water treatment techniques [1, 3–8,16–18,93–95].

Technique	Advantages	Disadvantages
Coagulation/ Flocculation	- High effectiveness for colloidal organics, turbidity, and suspended materials. - -Simple and widely used in conventional water plants.	-Excessive sludge generation -Low efficiency for trace contaminants and organic pollutants. -Depending on type and dose of the coagulant and precise pH,
Membrane Filtration	-Highly effectiveness to remove particulate, microorganisms, and macromolecule. -Highly water quality can obtain (especially NF/RO). -Modular systems with small footprints and scalable design.	-Membrane fouling (organic/ inorganic deposits) reduces flux and increases maintenance -High energy demand and operational costs. -contaminants do not degrade but concentrates them into a retentate phase.
Adsorption	-High flexibility and wide applicability to various contaminants. -Low operational complexity. -Can be effectiveness for contaminates of lower concentrations.	-Selectivity and regeneration of some adsorbents can be challenging. -Adsorbent efficiency can be reduced by competing ions and natural organic matter. -Adsorption performance depending on properties of media.

considerable biosorbent hydrogel material for uptake of (Pb(II), Cu(II), and Cd(II)) ions were fabricated by Radix Isatidis residues functionalized through grafting with acrylamide and acrylic acid, as illustrated in Fig.1a, [96]. The researchers explained that the synthesized hydrogel materials functioned as highly effective biosorbent for the elimination of metal ions from aqueous media. This approach offers a promising way to develop biosorbent materials and enable the cyclic utilization of Chinese herb residues [96]. The redox method was investigated for the preparation of Poly(acrylonitrile-co-acrylamide) [poly(AN-coAm)] using sodium bisulfite and potassium persulfate as initiators. Then, the obtained copolymers were treated with hydroxylamine hydrochloride to produce amidoxime terminal groups in the polyacrylonitrile (PAN) chains. The amidoxime group was shown to form a complexing ion-exchange network based on acrylonitrile for the removal of Cu(II) ions (111 mg g^{-1}) from aqueous solution [99]. Also, a free radical co-polymerization reaction approach was investigated to prepare polyacrylamide-based cryogels (macroporous polyacrylamide gel (MPAmG)) called cryogels to remove lead ions (Pb^{2+}) from aqueous media [100]. In this process, MPAmG were fabricated for 1.0 h at −12 °C by reacting acrylamide (Am), allyl glycidyl ether (AGE), and N, N-methylene-bis (acrylamide) (MBAAm) with epoxy functional groups (epoxy-PAm) at a concentration of 7.5%. Thereafter, MPAmG was reacted with tris(2-aminoethyl)amine (TREN) ligand groups, followed by bromoacetic acid (BA). The introduction of amide and carboxyl groups in the cryogels structure enabled the removal of lead from aqueous solutions. Under optimal conditions (pH 5 for 30 min), the MPAmG-TBA exhibited a lead removal capacity of 10.78 mg g^{-1} [100]. A modified macroporous polyacrylamide-based monolith was prepared as a new sorbent material to interact with Pb(II), Cd(II), and Cr(III) in aqueous media [102]. In this study, a microporous polyacrylamide-based monolith was modified with vinylsulfonic acid to introduce a negative surface charge, enabling the formation of complexes with heavy metal ions in aqueous media [102]. Fig. 1b represented the removal of concentrated industrially significant positive and negative heavy metal ions (Zn, Cu, Ni, and $(Cr_2O_7)^{2-}$) using ionized acrylamide-based copolymer/terpolymer hydrogels [103]. In this work, the hydrogel materials were prepared using the ionized polymer based on Acrylamide (Am, polymer backbone) grafted with co-monomers sodium p-styrenesulfonate (SS) and N, N-dimethylaminopropyl acrylamide (DMAPAm). They found that the SS:DMAPAm ratio significantly increased the adsorbent's adsorptive capacity. At a high SS ratio, leading to enhanced adsorption of the cationic metal ion. On the other hand, using a high DMAPAm ratio enhances the recovery of anionic metal ions. While using equal ratios, the removal of both cationic and anionic metal ions declined due to the counteractive nature of these co-monomers. Additionally, the capture ability of the hydrogels was noted to be directly proportional to their swelling efficiency. For regeneration and separation of cations and anions from the adsorbent, NaOH solutions were followed by HNO_3 [103]. A simple one-step synthesis method was investigated as a preparation process to fabricate a novel, low-cost, and green sodium alginate-polyacrylamide (Alg–PAm) composite aerogel for high-efficiency sorption of Pb(II) [104]. The synthesized Alg–PAm composite aerogel achieved 99.2% Pb(II) uptake and a high removal capacity of 252.2 mg g^{-1}. Alg–PAm has broad potential for treating wastewater contaminated with heavy metal ions. Another sodium alginate/cellulose nanofiber/polyacrylamide (SA/CNF/PAm) composite hydrogel microspheres were investigated for the removal of Pb(II) from wastewater [105]. In which sodium alginate was incorporated with cellulose nanofibers applying microfluidic strategy to form porous SA/CNF hydrogel microspheres, followed by grafting with polyacrylamide (PAm) to produce (SA/CNF/PAm) microspheres composite hydrogel. The presence of PAm enhanced the adsorption efficiency compared with original SA/CNF microspheres, with a maximum adsorption capacity of 676.97 mg/g for Pb[II] [105]. A free radical polymerization approach was investigated to prepare SA-PAm/GO hydrogel composites for the adsorption of Cu(II) and Pb(II) from water bodies, as demonstrated in Fig. 1c [106]. Under optimal parameters, the highest capture abilities for Cu(II) and Pb(II) were 68.76 and 240.69 mg g^{-1}, respectively. In addition, the SA-PAm/GO adsorbent maintains appropriate adsorption capacity after 5 cycles of adsorption-regeneration [106]. Also, the free radical solution and bulk polymerization approach were investigated to design a low-cost biocomposite SA-g-poly(AAm)/HL-$CoFe_2O_4$ hydrogel to remove Ni(II) heavy metal ions from aqueous medium [107]. The prepared biocomposite hydrogel was synthesized through grafting of polyacrylamide (PAm) onto sodium alginate (SA) and addition of a magnetic composite recognized as HL-$CoFe_2O_4$ (HL: hydrolyzed Luffa Cylindrica) [107]. The experimental results illustrated considerable removal efficiency of Ni onto the composites (follow for SA-g-PAm) (70.09), SA-g-PAm/HL (90.25%), and SA-g-PAm/HL-$CoFe_2O_4$ (93.83 %) with maximum interaction capacities of SA-g-PAm. (31.37 mg g^{-1}), SA-g-PAm)/HL (43.15 mg g^{-1}), and SA-g-PAm/HL-$CoFe_2O_4$ (45.19 mg g^{-1}). On the other hand, the removal efficiency of Ni suffers from a decrease in the presence of Ca^{2+} and Na^{+} in aqueous solution. Furthermore, after 8 cycles, the efficiency remained stable [107]. Fig. 2a shows the fabrication scheme of SA/sodium humate @ PAm (SA/SH@PAm) hydrogel beads by employing SA as the encapsulant, SH as the filler, and PAm as the outer layer to remove Cu(II) using batch and continuous investigations [108]. The experimental results revealed that ion exchange and chelation of Cu(II) by various functional groups (-COOH, -CO–NH, etc.) are the main adsorption mechanisms. Finally, the SA/SH@PAm showed excellent regeneration and selectivity properties [108]. The results reported for alginate/PAm systems [104–108] revealed that PAm plays avital role in construction of a stable and flexible 3D network that reinforces alginate that improves the interfacial adhesion and structural integrity of the hydrogel. In addition to the introduction of amide ($–CONH_2$) groups of PAm act as active binding sites which are beneficial to adsorb heavy metal ions [104,106]. Also, strong hydrogen bonding between PAm and alginate improves interfacial adhesion with the alginate matrixes and contributes to significantly enhancing swelling and adsorption performances with considerable mechanical stability.

A new bio-based, bilayer hydrogel composite composed of carboxymethyl cellulose (CMC) and PAm was investigated for heavy-metal wastewater purification, as represented in Fig. 2b [109].

The fabricated CMC/PAm composite hydrogel demonstrated high

Table 5
Applications of polyacrylamide and polyacrylate-based hydrogel materials in the removal of heavy metals.

Adsorbent	Pollutants	Q_o (mg/g)	Condition	Adsorption-Regeneration	Ref.
APAm	Ni	230	t = 180min, pH = 6, T = 50 °C	[a]	97
	Co	210			
Polyacrylamide hydrogels	Pb	442	t = 180min, pH = 4, T = 50 °C	5 0.1M of HCl 96.5%	98
poly(AN-coAm)	Cu(II)	111	t = 240min, pH = 5, T = 25 °C	[a]	99
MPAmG	Pb(II)	10.781	t = 30 min, pH = 5, T = 24.5 °C	[a]	100
Anionic polyacrylamide	UO_2^{2+}	111	t = 24 h, pH = 4, T = 45 °C	[a]	101
Polyacrylamide-based monolith	Cd(II)	22.8	t = 24 h, pH = 4, T = 25 °C	[a]	102
	Pb(II)	33.3			
	Cr(III)	66.7			
DMAPAm	Ni(II) Cu(II) Zn(II) $(Cr_2O_7)^{2-}$	[a]	[a]	3M HNO_3/NaOH	103
Alg–PAm	Pb(II)	252.2	t = 24 h, pH = 3, T = 25 °C	5 0.05 M HNO_3 97%	104
SA/CNF/PAm	Pb(II)	676.97	[a]	[a]	105
SA-PAm/GO	Cu(II)	68.76	t = 150 min, pH = 5, T = 25 °C	5	106
	Pb(II)	240.69		1 M HCL 80%/60%	
SA-g-PAm)	Ni	31.37	t = 100 min, pH = 6, T = 25 °C	8	107
SA-g-PAm)/HL		43.15		1.1 M HCl	
SA-g-PAm/HL-$CoFe_2O_4$		45.19		>70 %	
SA/SH@PAm	Cu	134.65	t = 800 min, pH = 5, T = 25 °C	10 1.2 mol/L HCl ≈70%	108
CMC/PAm	Cu(II) Pb(II) Cd(II)	[a]	t = 7h, pH = 5.5, T = 25 °C	3 EDTA solution (10 mL, 0.1 M) 67.1%, 83.3%, and 63.3%	109
CTS/PAmgel	Cd(II)	86.00	t = 6 h, pH = 5/6, T = 25 °C	5	110
	Cu(II)	99.44		1M HC/0.1 M NaOH	
	Pb(II)	138.41		90.7%, 91.1%, and 88.4%	
CTS/PAm/OP gel	Cr(VI)	80.43%	t = 240 min, pH = 4/5, T = 28 °C	0.1 M HCl, 0.1 M EDTA, and 0.1 M HNO_3 eluents	111
	Cu(II)	82.47%			
AM/AO/AEBI-CTS	Cu(II)	190.7	t = 6h, pH = 5, T = 25 °C	5	112
	Ni(II)	128.9		1 M HCl solution, 90 %	
CTS-gP(CMC-co-Am)	Cd	37.3	t = 90 min, pH = 10, T = 20 °C	[a]	113
Fe_3O_4 modified with PAm	Cu(II)	454.5	t = 90 min, pH = 6, T = 25 °C	[a]	114
	Ni(II)	222.2			
	Co(II)	312.5			
	Cd(II)	526.3			
GG/PAm/RH/Ulva	Cu(II)	50.25	t = 2h, pH = 4/4/9, T = 25 °C	4	115
	Pb(II)	45.24			
	MB	51.54			
GG/PAm/RH/Sarg	Cu(II)	73.52	t = 2h, pH = 4/4/9, T = 25 °C	4	115
	Pb(II)	52.63			
	MB	68.02			
(CAA-Ca(II)-FeS) hydrogel	Cd (II)	494.30	[a]	[a]	116
	Cu(II)	374.00			
	Pb(II)	783.20			
TOCNF-TMPTAP-APAm	Cu	240	t = 50 min, pH = 6, T = 25 °C	10 0.2 M of EDTA-2Na 80%	117
HPAMF	Cu	2.33 mmol g^{-1}	[a]	[a]	118
PEI-PAmCF	Cr(VI)		t = 12 min, pH = 3	5 90%	119
RIR/AA-co-AM hydrogel	Pb(II)	655.4	t = 120 min, pH = 5, T = 25 °C		120
	Cd(II)	367.2			
	Cu(II)	290.5			
PAm@TP hydrogel	Pb	27.3	t = 180 min, pH = 4.5	1 mol L^{-1} HCl	121
BSG-g-PAm	Cu(II)	95.12%	t = 70,70, and 95 min, pH = 4.0, 4.9 and 5.0, T = 50 °C	[a]	122
	Cd(II)	87.45 %			
	Pb(II)	84.65%			
PAm-CG composite	Pb(II)	0.622 mol/kg	[a]	[a]	123
PAm/Na-MMT	Ni(II)	99.3%	t = 24h, pH = 6, T = 45 °C	[a]	124
	Co(II)	98.7%			
Z-g-PAm	Cr (III)	44	[a]	[a]	125
	Pb(II)	345			
	Zn(II)	1046			

(*continued on next page*)

Table 5 (*continued*)

Adsorbent	Pollutants	Q_o (mg/g)	Condition	Adsorption-Regeneration	Ref.
CTMAB-PAm	Pb(II) Cr(VI)	184.88, 64.13	t = 24h, pH = 7, T = 27.5 °C t = 24h, T = 27.5 °C	[a]	126
Ppolyacrylamide–polystyrene/bentonite	Mg	84.2%	t = 12h, pH = 6, T = 45 °C	[a]	127
PAm-K	UO_2^{2+}	0.0656 mol kg^{-1}	pH = 4.5, T = 25 °C	[a]	128
HBP	Pb(II) Ni(II) Cd(II)	2.8950 2.6170 2.6136	t = 24h, pH = 5.6 and 9, T = 25 °C	[a]	129
PAm/HA-ATP	Ni(II)	64.3	t = 350 min, pH = 6 and 9, T = 25 °C	5 methanol + 0.1 mol/L NaOH (1:1, v/v) 70%	130
Ha-Am-PAm-Sep	Cu(II) Ni(II)	244 250	t = 60 min, pH = 5, T = 45 °C	4 0.1 mol l^{-1} solution of HCl 70%	131
Phy-PAm-Sep	Cu(II) Ni(II)	256.4 277	t = 60 min, pH = 5, T = 45 °C	4 1.1 mol l^{-1} solution of HCl 70%	131
PAm-PMC	Cu(II)	500	t = 60 min, pH = 6.5, T = 50 °C	3 0.05 mol/l of HCl 89%	132
g-PAm/OVerm	Pb(II)	219.4	t = 6h, pH = 5.5, T = 30 °C	5 1M HCl 90%	133
SP-C	Cd	211.86	t = 1h, pH = 6.5,	[a]	134
PAGSPs	Ni(II) Cr(VI) MO QY	75.18 125 32.25 55.55	[a]	[a]	135
S-PEMR	Ni Cu Cd Pb	42.06 % 93.14 % 89.68% 77.02 %	t = 6h, pH = 5.5, T = 30 °C	4	136
PHPAm/Fe_3O_4@SiO_2-SH	Hg(II) Pb(II)	256.41 227.27	t = 120 min, pH = 6.3	[a]	137
Fe_3O_4-PS-acrylic acid/acrylamide	Cu(II) Pb(II)	128 122	t = 120 min, pH = 7	3 1N HCL	138
PAm/FMWCNTs	Cu(II)	385.44	t = 120 min, pH = 4-6	0.1 M HCl 97.1%	139
UiO-66-NH_2-PAm-PET	Pb(II)	711.99	t = 240 min, pH = 5	6 methyl alcohol and 1 mol L-1 hydrochloric 88%	140
graphene/polyacrylamide	Ni(II)	110.25	t = 60 min, pH = 7, T = 25 °C	[a]	141
PAO-GO/PAm hydrogels	UO_2^{2+}	396.82	t = 70 min, pH = 6, T = 30 °C	[a]	142
Nanocomposite based on chitosan–polyethylene oxide/poly (acrylamide-*co*-acrylic acid)	Cu (II)	92%	t = 120 min, T = 25 °C	[a]	143
MoS_2@CPAmA MoS_2	Cr (VI)	800 237.1	t = 50 min, pH = 2	[a]	144
Zn-MOF-74/rGO/PAm	As(III)	282.4	t = 15 min, pH = 10, T = 25 °C	4 0.1M NaOH 75.6%	145
PAm/PAA/PDMTM	Cu(II) Cd(II) Pb(II)	92.33, 110.08 200.97	= 15 min, pH = 5, T = 25 °C	5	146
PAC@Fe_3O_4	Pb(II) Ni(II) Cu(II)	313.02 219.33 210.71	pH = 5, pH = 4, pH = 5	[a]	147
Fe-PGSH	cadmium	33.34			148
semi-IPN/PAm	Pb(II) Cd(II)	340.45 287.38	t = 30 min, pH = 4, T = 27 °C	5 1M HCl 84.1%, 70.7%	149
(PVA/PAm/PAA)/AC	Eu(III) Sm (III)	173.24 160.41	t = 180 min, pH = 4	[a]	150

[a] Not Detected.

affinity toward Cu(II), Pb(II), and Cd(II) ions, as well as multi-ion absorbability. Besides, the adsorbed Cu(II) ions in the hydrogel were in situ reduced to form uniform, dispersed Cu nanoparticles (NPs), and the resulting Cu-NPs-CMC/PAm hydrogel was used to reduce 4-nitrophenol to 4-aminophenol [109]. A double network EDTA-functionalized chitosan/polyacrylamide hydrogel prepared via a two-step strategy was investigated for wastewater treatment to eliminate Cd(II), Cu(II), and Pb(II) [110]. In the first step, ethylenediaminetetraacetic acid (EDTA)- cross-linked chitosan was followed by N, N-methylenebis(acrylamide) (MBA)- cross-linked polyacrylamide to form a CTS/PAm gel used for the removal of metal ions. The CTS/PAm gel exhibited a suitable maximum adsorption capacity of 86.00, 99.44, and 138.41 mg g^{-1} for Cd(II), Cu(II), and Pb(II), respectively. Additionally, the results showed that the CTS/PAm hydrogel exhibited acceptable mechanical strength and good recyclability [110]. For the investigated CMC/PAm hydrogels [109,110], the published works illustrated that PAm contributes to form a high density of cross-links, a 3D, sponge-like, and highly microporous morphology

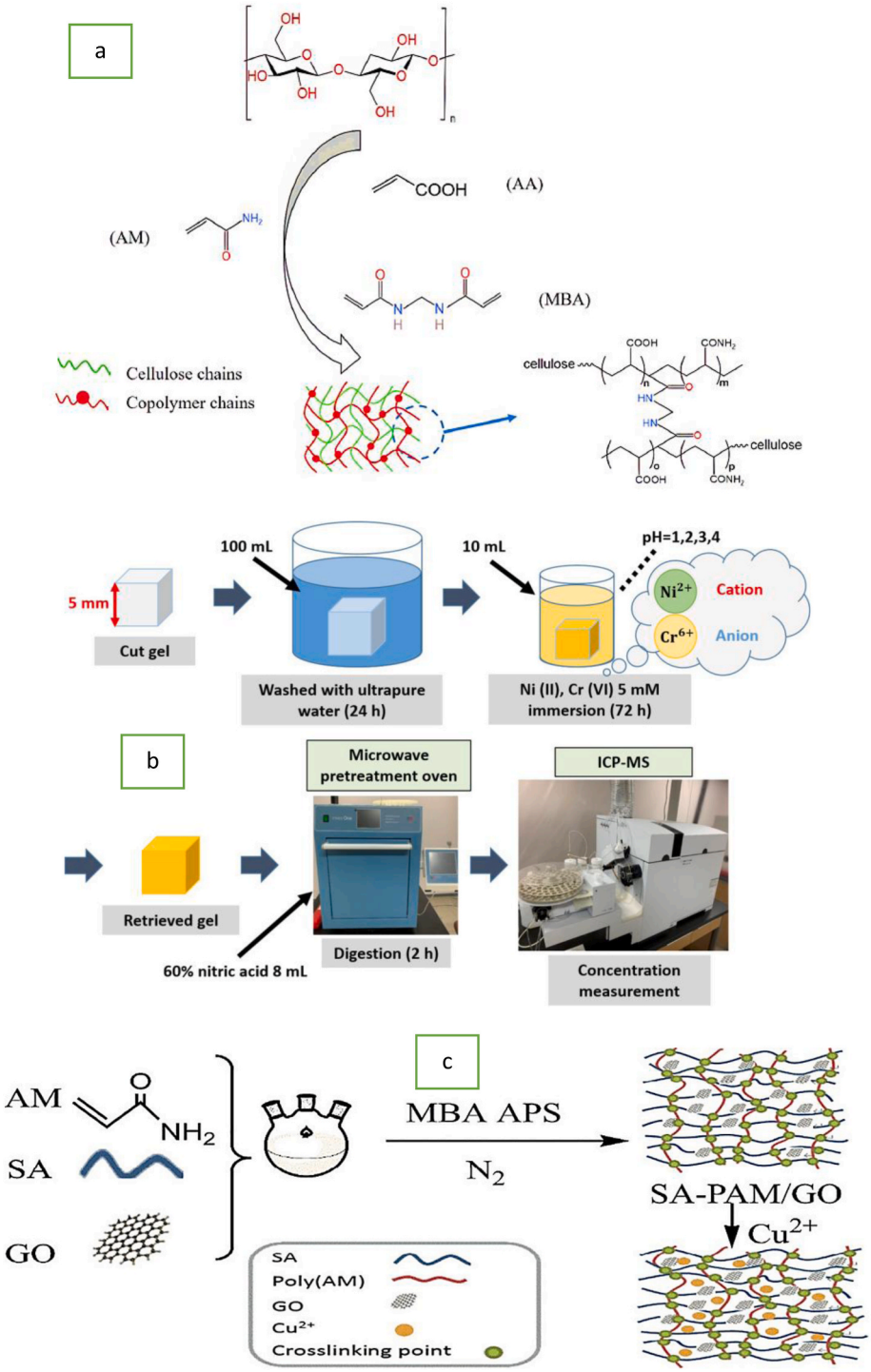

Fig. 1. (a) The preparation process of RIR/AA-co-AM hydrogel [96] (This figure has been adapted/reproduced from Ref. [96], with MDPI permission, copyright 2022), **(b)** Outlines of adsorption experiments of heavy metals by (AAm–SS–DMAPAm) terpolymer hydrogel [103] (This figure has been adapted/reproduced from Ref. [103], PLoS ONE permission, copyright 2024), and (c) Scheme of the fabrication of SA-PAm/GO hydrogel composites (106) (This figure has been adapted/reproduced from Ref. [106], Elsevier permission, copyright 2020).

reinforcing the fabricated hydrogels matrixes and providing these hydrogels with high mechanical strength as well as reduces excessive swelling or dissolution of CMC comparing with those of the pristine CMC-hydrogel [109,110]. The presence of amide groups of PAm functionalities increases the density of active sorption sites alongside with CMC's –COOH groups which allow the transportation of various molecules like H_2O and heavy metal ions across the hydrogels structural [109]. Also, they facilitate H-bonding and electrostatic interactions with CMC chains, promotes a uniform and cohesive network which leads to improve interfacial compatibility. In addition to PAm promotes hydrogel's density, swelling kinetics, and diffusion pathways, thereby optimizing adsorption performances.

Another novel fabricated CTS-BENT-g-AM/OP + MBA hydrogel composite, prepared by chemical cross-linking of radical chitosan with polyacrylamide and N, N′-Methylene bisacrylamide, and mixed with orange peel, was investigated for the removal of Cr(VI) and Cu(II) ions

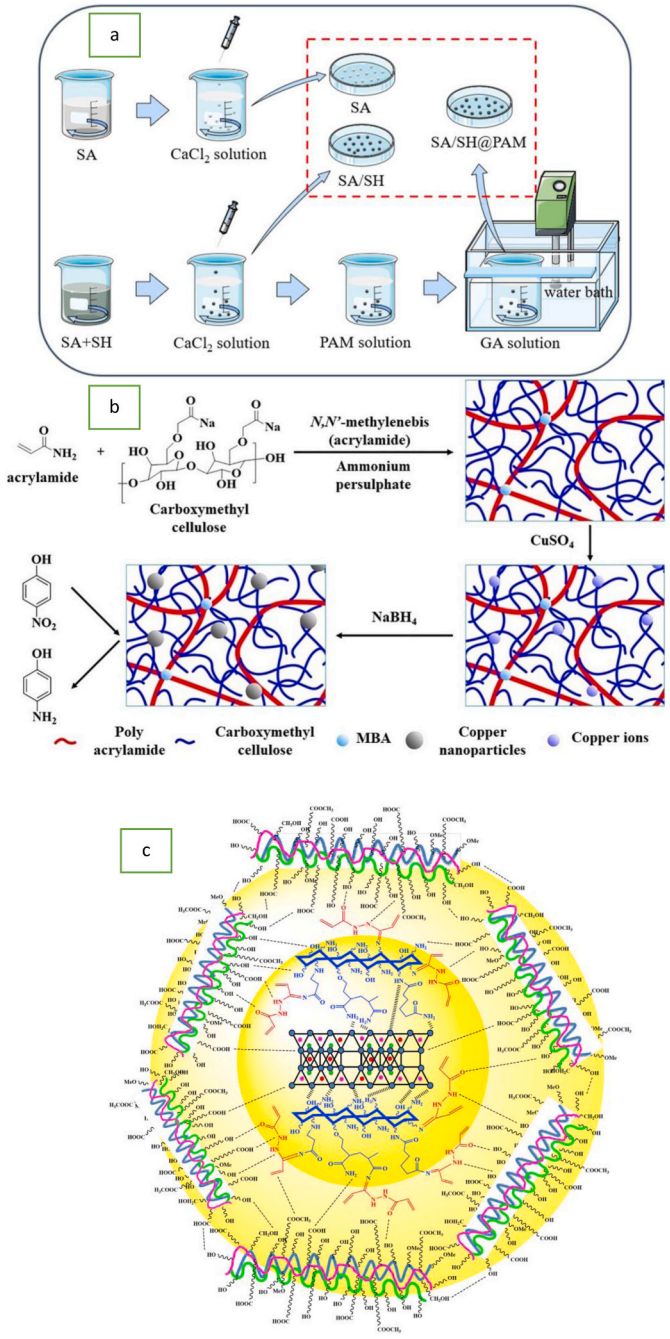

Fig. 2. Scheme of the fabrication of (a) SA, SA/SH, SA/SH@PAm [108] (This figure has been adapted/reproduced from Ref. [108], Springer permission, copyright 2024), **(b)** CMC/PAm composite hydrogels, sorption of Cu(II), formation of Cu@NPs in network of hydrogel, and the catalytic reactions of 4-NP into 4-AP [109] (This figure has been adapted/reproduced from Ref. [109], Elsevier permission, copyright 2019), and (c) CTS-BENT-g- AM/OP + MBA hydrogel composite (112) (This figure has been adapted/reproduced from Ref. [111], Elsevier permission, copyright 2020).

from wastewater, as shown in Fig. 2c [111]. The findings showed that the fabricated biosorbent -based hydrogel composite is cost-effective and promising hydrogel to eliminate heavy metal ion-contaminated water. Also, the free radical polymerization approach was used to prepare.

Amidoxime-modified chitosan (CTS) (AM/AO/AEBI-CTS) with a porous structure containing imidazoline groups through amidoximation of cyano groups, and cross-linked CTS was obtained by crosslinking imidazoline-modified polyacrylamide and CTS [112]. The experimental results showed that the AM/AO/AEBI-CTS exhibited good water wettability and excellent selectivity for Cu(II) over Ni(II). The experimental data showed that the fabricated material is a promising sorbent for removing heavy metals from wastewater [112]. Polyacrylamide-functionalized Fe_3O_4 nanoparticles are among the most attractive magnetic nanoparticles fabricated by the hydrothermal strategy, which develop a carbon-covered layer and polyacrylamide functionality to adsorb Cu(II), Ni(II), Co(II), and Cd(II) [114]. The stability of the prepared adsorbent in acidic solution may be due to the carbon coating and PAm surface functionalization. Moreover, PAm-coated Fe_3O_4 showed a higher removal percentage than the unmodified one, with the largest capture efficiency for Cu(II), Ni(II), Co(II), and Cd(II) [114].Recently, an innovative process was investigated and developed to remove hazardous contaminants, such as Pb(II), Cu(II), and methylene blue (MB), from aqueous media [115]. Green hydrogel composed of guar gum/polyacrylamide (GG/PAm) grafted with rice husk core (GG/PAm/RH) was prepared, thereafter mixed with Ulva fasciata (GG/PAm/RH/Ulva) and Sargassum dentifolium green algae (GG/PAm/RH/Sarg), as shown in Fig. 3a, [115]. Recyclability studies showed that the prepared hydrogels successfully removed the contamination over four adsorption–desorption cycles [115]. Fig. 3 b represents the synthesis and adsorption mechanism of a recent high-efficiency sorption process of Cu(II), Cd(II), and Pb(II) by a novel FeS-modified poly(acrylamide-co-2-acrylamido-2-methylpropane sulfonic acid)-g-carboxymethylcellulose-Ca(II) hydrogel (CAA-Ca(II)-FeS) [116]. A novel FeS-hydrogel was fabricated for the remediation of multiple heavy metals, with high selectivity and capacity. The overall results revealed that the prepared CAA-Ca(II)-FeS-hydrogel is a promising sorbent and provides an effective solution for removing heavy metals from complex contamination media.

Newly, owing to their sustainability, biocompatibility, eco-friendly nature, wide availability, and versatility in fabrication and chemical modification, naturally derived cellulose-based composite adsorbents have been recognized as suitable candidates for wastewater treatment applications [117–119]. Among them, cellulose nanofibers (CNFs) offer distinct advantages over other nanofibers, including high mechanical strength comparable to that of inorganic fibers, high transparency, low density, and outstanding physicochemical properties [117,118]. Consequently, CNFs have attracted considerable attention as effective reinforcing agents for polymer hydrogel composites, where they can synergistically enhance overall material performance [118]. So, a fabricated 3D lamellar porous cellulose nanofiber/polyacrylamide composite aerogel, prepared via a simple in-situ physical/chemical combination of anionic polyacrylamide and carbonylated cellulose nanofibers, followed by freeze-drying, was used for the removal of Cu (II), as shown in Fig. 3c [117]. In the TOCNF/PAm systems, the interactions are mainly controlled by inter/intrachain H- bonding interactions between the carboxylate groups ($–COO^-$) of TOCNF and the amide groups ($–CONH_2$) of PAm, with additional weak electrostatic interactions [117]. FTIR spectra confirms that PAm is successfully covalent crosslinked with TOCNF via TMPTAP crosslinking agent. Where FTIR spectra revealed that the bands of -OH groups in the TOCNF/TMPTAP/PAm spectra will be shifted to lower wavenumbers attribute to the formation of H-bond interactions between PAm and TOCNF in addition to the peaks of carboxylate groups ($–COO^-$) also decreased. In addition to, new bands ascribed to –COOH and amino functional groups appeared, respectively, approving the strong interactions between TOCNF, PAm and TMPTAP [117]. Therefore, abundant –COOH and amino functional groups were introduced to TOCNF structural, leading to improve adsorption active sites for heavy metals ions. On the other hand, chemical cross-linking double networks and H-bonding between PAm and TOCNF enhanced its underwater mechanical compressibility and water-stability [117]. The prepared aerogels exhibited high thermal stability, water stability, and an adsorption capacity of 240 mg g^{-1}. The adsorption mechanism is

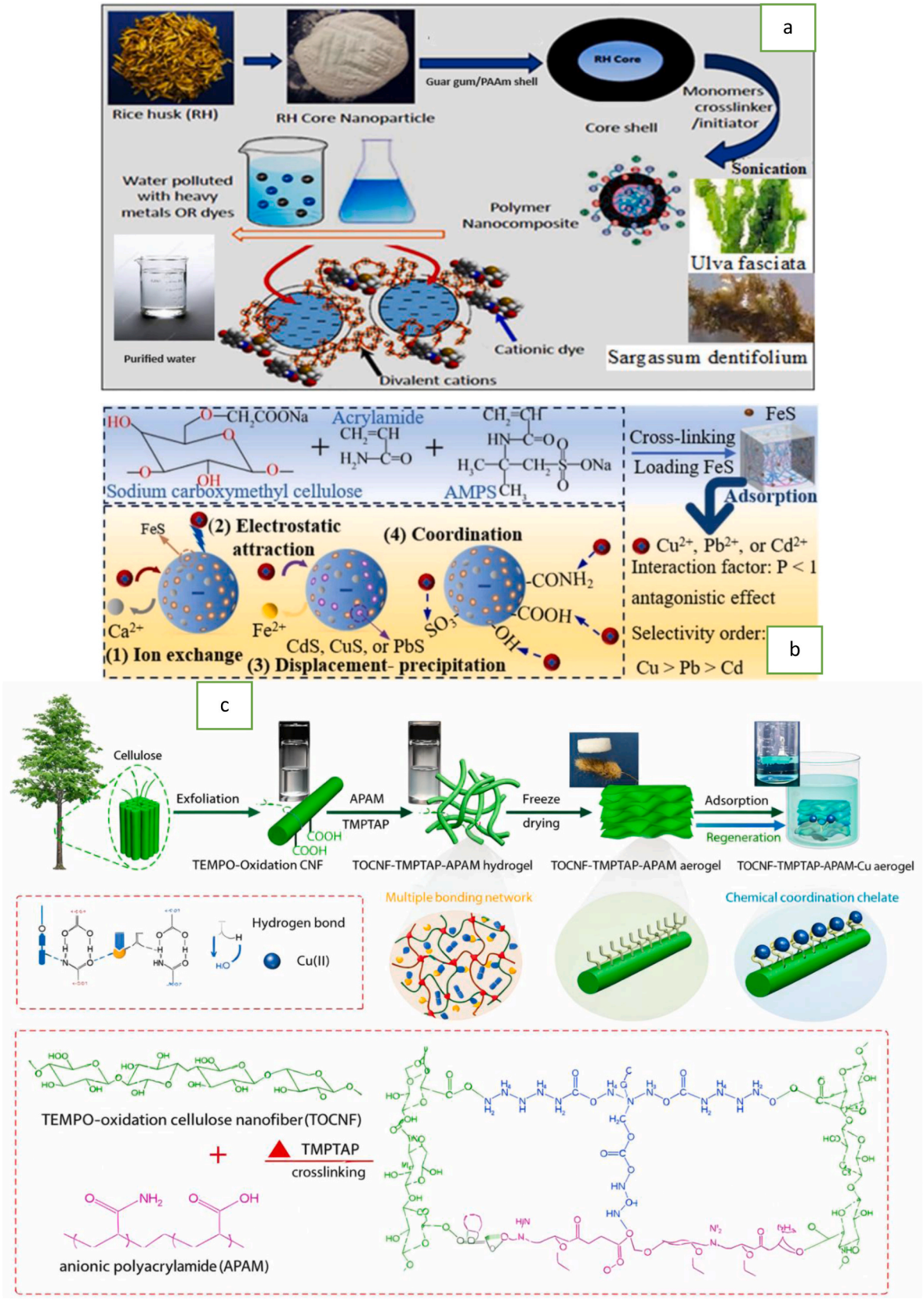

Fig. 3. Scheme of the preparation of (a) GG/PAm/RH/Ulva [115] (This figure has been adapted/reproduced from Ref. [115], Spriner permission, copyright 2024), **(b)** CAA-Ca(II) (CAA-Ca(II)-FeS hydrogels and sorption mechanism [116] (This figure has been adapted/reproduced from Ref. [116], Elsevier permission, copyright 2025), and (c) the facile fabrication of 3D lamellar porous TOCNF-TMPTAP-APAm aerogels to remove Cu(II) and regeneration (118) (This figure has been adapted/reproduced from Ref. [117], Elsevier permission, copyright 2022).

explained in terms of electrostatic attraction, chelation, and complex formation between the active sites and Cu(II) ions. Moreover, the aerogel possessed removal efficiency above 80% after 10 reuse cycles [117]. On the other hand, the incorporation of cellulose nanofiber (CNF) into HPAm hydrogels to fabricate novel classes of all physically cross-linking composite hydrogels to polyacrylamide/cellulose nanofiber (HPAmF) was investigated, comparing with the HPAm hydrogels, to uptake Cu(II) from aqueous media [118]. The addition of (2 wt%) CNF (2 wt%) leads to improved tensile strength by 632% compared to CNF-free hydrogels, besides enhancing the sorption capacity towards Cu (II) (2.33 mmol g^{-1}) about 86% over the pure hydrogel [118]. Another cellulose-based composite hydrogel (PEI-PAm-CF) was synthesized by simple cross-linking of polyethyleneimine/polyacrylamide (PEI/PAm) and cellulose with epichlorohydrin as the cross-linker and used for the adsorption of Cr(VI) [119]. It possessed a double-network structure and emitted blue fluorescence. Compared to (PEI-CF and PAm-CF), the PEI-PAm-CF displayed an interaction synergy effect to remove Cr(VI). Moreover, the adsorption process was not significantly affected by the presence of anions (NO_3^-, Cl^-, $H_2PO_4^-$, and CH_3COO-) and cations (Na^+, K^+, Mg^{2+}, Ca^{2+}, and Cr^{3+}), except SO_4^{2-}. Additionally, the removal performance only decreased by 7% after five adsorption/desorption cycles [119]. Summarily, PAm plays a dual role in CNF/PAm hydrogels matrixes as a hydrophilicity enhancer and networks stabilizer. Also, PAm constructs supportive 3D networks that support the rigid cellulose nanofiber frameworks, significantly improving the structural cohesion and mechanical strength of the prepared hydrogels. In addition, the hydrophilic amide groups of PAm contribute to enhanced swelling capacity and additional active adsorption sites for metal ions alongside the abundant carboxyl groups of CNF and improve interfacial compatibility through H- bonding with hydroxyl and carboxyl groups on CNF. Also, the hydrophilic nature of PAm significantly improves swelling performance, diffusion properties, and adsorption kinetics of the fabricated hydrogels [117–119].

Also, a series of 3D hydrogels with high porosity structure, Radix Isatidis residue/acrylic acid-co-acrylamide (RIR/AA-co-AM), Radix Isatidis residue/polyacrylamide (RIR/PAm), and Radix Isatidis residue/polyacrylic acid (RIR/PAA_4) were prepared for the removal of heavy metal ions Pb(II), Cu(II), and Cd(II) [120]. The findings revealed that RIR/PAA4 exhibited the highest swelling rate (9240%). At the same time, the RIR/AA-co-AM hydrogel showed the highest removal capacities of 655.4, 367.2, and 290.5 mg g^{-1} for Pb(II), Cd(II), and Cu(II), respectively. Recently, various eco-friendly, effective, and inexpensive adsorbents fabricated from natural waste materials grafted with polyacrylamide were investigated for the uptake of metal ions from aqueous media [121–123,152]. Polyacrylamide/Rice Husk hydrogel to remove Cd ions from aqueous solutions [152], a novel effiecient adsorbent Polyacrylamide@Tangerine Peel composite hydrogel to adsorb Pb(II) from wastewater [121], polyacrylamide grafted brewer's spent grain (BSG-g-PAm) as inexpensive sorbent material to eliminate heavy metals ions such as Cu(II), Cd(II) and Pb(II) from polluted streams [122], and the fabrication of effective and cost-effectiveness PAm-CG composite using in situ polymerization approach to eliminate Pb(II) from aqueous media [123]. Also, different preparation approaches were investigated to graft polyacrylamide with nanoclay [124], zeolite [125,153], bentonite [126,127], kaolinite [128], humic acid-bentonite [129], Attapulgite [130], sepiolite [131], pumice [132], vermiculite [133], silica [134]. These recent fabricated PAm-based materials were used to remove Co(II) and Ni(II) [124], Cu(II), Ni(II), and Zn(II) [153], Cr(III), Pb(II), and Zn(II) [125], Pb(II), Cr(VI) [126], Mn(II) [127], UO_2^{2+} [128], Ni(II), Cd(II) and Pb(II) [129], Ni(II) [130], Cu(II) and Ni(II) [131], Cu (II) [132], and Pb(II) [133,134] from aquatic media.

Despite the rapid expansion of nanomaterial-based adsorbents, the search for efficient, practical materials for water-treatment applications remains a significant challenge [154]. Therefore, the development of high-performance, sustainable, and economic materials has gained considerable attention to facilitate the practical deployment of adsorption technologies. Hydrogel-based materials have received great attention in this regard due to their strong potential for water purification applications [154]. Modifying the polymeric networks of hydrogels with nanomaterials to form hydrogel nanocomposites can substantially improve their promising performance and enhance essential properties, including mechanical integrity, swelling behavior, and regenerative capability [154]. These improvements are typically achieved through the incorporation of a variety of nanomaterials derived from different sources, such as waste foundry sand particles [135], manganese residues (EMR) silicate minerals [136], Fe_3O_4-magnetic nanoparticles [137], magnetic nanoparticles then blende with polystyrene waste [138], multiwalled carbon nanotubes [139], UiO-66-NH_2 on modified PET nonwoven fabric [140], graphene [141], ethylene diamine-reduced graphene oxide [142], chitosan–polyethylene oxide nanofibers [143], molybdenum disulphide (MoS_2) [144], zinc based metal-organic framework (Zn-MOF-74) [145],

PAm/PAA/PDMTM [146], and (PAC@Fe_3O_4) nanocomposite [147], into the hydrogel framework. In this regard, a new polyacrylamide grafted with waste foundry sand particles (PAGSPs) was investigated and developded to remove Ni(II) and Cr(VI) metal ions from water with adsorption capacities of 75.18 and 125 mg g^{-1} for Ni(II) and Cr(VI), respectivelly, in addition to adsorption of organic dyes such as methyl orange (MO) and quinoline yellow (QY) [135]. Also, a novel composite (S-PEMR) based on electrolytic manganese residues (EMR) silicate minerals-and polyacrylic acid-polyacrylamide double-network hydrogels was fabricated, as illustrated in Fig. 4a, to remove Ni (II), Cu(II), Cd (II), and Pb(II) [136]. The adsorption mechanism may involve chelation or coordination, ion exchange, interactions of O and N functional groups, and Si-O and Al-O interactions with the metal ions [136]. Fig. 4b represented the preparation of a novel thiol-rich PHPAm/Fe_3O_4@-SiO_2-SH nanocomposite hydrogel using partially hydrolyzed polyacrylamide (PHPAm) as a selective magnetic nanoadsorbent for effective removal of Hg(II) and Pb(II) from wastewater. The adsorption experiments showed that the prepared hydrogel can adsorb 256.41 mg Hg(II) and 227.27 mg Pb(II) [137]. Another smart nanoadsorbent, Fe_3O_4-PS-acrylic acid/acrylamide nanocomposite hydrogel, was synthesized with high saturation capacities for Cu(II) and Pb(II), and the hydrogel achieved the minimum magnetite content [138]. On the other hand, gamma radiation was applied as an initiator to prepare polyacrylamide/functionalized multiwalled carbon nanotubes (PAm/FMWCNTs), which were used to adsorb Cu(II) ions from wastewater [139]. Also, a practical and facile method was investigated to grow highly renewable UiO-66-NH_2-PAm-PET as MOF composite adsorbent materials to eliminate Pb(II) from water with excellent reusability and splendid stability [140]. Recently, other synthesized PAm-based nanomaterials were utilized to remove Ni(II) by graphene/polyacrylamide network hydrogel (GO-PAm) hydrogel [141], U(VI) Photothermal composite polyamidoxime-graphene oxide/polyacrylamide hydrogel (PAO-GO/PAm) [142], Cu(II) by chitosan–polyethylene oxide nanofibers and polyacrylamide-co-acrylic acid hydrogel [143], Cr (VI) by MoS_2@CPAmA [144], As(III) by (Zn-MOF-74/rGO/PAm) nanocomposites [145], CuII), Cd(II) and Pb(II) by PAm/PAA/PDMTM [146], and Pb(II), Ni(II), and Cu(II) from wastewater by (PAC@Fe_3O_4) nanocomposite [147]. Also, an iron-incorporated polyacrylamide-grafted shellac (Fe-PGSH) was prepared to eliminate Cd(II) from wastewater as a saturated monolayer, with an adsorption capacity of 33.34 mg g^{-1} [148]. A recent sustainable and efficient semi-interpenetrating polymer network (semi-IPN) structure based on *Acorus calamus* leaf lignin and acrylamide (AM) hydrogel as an eco-friendly adsorbent was fabricated to eliminate Pb(II) and Cd(II) ions [149]. The adsorption process is explained in terms of electrostatic interactions and chelation between metal ions and -OH and -NH groups [149]. Also, activated carbon (AC) derived from Sewage sludge of the wastewater treatment plant, activated with $ZnCl_2$, and finally, thermally exposed at 550 °C. Then, the prepared (AC) was modified with a terpolymer hydrogel of polyvinyl alcohol/polyacrylamide/polyacrylic

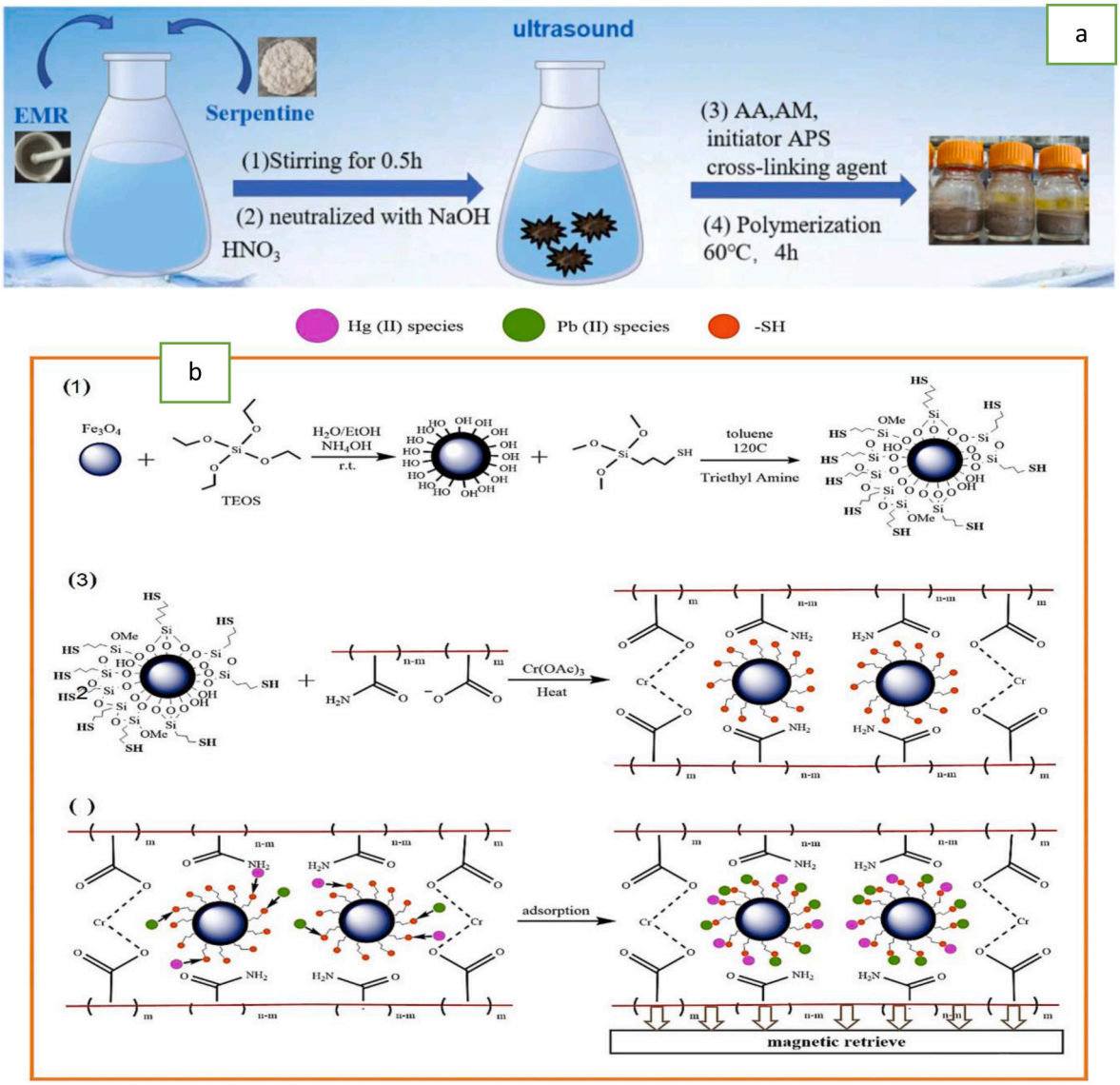

Fig. 4. Scheme of the fabrication of (a) S-PEMR hydrogel [136] (This figure has been adapted/reproduced from Ref. [136], Elsevier permission, copyright 2024), and **(b)** (**1**, **2**) PHPAm/Fe_3O_4@SiO_2-SH nanocomposites and (**3**) adsorption mechanism of Hg(II) and Pb(II) by PHPAm/Fe_3O_4@SiO_2-SH nanocomposites [137] (This figure has been adapted/reproduced from Ref. [137], Springer permission, copyright 2022).

acid (PVA/PAm/PAA) using γ-irradiation for the sorption of Eu(III) and Sm(III) ions from aqueous solutions. They noted that 1.0 g of the (PVA/PAm/PAA)/AC composite can absorb 35 g of water, 173.24 mg of Eu(III), and 160.41 mg of Sm(III). Moreover, the hydrogel composite exhibited excellent selectivity for Eu(III) and Sm(III) ions at pH 4 in the presence of cations such as Cd(II), Co(II), Sr(II), and Cs(I) [150]. Overall, PAm acts as a dispersion regulator and mechanical stabilizer in GO/PAm hydrogels systems. It forms a flexible and continuous polymeric framework that suppresses graphene oxide sheet aggregation and ensures their uniform dispersion within the hydrogels systems. The amide groups of PAm contribute additional interaction active sites such as coordination and H- bonding for metal ions. Moreover, PAm improves the dispersion and compatibility of GO within the hydrogels and enhances mechanical durability, adsorption performance, and reusability of the investigated hydrogels.

The data in Table 6 reveals a clear performance of PAm-based hydrogels through multiple synthesis routes, which introduce multifunctional active sites such as silicate, sulfonate, carboxylate, amide, amine, and hydroxyl, significantly enhancing adsorption performance. Overall, this data confirms that adsorption behavior is governed by the functionalization and hybridization strategies between polymer system and introduced functional entities, which are critical for optimizing PAm-based adsorbents.

3.2. Removal of dyes

Currently, the consequences of water pollution severely impact humanity, including contamination from plastics, heavy metals, and dyes. Among these, textile industry dye contamination is the primary pollutant with the worst effects [2,3]. Over 100,000 commercial dyes are in use globally, resulting in an estimated 700 million to 1.0 billion kilograms produced each year. It's estimated that 10 to 15% of these dyes are lost during production, entering effluents that may contaminate drinking water sources. These contaminants pose significant health risks, including pronounced physiological toxicity and significant disruption of reproductive systems. [3]. Furthermore, both flora and fauna are adversely impacted, as the presence of dyes disrupts water reoxygenation and reduces light penetration, critical factors for maintaining biological activity in natural ecosystems [3]. Accordingly, effluents from textile industries should undergo proper treatment to

Table 6
Overview of the PAm-based hydrogels and hybrid composites systems invstigated to remove heavy metal ions from aquatic media.

adsorbent	Composite type	Mass ratio	Functional group	Ref
Polyacrylamide hydrogels	Copolymer	–	Carboxylate, amide	98
Poly(AN-coAm)	Copolymer	2.0 g poly(AN-co-AM): 3.0 g hydroxylamine hydrochloride	Amidoxime, carboxyl, hydroxyl, and amide	99
MPAmG	Copolymer	7, 6 g Am: 3.2 g of MBAAm:1.0 ml AGE: 190 μl TEMED:152.6 mg APS	Carboxyl, hydroxyl, and amide	100
Anionic polyacrylamide	Copolymer	vinylsulfonic acid (0, 80, 100, 200, 500 and 600 μL; 25% w/v)	Sulfonate, carboxyl, hydroxyl, and amide	101
Polyacrylamide-based monolith	Copolymer	(0.3 g N-tert butylacrylamide/3.0 g methylated b-cyclodextrin) with 100 μL of 25% (w/v) VSA, 0.5 g PDA, 0.2 g MA, 0.2 g AS, 20 μL of 20% (w/v) APS, and 20 μL of 20% (v/v) TEMED in 0.1 M aqueous phosphate buffer	Sulfonate, carboxyl, hydroxyl, and amide	102
DMAPAm	Copolymerization	500 mM Am: 200 mM SS: 12.3 mM NMBA: 2.5 mM APS	Sulfonate, acrylate, carboxyl amine	103
Alg–PAm	Grafting	2.0 g SA: 2.0 g PAm	Carboxyl, hydroxyl, and amide	104
SA/CNF/PAm	Grafting	[a]	Carboxyl, hydroxyl, and amide	105
SA-PAm/GO	Free radical polymerization	[a]	Carboxyl, hydroxyl, and amide	106
SA-g-PAm/HL-$CoFe_2O_4$	Grafting	1:2 HL-$CoFe_2O_4$ ((2.5–20 wt%)	Hydroxyl and carboxyl,	107
SA/SH@PAm	Grafting	0.5 g SA: 0.15 g SH: 80 mL PAm	Carboxyl, hydroxyl, and amide	108
CMC/PAm	Free radical polymerization	3% CMC: 0.7g PAm	Carboxyl, amine and carbonyl	109
AM/CMC/AMPS	Free radical polymerization	1.0 g AM: 0.5 (2%) mL CMC: 0.24 g AMPS	Carboxyl, Sulfonate, amine, amide, and carbonyl	151
CTS/PAm gel	Free radical polymerization	0.5 CTS:1.0 PAm	Carboxyl, amine, and carbonyl	110
CTS/PAm/OP gel	Grafting	0.12 g CTS: 7.2 g AM: 0.072 g OP	Carboxyl, amine, amide, and carbonyl	111
AM/AO/AEBI-CTS	Free radical polymerization	3.0 g AM: 2.0 g AN: 0.2 g AEBI:1.0 g CTS	Amidoxime, amide, imidazoline ring, and hydroxyl	112
CTS-gP(CMC-co-Am)	Grafting	0.5 g CTS: 0.5 g CMC: 6.0 a.m.	Carboxyl, hydroxyl, amine, and carbonyl	113
Fe_3O_4 modified with PAm	Nanocomposite	0.05 g Fe_3O_4 : 0.5 g PAm	Hydroxyl, amine, and carbonyl	114
GG/PAm/RH/Ulva	Free radical polymerization	[a]	Hydroxyl, amine, silicate, and carbonyl	115
(CAA-Ca(II)-FeS) hydrogel	Grafting	[a]	Carboxyl, hydroxyl, amine and carbonyl	116
TOCNF-TMPTAP-APAm	Grafting	1.2 wt% TOCNF: 5.0 wt% APAm: 5 wt% TMPTAP	Carboxyl, carboxylate, hydroxyl, amine, amide	117
HPAmF	In situ polymerization	0.1 wt% CNF: 2.82 wt% SMA: 20 wt% AM	Carboxyl, carbonyl, hydroxyl, amide	118
PEI-PAmCF	Physical mixing	5.0 g PEI: 0.4g PAm: 10 mL CF	Carboxyl, hydroxyl, amide, amine	119
RIR/AA-co-AM hydrogel	Grafting	2.0 mL AA: 2.0 g AM: 0.2 g MBA	Carboxyl, hydroxyl, amide, and amine	120
PAm/RH	Free radical polymerization	10g:1.05M	Hydroxyl, amine and carbonyl	152
PAm@TP hydrogel	Grafting	1.0 g TP: 1.0 g PAm	Carboxyl, carbonyl, hydroxyl, amide, and amine	121
BSG-g-PAm	Grafting	10%BSG: 0.30 mol. PAm	Hydroxyl, amine and carbonyl	122
PAm-CG composite	In-situ polymerization	0.3 g BSA: 3 g AA: 1.0 g CG: 400 mg PER	Methylene, methyl, carboxylate, hydroxyl, amide	123
PAm/Na-MMT	Free radical polymerization	2.0 g PAm: 0.5 g Na-MMT, 1, 0.5: 2g	Alcohol, hydroxyl, amine, amide and silicate	124
zeolite-g-PAm	Nanocomposite	[a]	[a]	153
Z-g-PAm	Radiation-induced graft polymerization	2.0 g NZ:40 %w/w PAm	Silicate, amide, hydroxyle, and carbonyl	125
Ppolyacrylamide–polystyrene/bentonite	In situ polymerization	1.0 g bentonite,: 1.0 g PAm	Carbonyl polyacrylamide, silicate, amide, hydroxyle, amine	127
PAm-K	In situ polymerization	2.0 g Am:1.0 g kaolinite	Silicate, amide, hydroxyle, amine and carbonyl	128
HBP	US Patent No. 19,1992	85% HB5:15% PAM	Silicate, aluminate, amide, hydroxyle, amine, carboxylate, and carbonyl	129
PAm/HA-ATP	Free radical polymerization	1.4216 g Am: 0.1517 g ATP	Hydroxyl, amide, sulfonate, phenolic, carboxylate, and carbonyl	130
Ha-Am-PAm-Sep	Grafting	20 g Am:10 g Sep	Silicate, phosphate, amide, hydroxyle, amine, carboxylate, and carbonyl	131
PAm-PMC	Free radical polymerization	1.5 g Am: 0.45 g PMC	Silicate, amide, hydroxyle, carboxylate, and carbonyl	132
g-PAm/OVerm	Grafting	2.0 g OVerm: 0.6 g Am	Silanol, thiol, amide, hydroxyle, carboxylate, and carbonyl	133

(*continued on next page*)

Table 6 (*continued*)

adsorbent	Composite type	Mass ratio	Functional group	Ref
SP-C	Nanocomposite	0.5 g AS: 4 g Am	Silanol, amide, hydroxyle, and amine	134
PAGSPs	Nanocomposite	[a]	[a]	135
S-PEMR	Copolymer	2.0 g EMR: 1.12 g AM: 4.48 mL AA: 0.03 g MBAm	Silicate, aluminate, amide, carboxyl, hydroxyl, and amine	136
PHPAm/Fe_3O_4@SiO_2-SH	Nanocomposite	[a]	Thiol, mercapto, amide, hydroxyl, and amine	137
Fe_3O_4-PS-acrylic acid/acrylamide	Nanocomposite	(0.5, 1, and 2%) Fe_3O_4 : 0.50 g PS: 5 0 g AA: 5.0 g Am	Hydroxyl, amide, and carboxyl	138
PAm/FMWCNTs	Nanocomposite	[a]	Hydroxyl, amide, and carboxylate	139
Graphene/polyacrylamide	Nanocomposite	1.8 g Am: 5.0 mg TA: 4.0 mg GO	Carboxyl, hydroxyl, amine, ester, amide, carbonyl, eopoxy	141
PAO-GO/PAm hydrogels	Nanocomposite	(0.5–2.0 g L^{-1}): 500 mg	Amidoxime, carboxyl, epoxy, and hydroxyl	142
Nanocomposite based on chitosan–polyethylene oxide/poly(acrylamide-*co*-acrylic acid)	Nanocomposite	[a]	-$N^+(CH_3)_3$	143
MoS_2@CPAmA MoS_2	Nanocomposite	0.9073 g $Na_2MoO_4{\cdot}2H_2O$: 1.7127 g (CN_2H_4S): 0.5 g CPAmA	Quaternary ammonium, hydroxyl, amide, and carboxylate	144
Zn-MOF-74/rGO/PAm	Nanocomposite	125 mg Zn-MOF-74:125 mg rGO: 0.7 g Am	Amine, carbonyl, hydroxyl, and amide	145
PAm/PAA/PDMTM	Copolymer	0.50 g DMTM: 1.0 g AM: 0.50 mL AA: 6.0 mL DMTM: 50 mg APS: 50 mg MBA	Thiol, amide, carboxyl, carbonyl, hydroxyl, and amine	146
PAC@Fe_3O_4	Nanocomposite	7.5 g cell@Fe_3O_4: 0.05 g AIBN: 5.0 g Am	Carboxyl, amine, carbonyl, hydroxyl, and amide	147
Fe-PGSH	Copolymer	[a]	[a]	148
semi-IPN/PAm	Copolymer	[a]	Carboxyl, amine, carbonyl, hydroxyl, and amide	149
(PVA/PAm/PAA)/AC	Copolymer			150

[a] Not Detected.

eliminate toxic dyes before discharge into water bodies. The successful removal of dyes from aqueous media using hydrogels has attracted considerable interest due to their reusability, effective adsorption, recyclability, operational simplicity, eco-friendliness, and cost-effectiveness [155,156]. Many recent publications provide comprehensive studies of the progress made in investigating and developing neat and composite bio-based or synthetic polymeric hydrogels, such as polyacrylamide and polyacrylamide-based materials, as efficient candidates for removing diverse dye molecules from aqueous media [115,135,155[116,139,155,157–233. Table 7 presents applications of polyacrylamide-based hydrogel materials for the elimination of dyes from aqueous media [155, 257-233]. Recently, organically cross-linked PAm/hBN nanocomposite hydrogels were fabricated as effective adsorbents for methylene blue (MB), phenol red (PR), and methyl orange (MO) fromaqueous media [155]. In this respect, in the presence of hBN at 150 °C and for 8.0 h, organic cross-linkers (as N, N′-methylene bisacrylamide (MBS)) were reacted with PAm molecules [155].

Also, another promsing polyacrylamide basd hydrogel was investigated as superoleophobic membranes and synthesized by free radical co-polymerization via incorporating acrylic acid and β-cyclodextrin as monomer and crosslinking with MBS [156]. The fabricated underwater superoleophobic hydrogel membrane illustrated considerable adsorption performance for MB dye with effectively separated oil/water mixtures [156]. PAm hydrogel was also investigated to adsorb another cation dye, safranine (SF), from aqueous media [158]. Suggested mechanism of the adsorption of SF molecules onto the surface of PAm-hydrogel was demonstrated, as illustrated in Fig. 5a, [158]. In this suggested mechanism, the most impactful attraction forces between SF-species and the PAm-surface are attributed to electrostatic interactions. Also, this can be due to the electrostatic attractions between (+) charged available on PAm surfaces, such as amino groups (–NH_2) and (=O) groups, and (−) charged groups of SF species, in addition to n–n interactions and H- bonding [158].

A novel, efficient adsorbent, pentaazatetraethylene-sulfonated polyacrylamide (PAm-SO_3-N_5), was prepared to remove calmagite from aqueous media. The results showed that the largest equilibrium elimination of PAm-SO_3-N_5 for calmagite was 1732.5 mg g^{-1} eventually, after recycling the adsorbent for 7 runs, adsorption of the calmagite dye showed no significant loss [159]. Recently, bio-based hydrogel adsorbents have attracted significant attention due to their highly favorable properties, including high adsorption efficiency, well-interconnected porous structures, and large specific surface areas, all of which collectively enhance adsorption capacity and kinetics. Sodium alginate (SA) is among the most readily available biopolymers and is an excellent candidate for the fabrication of bio-based bioadsorbents [161]. SA is a naturally occurring polysaccharide polymer with non-toxicity, good biocompatibility, and degradability in addition to containing abundant functional groups, particularly hydroxyl (–OH) and carboxyl (–COOH) groups [162,166]. Structurally, it consists of linear copolymeric blocks of β-1,4-D-mannuronic acid (M units) and α-1,4-L-guluronic acid (G units), linked via 1–4 glycosidic bonds in different ratios [163]. Nevertheless, SA–based adsorbents remain suffering from limited adsorption capacity and prolonged adsorption times. These limitations necessitate the development of SA–based bioadsorbents with enhanced adsorption capacity and faster adsorption kinetics for practical applications. Therefore, many recent works have focused on modifying SA via physicochemical processes to incorporate additional functional groups, thereby enhancing its durability, mechanical stability, and adsorption capacity. Also, recent studies have investigated the fabrication of SA/PAm-based hydrogels using various approaches to remove different types of dyes [160–166]. Fig. 5b schematically illustrates the preparation of PAm/SA hydrogels via free-radical solution polymerization of acrylamide (AAm) in the presence of sodium alginate and the crosslinker $PEGDMA_{500}$ [161]. The adsorption capacity of the fabricated PAm/SA hydrogels with various SA contents was compared with that of the PAm hydrogel for MB adsorption. The results of swelling experiments showed that the fabricated PAm/SA hydrogels have a swelling range (12.72–25.52 $g_{water}\ g^{-1}_{dry\ gel}$) in water, which is higher than that of the PAm hydrogel (8.5 $g_{water}\ g^{-1}_{dry\ gel}$). Moreover, the highest saturation capacity of PAm/SA hydrogels towards MB was 90.90 mg/g, compared with 23.20 mg/g for PAm [161]. New biobased interconnect polymer network (IPN)-structured, extra-water-content (83%) crosslinked SA-PAm hydrogels were prepared to remove MB-dye from aqueous

Table 7
Applications of polyacrylamide and polyacrylate-based hydrogel materials to remove various types of organic dyes from aqueous media [155. 257-233].

adsorbent	pollutants	Qo (mg/g)	condition	adsorption-regeneration	reference
Neat-PAm	MB	11.1	t = 10 min, T = 25 °C		155
	PR	10.8			
	MO	10.2			
PAm/hBN Nanocomposite	MB	13.5	t = 10 min, T = 25 °C	5	155
Hydrogel	PR	13.1		D.L water and ethanol	
	MO	12.8			
PVA-g-PAm	MB	703	t = 20h, pH = 6,	5	157
	CV	863	T = 25 °C	23%	
	CR	174		30%	
				13%	
PAm	SF	640	t = 3h, pH = 5,	[a]	158
			T = 25 °C		
PAm-SO_3-N_5	calmagite	1732.5	t = 30 min, pH = 5.8,	7	159
			T = 25 °C	0.1 mol/L HCl	
SAG-g-PAm	MB	69.13	t = 8h, pH = 10,	[a]	160
			T = 25 °C		
PAm/SA	MB	90.90	t = 28h, pH = 7,	[a]	161
		23.20	T = 25 °C		
SA-PAm	MB	43.1	[a]	4	162
SA-PAm-CNC		44.1		distilled water	
SA-PAm-BC		47.1		55%	
SA-PAm-TOCN		57.1			
PAm/SA/Fe_3O_4@ZIF-8-8	CR	234.69	t = 600 min, pH = 6,	5	163
			T = 40 °C	ethanol	
				80%	
SA-g-P(AA-co-AmPS)/KL	MV	1361.1	t = 24h, pH = 7,	[a]	164
	R6G	1627.8	T = 25 °C		
	AK	563.5			
	XO	312.4			
hydrogel	CV	98.51 %	t = 80min, pH = 8,	8	165
hydrogel/Hap		98.46 %	T = 25 °C	1M HCl	
hydrogel/HAp/Cu-Fe LDH		98.72 %		94%	
CPAm-Dia/SA-La	AB 113	2907	t = 60min, pH = 2,	3	166
	CR	1578	T = 25 °C	EDTA and La(III) solutions	
				99.7%, 88.5%, and 66.5%	
Pcn-g-P(Am-*co*-SA) hydrogel	MG	5000	t = 6 min, pH = 7,	11	167
			T = 20 °C		
CMC-g-poly(AAm)	MV	76.09%	t = 60 min, pH = 9,	[a]	168
CMC-g-P(AAm)/CL	MB	83.11%	T = 25 °C		
CMC-g-P(AAm)/CL-Fe_3O_4	MV	85.91%			
	MB	92.89%			
	MV	90.11%			
	MB	95.01%			
HG	MB	12.3	t = 70min, pH = 8,	[a]	169
HG/BC		14.2	T = 25 °C		
HG/MTWBC		20.79			
Hyd	MB	85.74%	t = 50min, pH = 10,	6	170
Hyd/WS		91.74%	T = 25 °C	0.1 M HNO_3	
Hyd/WS/$CoFe_2O_4$		95.83%			
Hyd/WS/$CoFe_2O_4$/ZIF-67		97.72%			
PAm/CMC/MHNT hydrogel	MB	50.5	t = 120 min, pH = 11,	5	171
			T = 25 °C	0.1 M HCl	
				81.58%	
AM-AC/CMC-Ca	ST	1558.52	t = 60min, pH = 7.6,	6	172
			T = 25 °C	H_2O, NaOH, and HCl 0.1 M	
				88%	
PAm/CMC-CuS	RhB	19.86	[a]	5	173
	NR	208.33		Ethanol	
κC-g-PAm/bentonite	MB	156.25	t = 60min, pH = 11.6,	5	174
			T = 25 °C	Acetone	
				94%	
κC-g-P (AAc-co-AAm)/Kaolin	MG	118.42	t = 180min, pH = 6,	5	175
			T = 25 °C	0.1M HCl (67.27%)	
				0.1M NaOH (27.8%)	
APAm/DTPA-CTS/GO	MB	652.99	t = 100min, pH = 7,	6	176
			T = 30 °C	91%	
g-CCTS	MB	79.09	pH = 12, T = 20 °C	5	177
				76.64%	
(CTS/AM-CA) composite hydrogel.	MO	1080	[a]	5	177
	MG	1030			
VSi-CTS-g-PAm	MB	68.02	t = 24h, pH = 12,	[a]	178
			T = 50 °C		
PAm/chitosan hydrogel	MO	62.5	t = 10min, pH = 3,	[a]	179
			T = 25 °C		

(*continued on next page*)

Table 7 (*continued*)

adsorbent	pollutants	Qo (mg/g)	condition	adsorption-regeneration	reference
PAm/CTS	XO	177.5	t = 48h, pH = 2,	5	180
PAm		20.52	T = 35 °C	83.29%	
CTS/PLA	MO	769.23	t = 30 min, pH = 7,	7	181
CTS/PAm		303.03	T = 45 °C	1M NaOH	
				15/10%	
TiO_2-PAmCTS	Sirius yellow K-CF	1000	t = 90 min, pH = 2,	6	182
			T = 40 °C	HCl (0.1 M)	
				4.86%	
CH-PAm-ZnO	Sirius yellow K-CF	149.9	t = 90 min, pH = 2,	[a]	183
			T = 40 °C		
Jh-g-(PAm-co-PVAc)	CV	70.5	pH = 9.2, T = 30 °C	5	184
				25%	
CNF-PAm5%	MB	172.08	t = 60 min, pH = 7	4	185
				85%	
PAm/CNCs microspheres	MB	490.12	t = 120 min, pH = 7	5	186
				0.1M HCl	
				90%	
PAm/CG/FE	MB	48.30	t = 80 min, pH = 8	4	187
PAm		56.17		0.05 M of HCl	
				9%	
				30%	
PAm/BC/KIF	MB	60	t = 24h, pH = 10	3	188
hemi-g-PAm	MB	2300	t = 40 min, pH > 4,	[a]	189
			T = 25 °C		
CMC–CPAm–TA	Cu(II)	669.8	t = 60 min, pH = 6	5	190
	RhB	202.2	t = 90 min, pH = 5	D H_2O	
				79% Cu(II) 63% RhB	
SG@AA-co-AM	VGB	159.9	t = 30 min, pH = 8,	5	191
			T = 25 °C	0.1 M HCl	
				3.9%	
St-g-poly(AAM)	MG	5.9	t = 60 min, T = 25 °C	5	192
St-g-poly(AA)		47.2		1 M HNO_3	
St-g-AA(L)-AAM		59.5		84.54%	
St-g-AA(H)-AAM		52.6			
St-co (PAm/PAA)	MB	1700	t = 120 min, pH = 7,	4	193
			T = 25 °C	0.1 mol/L HCl	
				77%	
St-30/ZnO hydrogel composite	MB	993	t = 4h, pH = 6,	8	194
	CV	>90%	T = 25 °C	0.5 M NaOH solution	
	CR	<72%		83%	
	RO	12%			
PUL/PAm/AC	MB	591.4	t = 120min, pH = 8,	[a]	195
			T = 25 °C		
PUL/PAm/GO	MB	438.7	t = 140min, pH = 8,	5	196
			T = 25 °C	5%HCl	
				62.4%	
GG-g-poly (AC-co-PAm)	MV	998	t = 1h, pH = 7,	4	197
			T = 25 °C	HCl	
				77.75	
XG/AA/AAm/GO	MB	1008	t = 1h, pH = 7,	5	198
XG/AA/AAm		730.7	T = 25 °C	1.1 M HCl	
				86%	
GA-cl-poly(Am)	CV	90.90	t = 90min, pH = 9,	6	199
			T = 35 °C	67%	
GK-PAm	R6G	1244.71	[a]	[a]	200
PAm,	Basic fusion	33.22	t = 150min, pH = 11,	5	201
(GG-co-PAm)-10%,		30.21	T = 35 °C	Acetone	
(GG-co-PAm)-20%		18.11		85%	
V_2O_5-Gum Ghatti-Cl-Poly (AM-co-MAA	MB	35.21	t = 100min, pH = 9,	[a]	202
			T = 25 °C		
XG-g-PAm hydrogel	AR8	177	t = 20 min, pH = 1,	5	203
			T = 20 °C	1 M HCl	
				71.3 %	
Fe_3O_4@SF-PAm	MB	2025	[a]	5	204
				90%	
PAm-g-gelatin	CV	35.45	t = 60min, pH = 9,	10	205
PAm-g-gelatin/AC		39.865	T = 25 °C	acetone/ethanol	
PAm-g-gelatin/ACL/Mg-Fe LDH		44.952		90%	
PAm/PA/PDA	MB	350.67	t = 60min, pH = 4.5,	7	206
	MYB	*350.67*	T = 45 °C	pH 2.0 for cationic dye (NR, MV, and YMB) and	
	MV	*625.97*	t = 60min, pH = 10,	pH 11.0 for anionic dye	
	NR	*584.58*	T = 45 °C	(MB)	
			t = 60min, pH = 10,		
			T = 45 °C		
			t = 60min, pH = 5.5,		
			T = 45 °C		

(*continued on next page*)

Table 7 (*continued*)

adsorbent	pollutants	Qo (mg/g)	condition	adsorption-regeneration	reference
(GA/AAm)-ES/GO	AR	313.3	t = 480min, pH = 9	4 58.78%	207
Alg-g-poly(AAm)/CB nanocomposite hydrogel	MB	24.56	t = 60 min, pH = 6.0, T = 25 °C	[a]	208
PVA/PHPAm/GO semi-IPN nanocomposite hydrogel	MB	714.8	[a] t = 180 min, pH = 7, T = 30 °C	5 0.1M HCl	209
PVA/PHPA	MB	293	t = 180 min, pH = 7, T = 30 °C	5 0.1M HCl	209
Pn-g-PAm	MG	120.772	t = 30min, pH = 7, T = 25 °C	[a]	210
CPAmPEI/GO	MO	677.55	t = 1110 min, pH = 3, T = 30 °C	6 0.1 mol/L NaOH 19.45%	211
P(NIPAm-coAAc)/MoS_2	MB	1258	t = 6h, T = 40 °C	[a]	212
PAm/PAA/CHN hydrogel	MB	1056	t = 3 days, pH = 7, T = 25 °C	5 HCl & DH_2O 96%	213
(PAA-coPAm)-DPNR/Ag-TiO2	MB	206.42	t = 24h, pH = 7, T = 25 °C	5 0.5 M NaOH 90%	214
CMC-g-P(AAm)/MMT	MG	158.1 172.4	t = 24h, pH = 7.6, T = 25 °C	5	215
poly(GG-co-AAm-co-MAA) hydrogel	MV FB	233 200	t = 60 min, pH = 7.0, T = 30 °C	5 aceton 80% MV 86% FB	216
AAc-coAM)/AC	BB	114.4	t = 30 min, pH = 7, T = 40 °C	[a]	217
PAm PAA	RO-20	216.919 50.582	t = 95/65 min, pH = 3/2	[a]	218
PAm PAA	DR-31	155.279 143.884	t = 90/60 min, pH = 3/1.5	[a]	218
AA/AMA	Direct Brown 2	100%	t = 45 min, pH = 3	[a]	219
PAm-Agar/Clay@r-GO nanocomposite hydrogel	MB RhB MO	189 186 110.3	t = 5 h, pH = 10, T = 40 °C t = 5 h, pH = 10, T = 40 °C t = 12 h, pH = 10, T = 40 °C	4 2(M) HCl, 1 M NaOH 85%	220
zeolite hydrogel composite (ZHC) based on j-carrageenan (KC) and AQSOA-Z05	MB	682.67	pH = 7, T = 45 °C	6 100%	221
Fe_3O_4/PAm/LMSH Nanocomposite Hydrogel	CV MO	5.05 mg/g 0.72 mg/g	t = 10 h, pH = 7, T = 25 °C t = 2.5hr, pH = 7, T = 25 °C	[a]	222
PAm-talc talc	MB	0.0104 mol kg^{-1} 0.0124 mol kg^{-1}	pH = 5.2, T = 25 °C	[a]	223
poly(MAA-co-AAm)/Cl30B poly(MAA-co- AAm)	MB	98.57% 97.65%	t = 80 min, pH = 8, T = 25 °C	[a]	224
HPAm/SiO_2@XG	CV	342.19	t = 180 min, pH = 7, T = 30 °C	5 0.1 M HCl 71.5 %	225
PAm/MXene	MB	282.29	t = 360 min	[a]	226
PAm@TiO_2	CV	38.9	t = 24h, pH = 6.9, T = 25 °C	[a]	227
Ce/Ti-NRs/CMC/PAm	CR	22.44	t = 90, pH = 2.0, T = 25 °C	[a]	228
GO/PAm	Drimarene Brilliant Blue K-4BL	1000	t = 24h, pH = 8	5 4% HCl in 50/50 water/ethanol (v/v) 40%	229
Hyd/CB	MB	27.32	t = 60, pH = 7, T = 25 °C	4 1 M HNO_3 71.65%	230
Polyacrylamide and graphene oxide nanocomposite	MG	274	t = 24h	[a]	231
ZMC	OG	142.76	t = 60 min, pH = 2, T = 25 °C	20 0.01M NaOH 79.25%	232
PAm/B/CN	TC		t = 240 min, pH = 2, T = 25 °C	[a]	233

[a] Not detected.

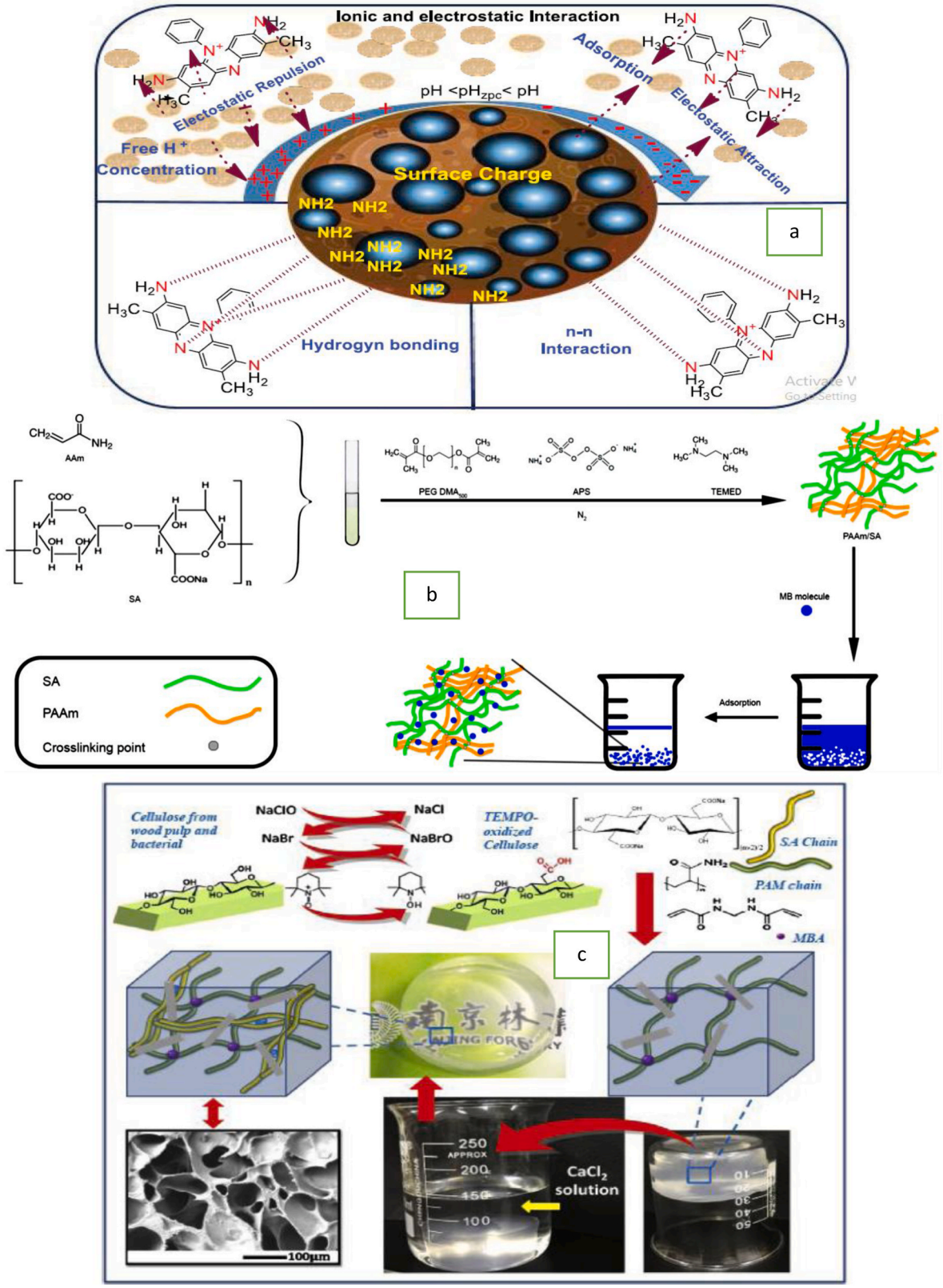

Fig. 5. Scheme of the (a) possible interactions mechanism of SF adsorption on PAm [158] (This figure has been adapted/reproduced from Ref. [158], Elsevier permission, copyright 2021), **(b)** Fabrication of PAm/SA hydrogels and mechanism of sorption of MB species onto PAm/SA hydrogel [161], (This figure has been adapted/reproduced from Ref. [161], Springer permission, copyright 2021), (c) fabrication process of crosslinked SA-PAm hydrogels [162], (This figure has been adapted/reproduced from Ref. [162], Elsevier permission, copyright 2018), and (d) fabrication magnetic PAm/SA/Fe_3O_4@ZIF-8 hydrogel beads [163](This figure has been adapted/reproduced from Ref. [11], Springer permission, copyright 2024.

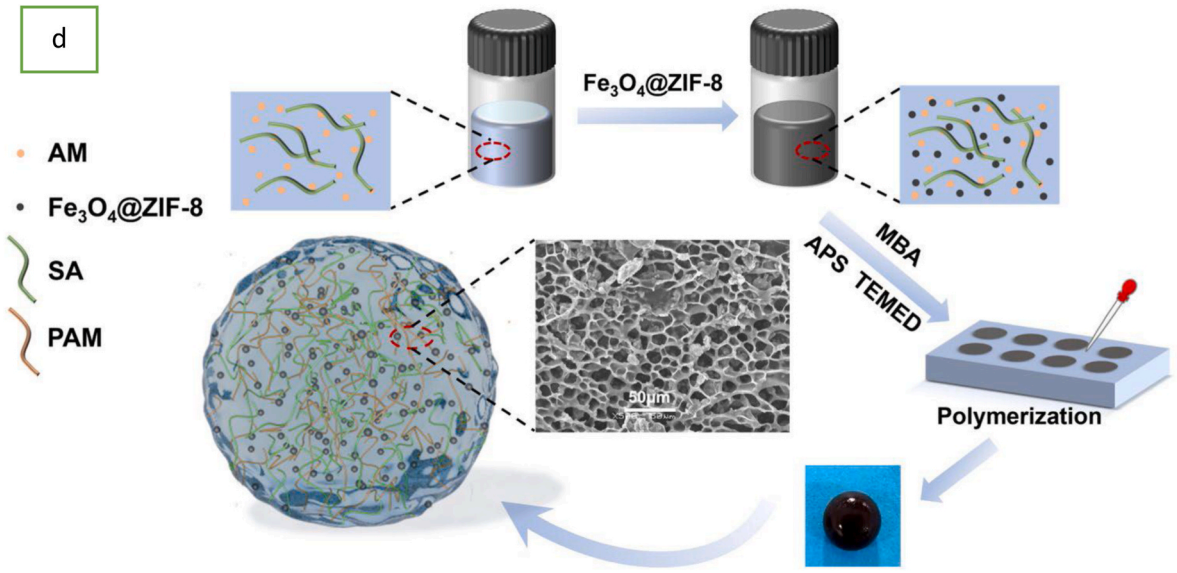

Fig. 5. (*continued*).

media [162]. As shown in Fig. 5c, the fabricated hydrogels were prepared via crosslinked polyacrylamide (PAm) with polyelectrolyte sodium alginate (SA) and then dispersed cellulose nanocrystals (CNCs), bacterial cellulose fibers (BCs), and 2,2,6,6-tetramethylpiperidine-1-oxy radical (TEMPO)-oxidized cellulose nanofibers (TOCNs) in the SA-PAm gel matrix [162]. The addition of BC enhances the compressive strength of the SA-PAm-BC hydrogel by 6.59-fold more than pure SA-PAm. While TOCNs will improve the adsorption capacity due to the existence of a carboxyl group, the adsorption capacity of SA-PAM-TOCN (57.1 mg g^{-1}) is more than 1.3-fold that of SA-PAm (43.1 mg g^{-1}). Moreover, the adsorption percentage decreases with each regeneration cycle and remains at 55% of its initial capacity after 3 cycles [162]. Recently, magnetic (PAm/SA/Fe_3O_4@ZIF-8) hydrogel beads with a semi-interpenetrating polymer network (SIPN) structure were investigated to combine the properties of both PAm/SA hydrogel and Fe_3O_4@ZIF-8 for the elimination of CR-dye species, as shown in Fig. 5d [163]. The addition of Fe_3O_4@ZIF-8 improves the adsorption behavior of PAm/SA of CR-dye to reach its maximum capacity of 234.69 mg g^{-1}. This is attributed to the involvement of multiple adsorption mechanisms: metal coordination, electrostatic attraction, H-bonding, and π-π stacking. Additionally, PAm/SA/Fe_3O_4@ZIF-8 showed high selectivity for CR-species adsorption and cyclic regeneration, with CR-dye uptake exceeding 80% of the initial removal efficiency [163]. During the last decade, various works were investigated to fabricate grafted polyacrylamide by sodium alginate to remove various types of dyes species from aqueous solutions, such as SA graft poly(acrylic acid-co-2-acrylamide-2-methyl-1-propanesulfonic acid)/kaolin (SA-g-P (AA-co-AMPS)/KL) hydrogel to remove methyl violet (MV), rhodamine 6G (R6G), acid chrome blue K (AK) and xylenol orange (XO) [164], hydrogel/HAp/Cu-Fe LDHto adsorb crystal violet (CV)-dye [165], green macroparticle composite (CPAm-Dia/SA-La) to eliminate AB 113 and CR-dye [166], and Pcn-g-P(Am-*co*-SA) hydrogel to adsorb malachite green (MG) species from aqueous Media [167].

For the studied SA/PAm hydrogels systems, PAm forms a reinforcing 3D network that improves the mechanical stability of the alginate systems and introduces amide functionalities (–$CONH_2$) groups that enhance the adsorption of dyes through H-bonding and electrostatic interactions. Moreover, PAm can improve polymer–polymer compatibility and limiting phase segregation, in addition to regulating swelling behavior and adsorption capacity of the investigated dyes.

Another of the most recent attractive approaches to the characterization of polyacrylamide hydrogel is the use of carboxymethyl cellulose (CMC) [168–173]. CMC is a functional cellulose derivative with excellent biodegradability, cost-effectiveness, and biocompatibility, making it attractive for diverse applications, including wastewater treatment. Owing to the presence of abundant (COO^-) and (OH^-) groups along its polymeric structure, CMC can effectively interact with pollutants through electrostatic forces, hydrogen bonding, and π–π interactions. To enhance the adsorption performance and mechanical strength of CMC-based hydrogels, a range of synthetic monomers, including acrylic acid, acrylamide, *N*-isopropylacrylamide, and itaconic acid, as well as their corresponding copolymers, may be grafted onto the biopolymer backbone via appropriate polymerization strategies [168]. In this regard, a free radical polymerization process was used to fabricate a novel sorbent CMC-g-P(AAm)/CL and CMC-g-poly(AAm)/CL-Fe_3O_4 as a novel magnetic biochar nanocomposite hydrogel sorbent to remove MB-dye and MV-dye species in a single and simultaneous state from aqueous media [168]. The proposed mechanisms of adsorption of MB-species and MV-species onto the fabricated nanocomposite hydrogel sorbents are depicted in Fig. 6a [168]. Another novel CMC-grafted poly(acrylamide)/magnetic biochar HG/MTWBC nanocomposite hydrogel was fabricated to eliminate MB species from aqueous solutions [169]. Also, the free radical polymerization method was applied to prepare a poly (AAm)-grafted CMC hydrogel (Hyd/WS/$CoFe_2O_4$/ZIF-67) adsorbent for the removal of MB from aqueous media, and the possible mechanisms of the investigated adsorption processes are shown in Fig. 6b [170]. A free-radical polymerization approach was used to fabricate a novel PAm/CMC/MHNT hydrogel [171]. The prepared polyacrylamide/sodium carboxymethyl cellulose/magnetic halloysite nanotube hydrogel is a cost-effective adsorbent for removing MB dye from wastewater [172].

Prepared bio-adsorbent by mixing of acrylamide (AM) reaction with a polysaccharide carboxymethyl cellulose (CMC)-modified activated carbon (AC) and final Ca(II) cross-linking polymerization to form macroparticle (AM-AC/CMC-Ca) hydrogel biocomposite was investigated to remove of Safranin T (ST) cationic dye with high swelling efficiency 3500% in distilled water and maximum adsorption capacity 1558.52 mg g^{-1} for ST dye [172]. Also, fabrication of floatable polyacrylamide/carboxymethyl cellulose-copper sulfide (PAm/CMC-CuS) hydrogels was investigated for selective capture of cationic dyes, Rhodamine B (RhB) and Neutral red (NR), from mixed solutions containing anionic dyes [173]. In addition, PAm/CMC-CuS hydrogel exhibits a higher removal rate and greater capture capacity than PAm/CMC hydrogel. Moreover, the PAm/CMC-CuS hydrogel

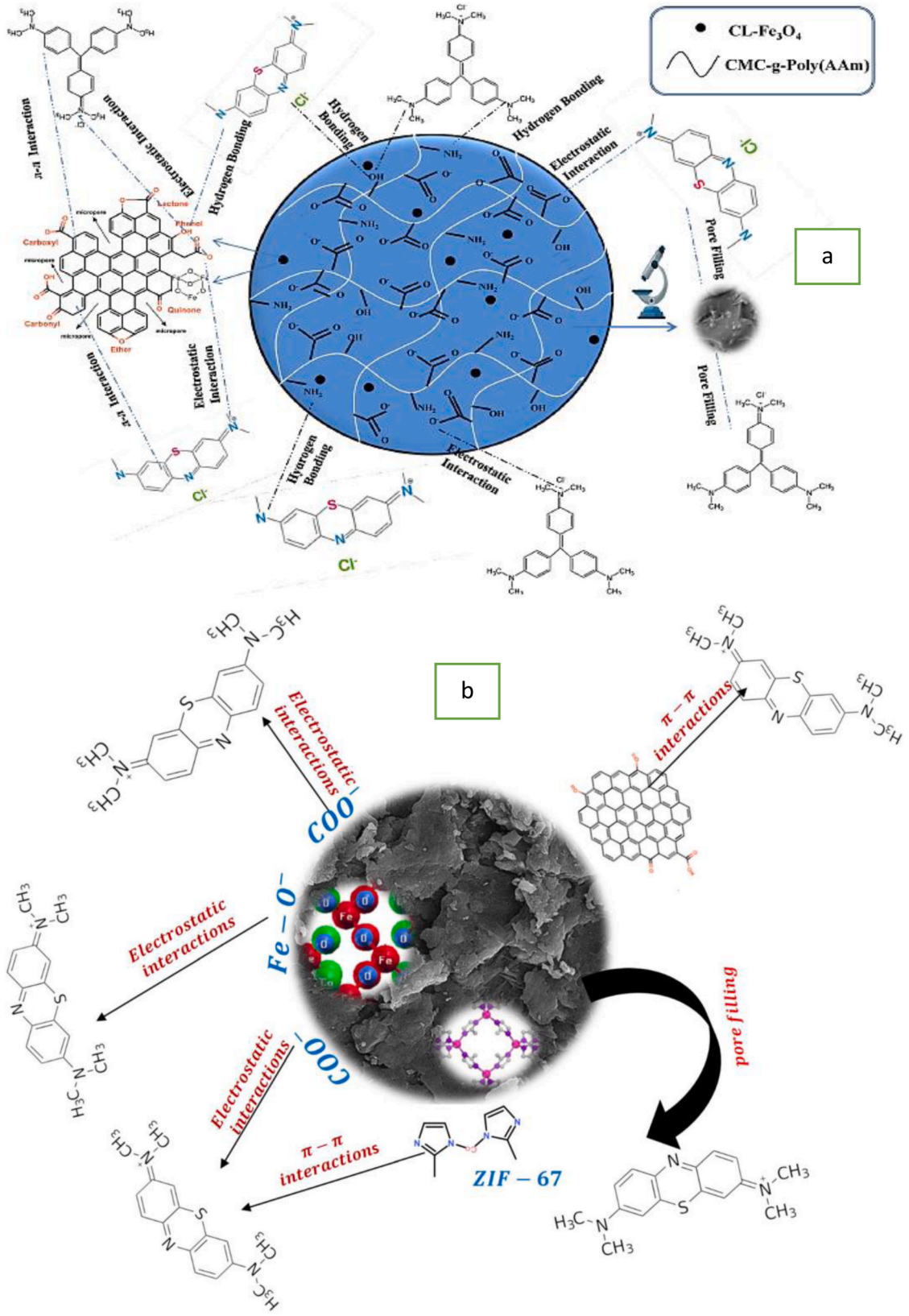

Fig. 6. Scheme of the (a) possible mechanisms of adsorption of MB-species and MV-species onto CMC-g-P(AAm)/CL-Fe_3O_4 nanocomposite hydrogels [168] (This figure has been adapted/reproduced from Ref. [168], Elsevier permission, copyright 2025), **(b)** possible mechanisms of adsorption of MB-species by Hyd/WS/Co-Fe_2O_4/ZIF-67 [170] (This figure has been adapted/reproduced from Ref. [170], Royal Society of Chemistry permission, copyright 2025), (c) fabrication route of APAm/DTPA-CTS/GO composite aerogel [176] (This figure has been adapted/reproduced from Ref. [176], Elsevier permission, copyright 2023), and (d) fabrication of CMC–CPAm–TA and sorption mechanisms for Cu(II) ions and rhodamine B [190](This figure has been adapted/reproduced from ref: 190, Springer permission, copyright 2024.

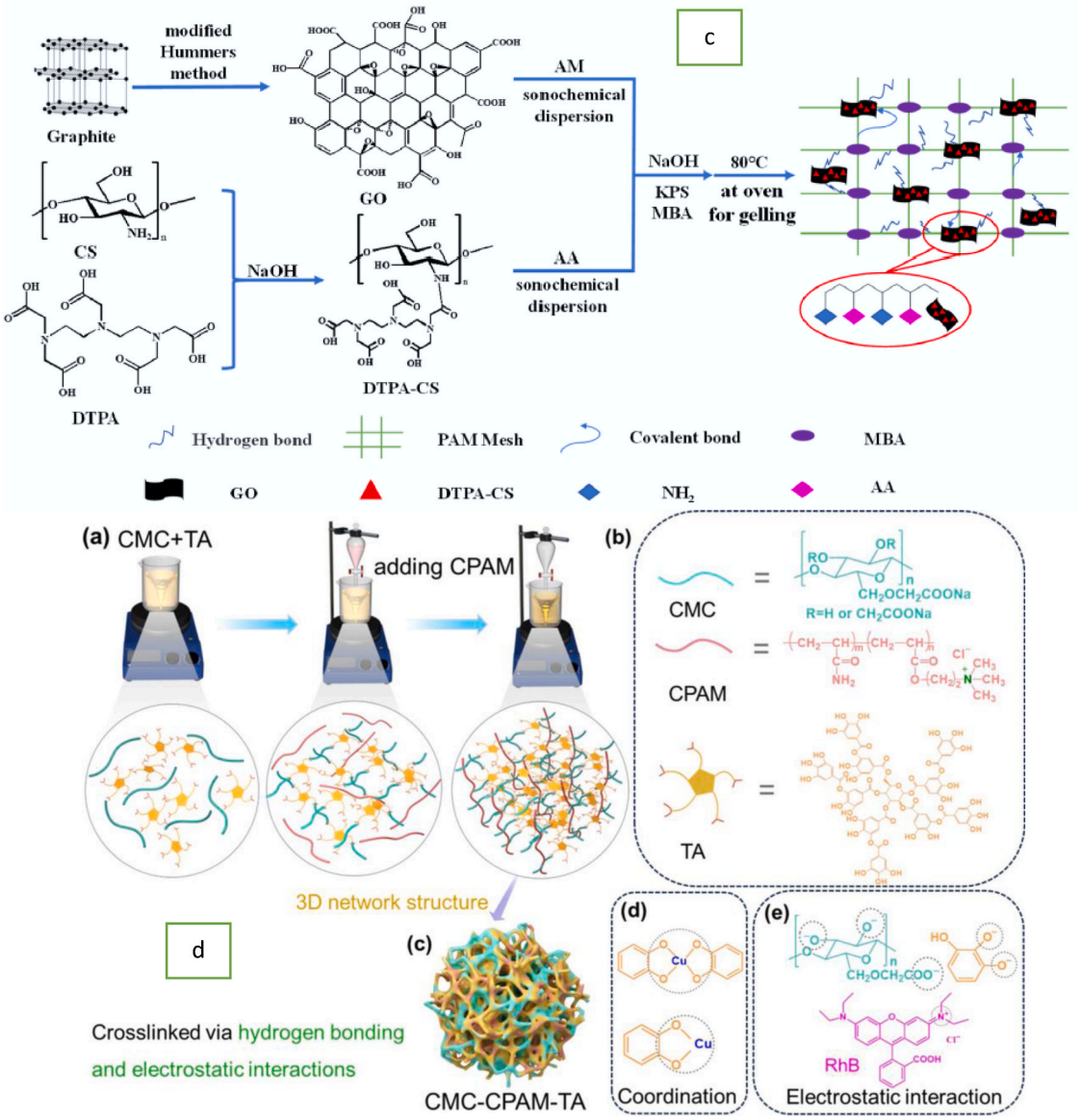

Fig. 6. (*continued*).

demonstrated suitable reusability and stability over 5 cycles [173].

Overall, PAm reinforces the prepared hydrogels in studied CMC/PAm systems by forming stable 3D frameworks. The presence of amide (–$CONH_2$) functional groups of PAm and CMC's carboxyl groups enhancing synergistic adsorption interactions with different dye species. Additionally, PAm improves interfacial compatibility and dispersion and contributes to controlled swelling kinetics and adsorption rates [168–173].

On the other hand, kappa-carrageenan (κC) is one of the most important natural components that can be used to graft polyacrylamide hydrogel onto fabrics to fabricate superabsorbent materials for removing dye species from aquatic media [174,175]. Kappa-carrageenan is a naturally derived, biodegradable and renewable polysaccharide extracted from red seaweeds and is extensively utilized as a gelling agent and viscosity modifier. Its wide range of industrial applications is primarily attributed to its remarkable gel-forming capability. Structurally, κ-carrageenan is composed of linear chains of alternating D-galactose and 3,6-anhydro-D-galactose residues, featuring variable sulfate group substitution. These sulfate groups endow the polymer with a pronounced anionic nature, which plays a key role in its physicochemical behavior [175]. Recently, a free-radical polymerization approach was applied to prepare a series of superabsorbent composite hydrogels, porous κC-g-PAm/bentonite, for adsorbing MB species [174], and porous κC-g-P(AAc-co-AAm)/kaolin for removing malachite green (MG) [175].

Chitosan (CTS) is a widely abundant natural amino-polysaccharide that is inexpensive, alkaline in nature, and characterized by high biocompatibility, non-toxicity, and hydrophilicity. In addition, its polymeric backbone is rich in amino (-NH_2) and hydroxyl (-OH) functional groups, which enhance its strong interaction ability with metal ions and dyes through H-bonding and chelation mechanisms. As a result, CTS is widely considered an eco-friendly and cost-effective functional material, and its abundant reactive sites enable it to be engineered into a variety of functional derivatives, making it highly effective for treating diverse industrial wastewater effluents [176–185]. Nevertheless, similar to many naturally derived polymers, CTS suffers from poor chemical stability, limited mechanical strength, and unsatisfactory adsorption capacity. Therefore, improving its properties through cross-linking is necessary to overcome these intrinsic limitations. Recently, a facile method was used to fabricate an efficient and recyclable adsorbent, the APAm/DTPA-CTS/GO composite aerogel, for the removal of MB-dye, as shown in Fig. 6c [176]. The prepared aerogel exhibited a high

adsorption capacity for MB (652.99 mg g^{-1} at 303 K), owing to multiple interaction mechanisms (electrostatic, H-bonding, and π-π conjugation). Moreover, the aerogel maintained a high adsorption capacity (600 mg g^{-1}) even after 6 runs [176]. A magnetite chitosan/poly (acrylamide-co-crotonic acid) hydrogel was also recently synthesized via a one-pot free-radical polymerization process as a promising adsorbent for the eco-friendly removal of MO-dye and MG-dye species from wastewater [177]. During the last years, novel polyacrylamide-modify-chitosan adsorbent materials, such as VSi-CTS-PAm [178], PAm/chitosan hydrogel [179], PAm/CTS [180], Pcn-g-P(Am-co-SA) [181], TiO_2-PAm-CTS [182], CH-PAm-ZnO [183], and Jh-g-(PAm-co-PVAc) [184] hydrogel, to remove MB-species [178], MO- dye [179], XO-dye [180], MO-dye [181], K-CF dye [182,183], and CV-dye [184], respectively, from aqueous media.

Among naturally occurring biopolymers, cellulose is the most abundant renewable polymer, widely distributed across living organisms and distinguished by its high content of (-OH) groups. Its renewable origin, biodegradability, non-toxic nature, low cost, and outstanding biocompatibility make cellulose an attractive platform for adsorbent fabrication. Consequently, it has attracted considerable interest in chemical modification, primarily due to the abundance of reactive hydroxyl groups along its molecular backbone. These structural features enable the grafting of diverse functional groups, including amino, amide, carboxyl, and carbonyl sulfide groups, onto the cellulose surface via different modification approaches [185–190]. Therefore, recent work has reported significant progress in the fabrication and characterization of polyacrylamide-based cellulosic materials as green, efficient, multifunctional wastewater treatment agents, especially for various types of dyes [185–190]. Synthesis of nanocellulose (CNF) and polyacrylamide (PAm) gel network was investigated through a one-step synthesis and followed by modification with NaOH to eliminate MB-dye from aqueous media [185]. The fabricated CNF-PAm5% exhibits favorable adsorption behavior toward MB-dye species, with increasing NaOH concentration, reaching 172.08 mg g^{-1}, and maintaining 85% adsorption efficiency after 4 reuse cycles [185]. A reversed-phase suspension strategy was applied to prepare cellulose composite microspheres through the addition of cellulose nanocrystals (CNCs) into polyacrylamide (PAm), followed by partial hydrolysis to fabricate CNC-APAm composite microspheres [186]. The adsorption experiments showed that the prepared CNC-APAm composite microspheres exhibit excellent adsorption performance toward MB dye, which follows the quasi-secondary kinetic model and the Langmuir adsorption model [186]. Another eco-friendly, reusable, biodegradable, cost-effective, and nontoxic adsorbent, polyacrylamide/cellulose hydrogel incorporated with fuller's earth (PAm/CG/FE), was investigated using a free-radical polymerization approach for the removal of MB-dye. The addition of cellulose and fuller's earth to polyacrylamide clearly improved structural stability, thermal stability, and adsorption performance for MB species [187]. The development of a bio-composite hydrogel based on a mixture of polyacrylamide (PAm), bacterial cellulose (BC), and keratin intermediate filaments (KIF) derived from human hair was studied and used for the adsorption of MB-dye from aqueous solutions [188]. The addition of 2% KIF hydrogel will achieve an optimized compressive strength of 0.4 MPa. Batch adsorption experiments presented an adsorption capacity of 60 mg g^{-1} for methylene blue over 12 h. Adsorption was fitted to the pseudo-second-order and the Freundlich isotherm models, suggesting a heterogeneous mechanism driven by electrostatic interactions and π–π stacking [188]. The fabricated hydrogel offers an eco-friendly solution for the continuous removal of dye species and wastewater treatment. Also, recent hemicellulose-graft-polyacrylamide (hemi-g-PAm) hydrogel [189] and a novel carboxymethyl cellulose/cationic polyacrylamide/tannic acid (CMC–CPAm–TA) [190] were synthesized and used as effective adsorbents to remove MB-containing wastewater [189], Cu(II) ions, and rhodamine B (RhB) [190] from aqueous media. Fig. 6d illustrates the fabrication process of CMC–CPAm–TA and sorption mechanisms for Cu (II) ions and RhB-dye onto the prepared adsorbent [190]. As reported in the literature, PAm acts as hydrophilicity enhancer and network regulator in CNF/PAm hydrogels and forms interpenetrating networks with CNF matrixes. Its amide (–$CONH_2$) groups interact synergistically with the carboxyl groups of CNF to enhance the adsorption of dyes through H-bonding and dipole–dipole interactions, and significantly improves swelling performance, pore accessibility, and diffusion kinetics [185–190].

Starch is another promising naturally occurring, biodegradable polysaccharide composed of linear amylose and branched amylopectin, sourced from a wide range of plants. Its abundance, low cost, and hydroxyl-rich molecular framework make starch a highly attractive precursor for the fabrication of renewable, biodegradable hydrogels. In addition, its non-toxicity, environmental compatibility, renewability, and ease of availability further support its use in sustainable material design. Despite these advantages, the direct use of starch as an adsorbent is constrained by inherent limitations, including poor mechanical strength, limited chemical stability, and challenges with separation and reuse. Copolymerization of starch with petroleum-based polymers has been proposed as an effective strategy to achieve both environmental and economic benefits; however, further performance enhancement is often required. Consequently, a variety of modification techniques have been investigated, among which chemical modification is the most prevalent, owing to its ability to improve starch solubility, swelling capacity, and adsorption efficiency. In recent years, copolymerization strategies that integrate natural starch with hydrophilic synthetic polymers have emerged as a promising solution to these limitations. This approach enables the formation of copolymers with tailored and improved properties by synergistically combining the strengths of both polymer types. While hydrophilic synthetic polymers impart enhanced water absorption, mechanical robustness, and structural stability, starch contributes biodegradability and environmental sustainability, resulting in materials well-suited for advanced adsorption applications [191–194]. So, free radical polymerization approaches were used to fabricate a novel sorbent material, starch grafted polyacrylic acid copolymer polyacrylamide (SG@AA-co-AM), for adsorbing Victoria green B (VGB) dye from wastewater [191]. The fabrication and adsorption mechanisms are as follows: starch-based free radicals undergo free-radical copolymerization with acrylic acid (AA) and acrylamide (AM), yielding the graft copolymer sorbent SG@AA-co-AM. In this process, AA and AM are grafted onto the starch backbone via the hydroxyl groups at C-2, C-3, and C-6. The incorporation of these functional groups increases the availability of active sorption sites within the SG@AA-co-AM structure, thereby enhancing its effectiveness to remove VGB-dye from aqueous media [191]. Also, new renewable and eco-friendly polysaccharide hydrogels, St-g-AA(L)-AAM and St-g-AA (H)-AAM, were fabricated via aqueous solution polymerization by grafting polyacrylic acid and acrylamide to remove Malachite Green (MG) dye [192]. The negative functional groups, such as –COOH, –COO^-, and –$CONH_2$, on the surface of the prepared hydrogels play a vital role in improving separation efficiency through electrostatic interactions with the positively charged MG–species [192]. Another recent novel adsorbent material was fabricated, such as St-co (PAm/PAA) [193] and St-S30/ZnO hydrogel composite [194] for the efficient removal of (MB) [194], MB-dye, CV-dye, reactive orange (RO), and congo red (CR) [194], respectively, from aqueous solutions.

Similarly, polysaccharides are naturally occurring macromolecules and constitute one of the most extensive classes of natural compounds. They are distinguished by their excellent biological and physicochemical properties, including biocompatibility, biodegradability, non-toxicity, and effective adsorption capacity. Nevertheless, the direct use of unmodified polysaccharides is often limited by inherent constraints. Consequently, chemical modifications have become a key approach to addressing these limitations and enhancing the applicability of polysaccharides. Through techniques such as grafting and cross-linking, polysaccharides can be converted into a wide range of material forms,

including composites, fibers, membranes, and hydrogel networks. Pullulan (PUL) is an inexpensive and readily available polysaccharide that has gained considerable attention due to its excellent biocompatibility and environmentally friendly characteristics. The presence of abundant hydrophilic functional groups, together with its inherent structural stability, makes PUL a promising candidate for hydrogel fabrication. Furthermore, PUL-based materials are considered pollution-free and have been widely investigated owing to their superior biodegradability and significant promise for advanced material applications [195,196]. In recent years, a simple synthetic approach was investigated to fabricate composite hydrogels, such as pullulan polysaccharide/polyacrylamide/activated carbon (PUL/PAm/AC-composites) [195] and another PUL/PAm/GO composites [196] to adsorb methylene blue (MB) from water. In the PUL/PAm/AC hydrogel composites, PAm acted as a hydrogel matrix, the PUL (improved the mechanical strength) and the activated carbon AC, promoted extra active sites and enhanced the adsorption processes of MB-species from water. The PUL/PAm/AC provided the highest MB uptake capacity, 591.4 mg/g at 298 K, pH 10, and a PUL: AC ratio of 6:1 [195]. Also, the prepared hydrogel PUL/-PAm/GO composites consisted of PAm as the carrier, mixed with PU, and loaded with GO to remove MB-dye. The results demonstrated that the rate of uptake of MB-species by PUL/PAm/GO was 83.2% within 140 min, and the saturation ability was 438.7 mg g^{-1} [196]. Similarly, other polysaccharide-based natural polymers, including guar gum, gum ghatti, and xanthan gum, are among the most widely employed raw materials in various applications. The favorable characteristics of these materials, such as economic viability, environmental safety, biodegradability, and renewability, have attracted considerable research attention compared with many synthetic or composite polymers, leading to growing research interest. Despite these advantages, natural gums in their pristine form suffer from several shortcomings, including low specific surface area, poor thermal stability, processing challenges, insolubility in most common organic solvents, and insufficient mechanical strength, which collectively limit their broader utilization. Consequently, chemical modification through graft copolymerization has emerged as an effective approach to enhance their physicochemical properties. Grafted biopolymers typically exhibit improved mechanical performance, biocompatibility, and greater structural flexibility compared with their unmodified forms, making them promising candidates for addressing the challenge of toxic wastewater effluents. These modifications significantly improve both the structural integrity and chemical functionality of the biopolymers, thereby enhancing their performance and establishing them as versatile and efficient materials for advanced environmental and industrial applications [197–203]. GG-g-poly(AC-co-PAm) hydrogel was fabricated by a free radical strategy using methyl violet (MV) dye from aqueous media, where guar gum (GG) was blended with copolymer mixture of polyacrylamide (PAm) and acrylic acid (AA), using potassium persulfate (KPS) (initiator) and N, N-methylene diacrylamide (MBA) (crosslinker) [197]. Also, the free radical polymerization approach was investigated to synthesize (XG/AA/Aam/GO) hydrogel nanocomposite [198], consisting of xanthan gum(XG), acrylic acid, acrylamide, and graphene oxide, as shown in Fig. 7a, for the adsorption of (MB)-dye removal. Suggested chemisorption mechanism of MB-species onto

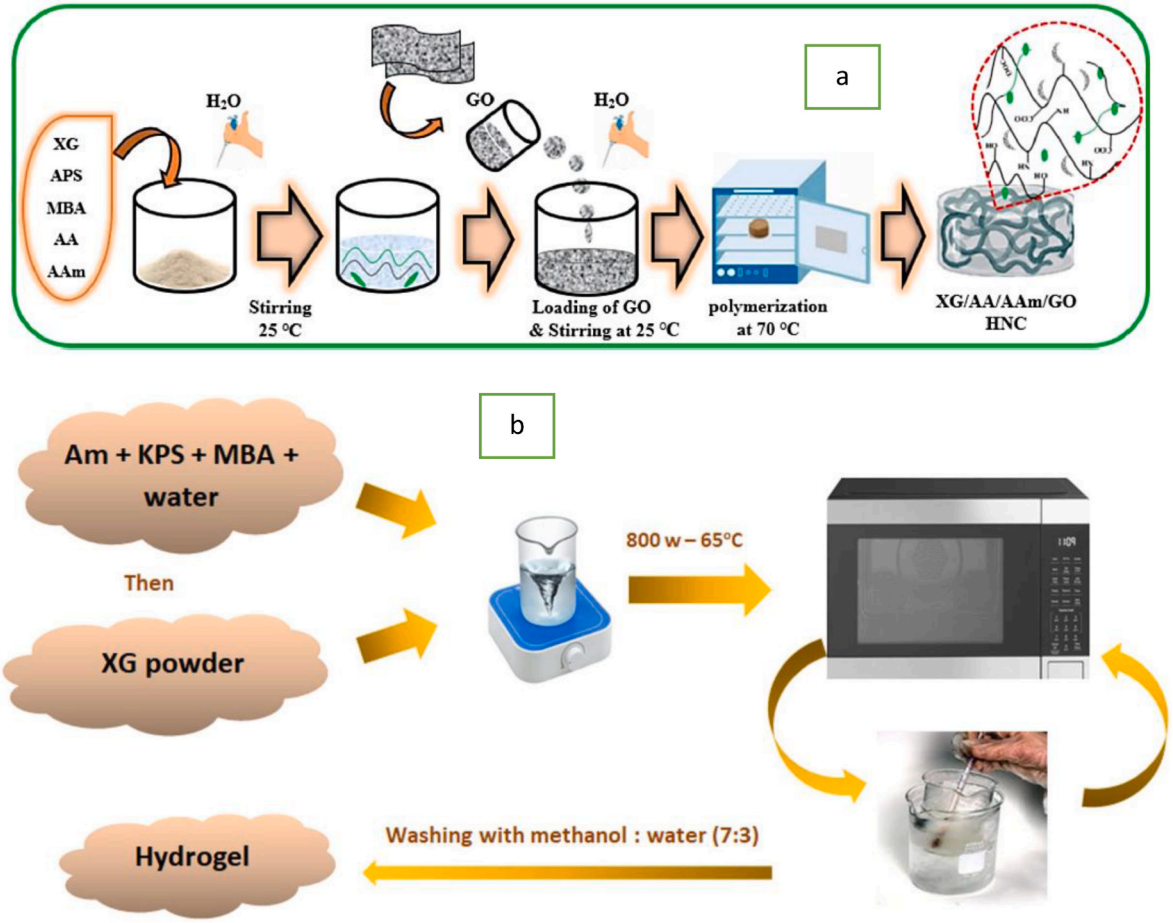

Fig. 7. Scheme of the (a) fabrication of XG/AA/Aam/GO nanocomposite hydrogels [198] (This figure has been adapted/reproduced from Ref. [198], Elsevier permission, copyright 2025) and **(b)** fabrication of XG-g-PAm hydrogel by microwave-assisted synthesis process [203] (This figure has been adapted/reproduced from Ref. [203], Springer permission, copyright 2025).

XG/AA/Aam/GO hydrogel nanocomposite involves covalent and hydrogen bonds [198]. A novel nanohydrogel GA-cl-poly(AAm)NHG adsorbent nanomaterial consisted of gum Arabic (GA) with poly (AAm)) was also fabricated for the adsorption of CV-dye from aqueous medium and the possible interactions between GA-cl-poly(AAm)NHG and CV-species [199]. Other types of gum were grafted with polyacrylamide by various technique to prepare promising effectiveness hydrogel adsorbents, such as gum karaya (Gk) with polyacrylamide (PAm) to form hydrogel polymer followed by in-situ dispersion of nickel sulphide nanoparticles to adsorb rhodamine 6G dye (R6G) [200], gellan gum/polyacrylamide(GG-co-PAm) hydrogel via free-radical polymerization, grafting different doses of gellan gum as a biopolymer backbone for removal basic fuchsin dye [201], Core-shell V_2O_5- grafted Gum ghatti mixed with poly(acrylamide-co-methacrylic acid) to form (V_2O_5-Gum Ghatti-Cl-Poly (AAM-co-MAA) adsorbent to eliminate MB-dye from water [202], and fabrication of XG-g-PAm hydrogel by microwave assisted approache using xanthan gum (XG) grafited polyacrylamide with MBA as a crosslinker and KPS as an initiator to eliminated Acid red 8 dye (AR8)-dye from aqueous from an aquatic environment [203].

In recent years, the grafting of polyacrylamide onto biomaterials such as silk fibroin (SF), gelatin, and phytic acid has attracted considerable attention for the development of eco-friendly adsorbent materials to remove organic dyes from aquatic media. This prominence is attributed to their abundance, environmental friendliness, biodegradability, biocompatibility, and nontoxic characteristics. Recently, a novel magnetic hybrid hydrogel (Fe_3O_4@SF-PAm) was fabricated via a combination of free radical polymerization and in situ co-precipitation to remove cationic dyes, including MB, CV, and Rhodamine B. The prepared hydrogel can be reused for 5 cycles, with elimination percentage for MB species exceeding 90% [204]. Also, the free radical polymerization method was used to prepare a promising, effective PAm-g-gelatin/ACL/Mg–Fe LDH composite hydrogel adsorbent biomaterial to eliminate CV species from wastewater [205]. Another 3D porous polyacrylamide/phytic acid/polydopamine (PAm/PA/PDA) hydrogel was synthesized to remove either anionic or cationic dyes, such as MB-dye, YMB-dye, MV-dye, and NR-dye [206]. The fabricated PAm/PA/PDA hydrogel showed high removal capacities (>350.67 mg g−1) for the selected dyes due to strong π-π stacking and anion-cation interactions, in addition to its easy recovery from water after the adsorption process and regeneration by adjusting solution pH values [206].

While hydrogels possess considerable potential for removing diverse organic dyes from aqueous solutions, their widespread application in wastewater treatment is restricted by poor mechanical stability and slow adsorption kinetics, leading to prolonged equilibrium periods. To overcome these limitations and challenges and improve their applicability, the development of hybrid and nanocomposite hydrogels has gained significant attention. The introduction of various fillers (e.g., graphene oxide (GO), clays, and related nanomaterials), a second polymer, or a combination of both into the hydrogel framework results in composite systems with significantly improved thermal stability, mechanical strength, chemical resistance, and adsorption performance and adsorption capacity. Moreover, nanocomposite hydrogels typically exhibit higher surface area and larger hydrodynamic radii than neat polymer hydrogels. These property enhancements are largely attributed to strong synergistic interactions between the polymer matrix and the incorporated nanofillers. Among the different fabrication routes, semi-interpenetrating polymer network (semi-IPN) nanocomposite hydrogels are considered particularly effective. To improve the handling and recyclability of polyacrylamide-based hydrogel nanocomposites, several recent studies have been published. Gamma radiation-induced copolymerization and crosslinking approaches were investigated to prepare a copolymer hydrogel based on (Gum Acacia/Acrylamide)-calcinated Eggshell/Graphene oxide (GA/AAm)-ES/GO for adsorption of cationic dye Astrazon red 6B (AR) from an aqueous media with adsorption ability of 313.3 mg g^{-1} and good recyclability over three rounds [207]. Also, free radical polymerization process was utilized to fabricate novel alginate (Alg) based nanocomposite hydrogels for the adsorption of MB-species from aquatic media [208]. The fabricated hydrogel matrix (Alg-g-poly(AAm) hydrogel) was embedded with different concentrations (0–12.5 wt%) of carbon black (CB) nanoparticles, forming Alg-g-poly(AAm)/CB nanocomposite hydrogel, which has a considerable adsorption performance, thermal stability, roughness, and surface area compared to Alg-g-poly(AAm) hydrogel [208]. Likewise, semi-interpenetrating polymer network (IPN) nanocomposite hydrogels are investigated as compatible blends of two polymers, with only one component chemically cross-linked. Simultaneously, the second component integrates into the network via non-covalent interactions, without forming covalent bonds between the two polymers. Accordingly, an eco-friendly PVA/PHPAm/GO semi-interpenetrating polymer network (semi-IPN) nanocomposite hydrogel was synthesized as an efficient adsorbent for methylene blue (MB) from aqueous solutions [209]. This hydrogel comprises poly(vinyl alcohol) (PVA) chains and graphene oxide (GO) nanosheets embedded within a cross-linked, partially hydrolyzed PAm network, and synthesized through a one-step internal ionic gelation process in an aqueous medium [209]. Compared with empty hydrogels, the swelling ability, thermal stability, and adsorption efficiency of the PVA/PHPAm/GO semi-IPN nanocomposite hydrogel were improved due to the incorporation of GO [209].

Over the past few years, increasing attention has been directed toward natural polysaccharide-based materials, such as pine gum (Pn)–based hydrogels [210] and *Nicandra physaloides* (L.) Gaertn seed gum (NPG)–based hydrogels [211], owing to their effectiveness as adsorbents for wastewater treatment. These natural polysaccharides are abundant, biodegradable, cost-effective, and eco-friendly, and they are decorated with various active groups that are advantageous for wastewater remediation applications. Notably, the excitance of COOH and C=C groups enables facile chemical functionalization through reactions with various agents, rendering these polysaccharides an ideal backbone for the fabrication of hydrogel adsorbent materials. Consequently, pine gum (Pn) and *Nicandra physaloides* (L.) Gaertn seed gum (NPG) has emerged as a promising candidate for wastewater purification, in line with rising interest in developing adsorbents derived from sustainable natural resources. Polysaccharide-based hydrogels exhibit several desirable characteristics, such as facile synthesis, high water uptake, high porosity, ease of operation, and diverse morphologies, all of which contribute to efficient pollutant mitigation. NPG is structurally composed of galactose, glucose, galacturonic acid, and rhamnose units. During gel formation, its spherical molecular units align end-to-end to form chain-like structures with branching nodes. This network can be further chelated with other substances, resulting in a three-dimensional porous architecture. Therefore, significant research efforts have focused on enhancing the adsorption performance of these hydrogels by incorporating nanomaterials or chemically modifying natural polymers to improve dye removal [210,211]. A free radical polymerization approach was used to prepare a novel (Pn-g-PAm) hydrogel, with Pn as the backbone and PAm as the monomer, for the removal of Malachite green (MG) dye. The fabricated hydrogel achieved high swelling efficiency (1325 %), high specific surface area (34.973 $m^2 g^{-1}$), pore volume (0.104 cc g^{-1}), and maximum adsorption capacity (120.772 mg/g) [210]. Also, an amino-functionalized CPAm/PEI/GO composite was fabricated using a mild strategy by reacting acrylamide (AM), methacryloxyethyltrimethyl ammonium chloride, polyethyleneimine ethoxylated (PEI), and graphene oxide (GO) for the adsorption of the MO-dye from aqueous media, with a high adsorption capacity of 677.55 mg g^{-1} [211].

Polyacrylic acid (PAA) is a hydrophilic, cost-effective polymer with good mechanical stability and high sensitivity to external stimuli. Accordingly, considerable efforts have been devoted to fabricating hydrogels based on PAm and PAA systems. The copolymerization of

PAm with PAA yields a functional copolymer capable of chelating a wide range of pollutants, thereby exhibiting superior adsorption properties. This capability is attributed to the ionizable and hydrophilic– COO-, -COOH, and other groups present in the AAc units, which serve as efficient chelation sites. Consequently, the synthesized composite hydrogel exhibits improved swelling behavior, adsorption capacity, pH responsiveness, and overall performance compared with single-component hydrogels [212–219]. A free-radical polymerization approach initiated by ultraviolet light was investigated to prepare a P(NIPAm-co-AAc)/-MoS_2 composite hydrogel as a suitable sorbent for MB species in aquatic media [212]. P(NIPAm-co-AAc)/MoS_2 composite hydrogel was fabricated by polymerization of N-isopropylacrylamide (NIPAm), acrylic acid (AAc) (monomers), N, N′-methylenebisacrylamide (MBA) (cross-linking agent), and molybdenum disulfide (MoS_2) (functional particles) [212]. Also, the free-radical polymerization technique was employed to fabricate a PAm/PAA/CHN hydrogel adsorbent by copolymerizing acrylamide acid and acrylic monomers with inorganic CHN as crosslinkers to adsorb MB species from wastewater [213]. Another adsorbents hydrogels synthesized through the copolymerization of PAm with PAA to eliminate various dyes species were developded and fabricated recently, such as PAA-coPAm)-DPNR/Ag-TiO_2 for adsorption of MB-dye [214], CMC-g-P(AAm)/MMT copolymer hydrogel to remove MG-species [215], poly(GG-*co*-AAm-*co*-MAA) hydrogel to eliminate MV- dye and FB-dye [216], (AAc-co-AM)/AC hydrogel to adsorb BB-dye [217], polyacrylamide (PAm) and polyacrylic acid (PAA) hydrogels to remove RO-20 and DR-31dyes [218], and poly(AA-co-AMA) copolymer for adsorption removal of azo dyes [219] from aqueous solutions.

In recent years, numerous adsorbents, particularly various types of clay minerals, have been widely explored for the removal of dyes from aqueous solutions. Clays possess a strong capacity to adsorb heavy metal and organic dye pollutants due to their advantageous physicochemical properties, including a layered morphology, a high specific surface area, and an elevated cation-exchange capacity. As a result, incorporating clay-based fillers into hydrogel polymer matrices not only enhances the structural and functional properties of the hydrogels but also substantially increases their adsorption efficiency. The use of nanosized clay fillers to reinforce polymer networks yields hydrogel nanocomposites with superior adsorption performance [220–224].

Therefore, an in situ free radical polymerization approach was investigated to fabricate PAm-Agar/Clay@r-GO nanocomposite hydrogel via incorporating the nanoclay modified by GO (Clay@GO) within the (PAm-Agar) double network hydrogel [220]. The prepared nanocomposite hydrogel demonstrates excellent removal efficiency for both anionic and cationic dyes, achieving rapid adsorption equilibrium [220]. Additionally, graft copolymerization was used to synthesize a zeolite hydrogel composite (ZHC) based on AQSOA-Z05 and $_k$-carrageenan.

(KC) as a potential sorbent for adsorbing cationic dyes from contaminated wastewater [221]. Another magnetic Fe_3O_4/PAm/LMSH nanocomposite hydrogel was prepared via in situ free-radical polymerization to remove CV-dye and MO-dye from aquatic media [222]. Talc is another important naturally occurring hydrated magnesium silicate mineral with the chemical formula $Mg_3Si_4O_{10}(OH)_2$. Structurally, pure talc is composed of a central brucite-type ($MgO{\cdot}H_2O$) layer positioned between two tetrahedral silica (SiO_2) sheets, resulting in a distinctive layered configuration [223]. Therefore, it is used to form a new adsorbent material, polyacrylamide (an inert polymer)-talc (PAm-talc), for the adsorption of MB from aqueous media [223].

Another clay recognized as a promising adsorbent is montmorillonite (MMT). It is a low-cost adsorbent with a high cation-exchange capacity, enabling effective adsorption of cationic pollutants due to its substantial negative surface charge. Cloisite 30B is a naturally derived MMT clay whose surface has been organically modified with quaternary ammonium salts [224]. Therefore, the adsorption performance of Cloisite 30B grafted poly(methacrylic acid-co-acrylamide) prepared by the radical polymerization method was investigated to prepare (poly (MAA-co-AAm)/Cl30B) nanocomposite hydrogels [224]. Poly (MAA-co-AAm)/Cl30B hydrogel is a promising adsorbent for MB species and is recommended for the treatment of colored wastewater [224].

To significantly improve the adsorption capacity and mechanical performance of polymer-based hydrogels, nanomaterials are commonly incorporated into their flexible polymeric frameworks. Among these systems, nanocomposite hydrogels have emerged as particularly effective adsorbents due to the persistent synergistic interactions between nanofillers and the polymer matrix. These interactions impart superior thermomechanical properties and a higher hydrodynamic radius than those of pristine polymer hydrogels. In addition, nanoscale adsorbents typically exhibit enhanced performance compared to micron-sized materials, owing to their high specific surface area and reduced internal diffusion limitations. Novel polymer architectures can be developed by blending natural and synthetic polymers with complementary characteristics. The successful fabrication of such binary blends relies heavily on the careful selection of compatible polymer pairs. In this regard, the availability of suitable functional groups that serve as effective binding sites is essential for efficient dye adsorption and for maintaining polymer compatibility, thereby facilitating network formation through strong physical intermolecular interactions [225–229]. Therefore, considerable effort has been devoted to enhancing the adsorption capacity and mechanical performance of polymer-based nanocomposite hydrogels for the removal of dyes from aqueous media [225–233]. Recently, a novel HPAm/SiO_2@XG multifunctional self-assembling nanocomposite hydrogel was rationally designed and synthesized through an environmentally benign gelation process in water, without the incorporation of any chemical crosslinkers. The formation of the hydrogel network is dominated by multiple hydrogen-bonding interactions between xanthan gum (XG), partially hydrolyzed polyacrylamide (HPAm), and the silanol groups present on silica nanoparticles. The resulting material exhibits enhanced adsorption of CV species. This can be attributed to the increased surface area resulting from the uniform distribution of SiO_2 nanoparticles, along with the enhanced density of reactive functional groups within the blended HPAm/XG polymer matrix [225]. A sol-gel approach was applied to fabricate a 3D porous structure (PAm/MXene) composed of 3% wt polyacrylamide (PAm) and Ti_3C_2Tx-MXene nanosheets to eliminate MB species from aqueous solutions [226]. PAm/MXene hydrogel exhibited excellent sensitivity to an electric field and high cyclic compression-resilience, with considerable electrosorption saturation of MB-dye species reaching 282.29 mg/g [226].

Also, a crosslinking process was applied to prepare a polyacrylamide-titanium dioxide (PAm@TiO_2) nanocomposite to eliminate CV-dye from water, as shown in Fig. 8a [227]. The adsorption mechanism of CV species onto the PAm@TiO_2 nanocomposite can be explained as a two-step process. Initially, CV molecules migrate from the bulk solution to the adsorbent's outer surface. This is followed by diffusion through the boundary layer and into the internal pores of PAm@TiO_2 nanocomposite. Electrostatic interactions are the main factor governing the adsorption process, while hydrogen bonding and n–π interactions also play supportive roles in the overall mechanism [227]. A novel Ce/Ti-NRs/CMC/PAm hydrogel was developded and investigated in photocatalytic degradation of CR-dye [228]. The fabricated hydrogel illustrates considerable degradation capacity and ability to simultaneously adsorb-degrade the dye via the PAm/CMC crosslinked hydrogels networks with photocatalytic degradation driven by embedded cerium titanate nanorods, showing superior simultaneously adsorb-degrade photo catalytic activity up to 91.68% with adsorption capacity of 22.44 mg g^{-1} [228]. Also, free radical polymerization was investigated to prepare a series of GO/PAm composite hydrogels for the uptake of Drimarene Brilliant Blue K-4BL molecules from wastewater. The experimental results demonstrate that Polyacrylamide hydrogels reinforced with graphene oxide (GO) nanoparticles exhibit improved thermo-mechanical stability and increased their adsorption capacity by approximately tenfold compared to an unmodified polyacrylamide

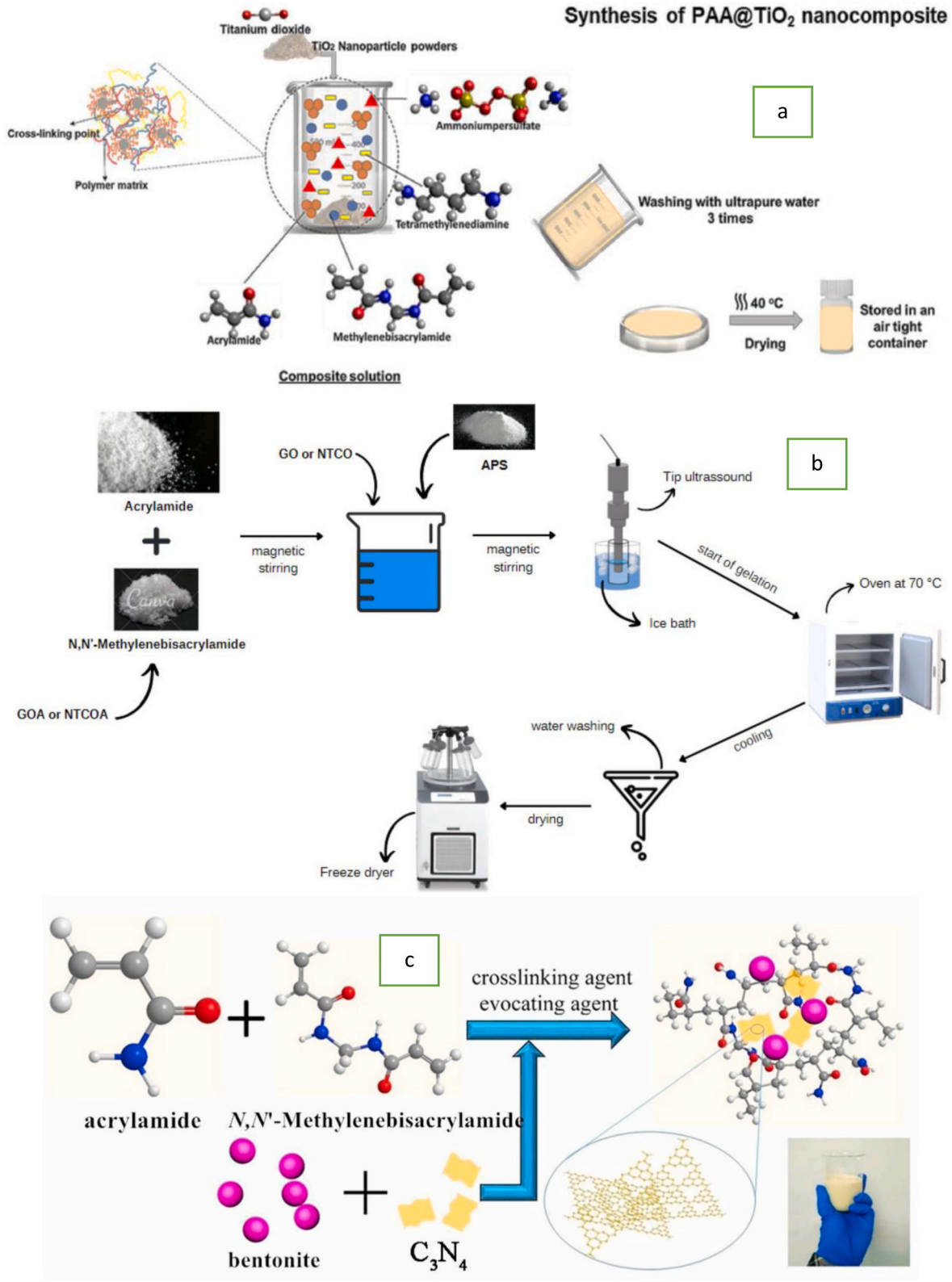

Fig. 8. Scheme of the fabrication of (a) PAm@TiO_2 nanocomposite hydrogels [227] (This figure has been adapted/reproduced from Ref. [227] Springer permission, copyright 2024), **(b)** polyacrylamide and nanocomposite hydrogels [231] (This figure has been adapted/reproduced from Ref. [231] Springer permission, copyright 2022), and (c) PAm/bentonite/g-C_3N_4 3D-hydrogel [233] (This figure has been adapted/reproduced from Ref. [233], Elsevier permission, copyright 2018).

hydrogel [229]. Also, a novel CMC-grafted poly(acrylamide) nanocomposite hydrogel was fabricated via free-radical graft polymerization, with acrylamide grafted onto the carboxymethyl cellulose backbone (Hyd), for the adsorption of MBdye from aqueous medium, with a saturation ability of 27.32 mg g^{-1} [230]. On the other hand, polyacrylamide-grafted graphene oxide and carbon nanotubes (CNTs) (GO@PAm) nanocomposite hydrogels were fabricated via in situ polymerization, as shown in Fig. 8b, to remove MG molecules from aqueous

solutions [231]. Over the last few years, the surface of PAm was modified with ZnO nanorods (ZNR) to form a ZNR-modified composite PAC (ZMC) for studying its adsorption behavior of Orange G (OG) [232]. The prepared gel showed higher removal efficiency than PAm. The ZMC achieved a maximum capture efficiency of 142.79 mg g^{-1} for OG and could be reused 20 times, retaining 80% of its initial performance [233]. A facile technique was investigated as a green process for the synthesis of a series of inexpensive, separation-free PAm/B/CN 3D-hydrogels, as shown in Fig. 8c, which conform to the subject of clean production [233].

Table 8 represents a summary table for the studied polyacrylamide (PAm)-based hydrogel materials investigated in this review for the adsorption processes of dyes from aqueous solution. The data highlights the composite types, mass ratio, and their corresponding functional groups. It is clear that, the synergistic modification processes of PAm significantly enrich surface chemistry and play a critical role for designing multifunctional polyacrylamide (PAm)-based hydrogel adsorbents with enhanced adsorption performance.

Generally, as reported in the pervious works, PAm can be described as a matrix former and dispersion facilitator in the studied GO/PAm hydrogels systems and forms a continuous polymeric network embedding GO nanosheets. It provides additional adsorption active sites for via amide groups alongside GO's oxygenated functionalities and improves interfacial dispersion and stability of GO. Moreover, it contributes to enhanced mechanical strength, elasticity, and accessibility of adsorption active sites for the investigated dye molecules.

Overall, the published works confirm and highlight the vital role of synergism of pure PAm hydrogel with other investigated materials to form hydrogel-based materials and improve their performances, as represented in Table 9 18–68,85–92. The enhancements in the performance reported to the studied hydrogel-based materials are not only attributed to the added components, but rather to the synergistic interplay between them and the PAm network. The improvements observed can be attributed to the reinforced structures, additional functional groups, and multi-interaction mechanisms introduced by secondary materials in addition to the hydrophilic, high swelling capacity, and flexible network of PAm hydrogel. It is important to note that PAm hydrogel remains the fundamental structural and functional platform, and the design of high-performance hydrogel systems should be viewed as cooperative interactions rather than independent contributions of additives to fabricate promising hydrogel-based materials.

3.3. Investigated adsorption mechanisms of pollutants by PAm-based hydrogels

The adsorption performances of PAm-based hydrogels do not arise from by a single mechanism, but rather by a synergistic combination of mechanisms that can be systematically discussed based on the nature and transformation of their functional groups such as amide (–$CONH_2$), carboxylate (–COOH/–COO^-), and amine (–NH_2) functionalities which can form specific interactions pathways with various types of pollutants. Scheme 8 represented the most common adsorption mechanisms of PAm-based hydrogels for heavy metal ions and dyes. Chelation/coordination interactions is the predominant mechanism for adsorption of heavy metal ions, arising from the interactions of metal ions with electron-donating atoms (N and O) in amide, amine, and carboxyl groups to form stable complexes involving lone pair electrons of N and O atoms in –$CONH_2$, –COO^-, and –NH_2 groups, and can be verified by FTIR spectral shifts (amide and carboxyl bands) and XPS binding energy changes (N 1s and O 1s) which approve the formation of metal–ligand complexes. On the other hand, electrostatic interactions primarily governing the adsorption of charged dyes, particularly in the presence of COO^- or protonated –NH_3^+ groups, with Zeta potential measurements demonstrating pH-dependent surface charge variation. Hydrogen bonding contributes as complementary mechanisms, improving the affinity toward polar organic pollutants through interactions with

Table 8
Overview of PAm-based hydrogels and hybrid composites investigated to remove various types of dyes from aqueous solutions.

adsorbent	Composite type	Mass ratio	Functional group	Ref
PAm/hBN	Nanocomposite	200 mg PAM (4.0 wt%): 0.01 wt% (of total weight of the gel) hBN	Carbonyl, amine, amide,	155
PAm based hydrogel incorporating β-cyclodextrin and acrylic acid	Copolymer	0.24 g (β-CD): 7.76 g Am: 2.0 mL AA: 0.01 g MBA: 0.05 g APS	Vinyl, hydroxyl, carboxylate, amide, and carbonyl	156
PVA-g-PAm	Copolymer	AM: PVA (0 wt %, 25 wt%, 50 wt%, 75 wt %, and 100 wt %)	Silanol, carboxalic, hydroxyl, amide, and carbonyl	157
PAm	Copolymer	**	Hydroxyl, carboxylate, amide, and carbonyl	158
PAm-SO_3-N_5	Physical Mixing	4.27 g Am: 1.46 g AAMPS: 1.46 g MBA: 75 mL EtOH	Sulfonic, hydroxyl, carboxylate, amide, and carbonyl	159
SAG-g-PAm	Copolymer	1.0 g SAG: 6.0-10.0 M Am (in 10 mL)	Hydroxyl, carboxylate, amide, and carbonyl	160
PAm/SA	Free radical	1.0 g Am: 1.0 g SA	Carboxyl, amide, hydroxyl, and carbonyl	161
SA-PAm-TOCN	Nanocomposite	0.6 g SA:3.6 g AM	Hydroxyl, carboxyl, amino, and carbonyl	162
PAm/SA/Fe_3O_4@ZIF-8-8	Free radical	0.5g Am: 0.05g SA: 0.05 MBA: 0.03 g APS	Hydroxyl, carboxyl, amide, carboxylate	163
SA-g-P(AA-co-AmPS)/KL	free radical	0.36 g SA:7.2 g AA:0.72 g AMPS: 0.42 KLg	Carboxyl, sulphonic, amide	164
HAp/Cu-Fe LDH	Nanocomposite	0.5 g SA: 1.0 g (AM): 0-10 wt % Cu-Fe LDH	Carbonate, phosphate, amide, hydroxyl, and carboxyl	165
CPAm-Dia/SA-La	Copolymer	8 g/L CPAM-Dia: 20 g/L SA: 40 g/L $La(NO_3)_3$	Hydroxyl, carboxyl, carboxylate,	166
Pcn-g-P(Am-*co*-SA) hydrogel	Copolymer	1.0 g Pen:1.0-6.0 g Am: 0.3 g KPS	Carboxyl, hydroxyl, amide, and sulfonate	167
CMC-g-poly (AAm)/CL-Fe_3O_4	Nanocomposite	2.5 g of CMC:X g Am: 10 wt% CL-Fe_3O_4	Carboxyl, hydroxyl, amide, and carbonyl	168
HG/MTWBC	Nanocomposite	0.33 g CMC: 1.2 g Am: 10 wt % MTWBC	Carboxyl, hydroxyl, amine, and carbonyl	169
Hyd/WS/$CoFe_2O4$/ZIF-67	Nanocomposite	0.33 g CMC: 1.2 g Am: 0.3 g KBS: 0.03 g MBA	Carboxyl, hydroxyl, amine, and carbonyl	170
PAm/CMC/MHNT	Nanocomposite	0.33 g CMC: 1.0 g Am: 0.03 g MBA: 2.5-20 wt% MHNT	Aluminosilicate, silicate, carboxyl, hydroxyl, amide, and carbonyl	171
AM-AC/CMC-Ca	Nanocomposite	(0.01–0.05 g) AC: (0.1–0.5 g) Am: (0.10–2.0 g)	Carboxyl, hydroxyl, amine, amide, and carbonyl	172

(*continued on next page*)

Table 8 (*continued*)

adsorbent	Composite type	Mass ratio	Functional group	Ref
		CMC: (10–40 g/L) $CaCl_2$		
PAm/CMC-CuS	Copolymer	**	Carboxyl, hydroxyl, amide, and carbonyl	173
κC-g-PAm/ bentonite	Copolymer	1.0–3.0 g κC: 2.0 g Am: 3.0-1.0 g bentonite	Silicate, sulfonate, hydroxyl, amide, and carboxylate	174
κC-g-P(AAc-co-AAm)/Kaolin	Copolymer	0.1-1.0 g Kaolin: 2-10 mL AAc: 2.0-6.0 g Am: 0.01 g-1.0 g KPS	Hydroxyl, amide, carboxyl, and carbonyl	175
APAm/DTPA-CTS/GO	Copolymer	1.0 g Am: 7.32 g DTPA: 2.0 g CTS: 2.0 AA: 5.56 g DTPA-CS: 5.0 mg/mL GO	Amine, hydroxyl, carboxyl, hydroxyl, and amide	176
g-CCTS	Grafting	0.5 mL AA: 0.2 g Am: 1.0 g g-CTS: 0.2 g MBA	Amine, amide, and carboxyl	177
VSi-CTS-g-PAm	Physical mixing	10 mL VSi: 4.0 g CTS: (0.3-0.9g) Am	Amine, amide, hydroxyl, and carbonyl groups	178
PAm/chitosan hydrogel	Nanocomposite	1.441 g PAm: 0.144 g CTS	Hydroxyl, amine, amide, carboxylate, and nitrile	179
(PAm/CTS)	Nanocomposite	(0.1- 0.8) g CTS: 2.9 g Am: 0.1 g MBAA: 0.1 g SDS	Amine, amide, carboxyl, and carbonyl	180
Pcn-g-P(Am-co-SA)	Copolymer	6.0 g Am:0.3 g KPS: 1.5 g AA: 5.87 g SA: 0.0316 g MBA	Carboxyl, amine, hydroxyl, amide, sulfonate: and carbonyl	181
TiO_2-PAm-CTS	Nanocomposite	0.5 g APS: 7.5 g Am: 1.0 g TiO_2: 1.0 g MBA	Amine, hydroxyl, amide, and carbonyl	182
CH-PAA-ZnO	Nanocomposite	2.5 g CTS: 0.5 ABS: 7.5 g Am: 0.6 g Zn $(NO_3)_2$	Hydroxyl, amine: and amide	183
Jh-g-(PAm-co-PVAc)	Copolymer	0.2 g Jh gum: 0.00562 M/L Am: 0.3699 mM/L KPS: 0.0464 M/L Vac: 0.324 mM/L MBA	Acetate, carboxyl, amine, hydroxyl, and amide	184
CNF-PAm	Copolymer	2.7 g Am:0.0224 g APS: 0.01 g MBA	Carboxyl, amine, hydroxyl, and amide	185
PAm/CNCs microspheres	Physical mixing	6.0 g CNCs: 10 g Am	Salfonic ester, hydroxyl, amide, and carbonyl	186
PAm/CG/FE	Physical mixing	2.0 g Am: 0.6 g CG: 0.4 g FE	Hydroxyl, amide, and carbonyl	187
KIF/BC/PAm	Physical mixing	0.5-2.0 (w/v) KIF: 0.3 g BC: 5 % (w/v) Am	Hydroxyl, amide, thiol, carboxyl, and carbonyl	188
hemi-g-PAm	Physical mixing	1.0 g EIHs: 5.0 g Am: 0.1 g MBA:	Acylamino, carboxyl, hydroxyl, amide, and carbonyl	189
CMC–CPAm–TA	Physical mixing	1.0 CPAm: 2.0 CMC: 1.0 g TA	Amino, amide, hydroxyl, carboxyl, and carbonyl sulfide	190
SG@AA-co-AM	Copolymer	1.0 g SG: 0.216 g KPS 2.536 mL AA: 2.627 g Am	Carboxyl, hydroxyl, amide, carboxylic ester, and carbonyl	191
St-g-(AA-AAM)	Copolymer	4.5 g St: X g (AA + Am + MBA)	Hydroxyl, amide, carboxyl, and carbonyl	192
St-co (PAm/PAA)	Copolymer	0.5 g CMC: 0.3 g PAm: 0.67 g AA: 0.015 g MBA	Carboxyl, hydroxyl, amide, and carbonyl	193
St-30/ZnO	Copolymer	7.5 g PAm: 7.5 g (St + PVA): 0.1 g (SiO_2-coated ZnO)	Hydroxyl, amide, sulfonate, silanol, Carboxyl, and carbonyl	194
PUL/PAm/AC	Physical mixing	0.5 g PUL: X g (AM, BIS, and KPS)	Carboxyl, hydroxyl, amide, and carbonyl	195
PUL/PAm/GO	Physical mixing	0.5 g PUL: 2.5 g Am: X g GO: 0.1 g BIS:0.125 g KPS	Carboxyl, hydroxyl, amide, and carbonyl	196
GG-g-poly (AC-co-PAm)	Grafting	1.0 g GG: 0.5 g (Am + AC): 0.05 g KPS: 0.08 g MBA	Carboxyl, hydroxyl, amide, and carbonyl	197
XG/AA/AAm/ GO	Nanocomposite	0.1 g XG: 2.0 mL AA: 2.0 mL Am: 0.053 g ABS: 0.0932 g MBA	Carboxyl, hydroxyl, amino, sulfur, amide, and carbonyl	198
GA-cl-poly (AAm)	Nanocomposite	5% GA: 0.2M Am	Carboxyl, hydroxyl, amide, imine, and carbonyl	199
GK-PAm	Nanocomposite	1.0 g GK: (0.5-1.5) g Am	Carboxyl, hydroxyl, amide, and carbonyl	200
GG-co-PAm	Copolymer	0.2 g GG: 0.11 MBS: 2.0 g Am: 0.05 APS	Carboxyl, hydroxyl, amide, and carbonyl	201
V_2O_5-Gum ghatti poly (AAM-co-MAA)	Copolymer	1.0 g V_2O_5: X g GG: 30 mg KPS: 20 mg ABC: 50 mg MBA: 1.0 g Am: 2.0 mL MAA	Carboxyl, hydroxyl, amide, and carbonyl	202
XG-g-PAm	Grafting	(1.0 – 10) g Am:1.0 XG: 0.3 g KPS	Carboxyl, hydroxyl, methyl, amide, and carbonyl	203
Fe_3O_4@SF-PAm	Grafting	0.2 g SF: 0.5 g/mL Am: 50 mL Fe_3O_4	Amine, hydroxyl, amide, and carboxyl	204
PAm-g-gelatin/ ACL/Mg–Fe LDH	Copolymer	1.0 g Am: 0.5 g grlatin: 0.15 g ACL/Mg–Fe LDH: 0.033 KPS	Amine, hydroxyl, amide, and carbonyl	205
(GA/AAm)-ES/ GO	Nanocomposite	ES or ES/GO (1:1) with (GA/AAm) (3/7) wt %	Vinyl, epoxy, hydroxyl, amide, and carbonyl	207
PVA/PHPAm/ GO semi-IPN	Nanocomposite	37.5 mg PVA: 87.5 mg PHPAm: 10 mg GO	Amine, epoxide, carboxylate, hydroxyl, amide, and carbonyl	209
Pn-g-poly(AAm)	Grafting	0.5 wt % Pn:1.4 g Am: 0.013 g MBA: 0.005 g APS	Carboxyl, hydroxyl, amide, and carbonyl	210
CPAmPEI/GO	Physical mixing	1.0 g AM: 5 mg/mL GO: 20 mg/mL APS:	Ester, carboxyl, amine, hydroxyl, amide, and carbonyl	211

(*continued on next page*)

Table 8 (*continued*)

adsorbent	Composite type	Mass ratio	Functional group	Ref
		20 mg/mL MBA: 2.0 g METAC: 1.5 g/mL PEL		
P(NIPAm-co-AAc)/MoS_2	Copolymer	1.0 g NIPAM:0.1 g AAc: 0.025 g MoS_2	Carboxyl, hydroxyl, amide, and carbonyl	212
PAm/PAA/CHN	Copolymer	6.0 mL AA: 0.2 g Am: 0.03 g APS	Carboxyl, hydroxyl, amide, and carbonyl	213
(PAA-co-PAm)-DPNR/Ag-TiO_2	Copolymer	X g (PAA-co-PAM): 1% w/v $AgNO_3$: 10%w/v TiO_2	Carboxyl, hydroxyl, amide, and carbonyl	214
CMC-g-P(AAm)/MMT	Copolymer	1.0 g CMC: 0.43 g/ml Am: (0–20 wt%) MMT:	Vinyl, carboxyl, hydroxyl, amide, and carbonyl	215
poly(GG-co-AAm-co-MAA)	Copolymer	0.4 g GG: 2.0 g Am: 2.0 mL MAA	Carboxyl, hydroxyl, amide, and carbonyl	216
(AAc-co-AM)/AC	Nanocomposite	5.0 mL AAc: 1.0 g Am: 0.1 g AC: 0.003 g KPS: 0.008 g MBA	Carboxyl, hydroxyl, amide, and carbonyl	217
PAm PAA	Physical mixing	**	Carboxyl, hydroxyl, amide, and carbonyl	218
AA/AMA	Copolymer	AA/AMA (25/75, 50/50, and 75/25): 0.0001 mmol AIBN	Amine, vinyl, amide, and carbonyl	219
PAm-Agar/Clay@r-GO	Nanocomposite	0.87 M Am: 0.3 g Agar: (1.0-5.0) wt % (Clay@GO): 0.7 mM MBA	Silanol, hydroxyl, amide, carboxyl, and carbonyl	220
zeolite hydrogel composite (ZHC) based on j-carrageenan (KC) and AQSOA-Z05	Copolymer	100 mg APS: 150 mg MBA: 1.0 g AM:0.2 g MAA	Sulfat, Silanol, hydroxyl, amide, carboxyl, and carbonyl	221
Fe_3O_4/PAm/LMSH	Nanocomposite	**	**	222
PAm-talc	Physical mixing	2.0 g Am: 0.4 g MB: 1.0 mL APS:100 μL TEMED.	Siloxane, hydroxyl, carboxyl, amide, and carbonyl	223
poly(MAA-co-AAm)/Cl30B	Nanocomposite	2.0 g Am: 0.02 g MBA: 4.8 mL MMA: 0.1 g PPS	Siloxane, ester, vinyl, hydroxyl, amide, carboxyl, and carbonyl	224
HPAm/SiO_2@XG	Nanocomposite	150 mg (HPAM): 150 mg (25 wt% of HPAM) SiO_2@XG	Silanol, carboxyl, hydroxyl, amide, and carbonyl	225
PAm/MXene	Physical mixing	4.0 Am: 4.5 mg/mL MXene: 0.2 wt %APS: 0.4 mL TMEDA	Hydroxyl, amide, florate, carboxyl, and carbonyl	226
PAA@TiO_2	Nanocomposite	2.0 g AA:1.0 g TiO_2: 0.2 g MBSA: 200 μL TEMED: 1.0 g APS	Amine, hydroxyl, amide, and carbonyl	227
Ce/Ti-NRs/CMC/PAm	Copolymer	(2 g/100 ml) CMC: (2 g/100 mL) PAm: (0.05 g/10 mL) Ce/Ti-NRs: 1, 0.12 g APS: 0.12 g MBA	Sulfonic, hydroxyl, carboxyl, amide, and carbonyl	228
GO/PAm	Nanocomposite	0.2 g GO: 2.0 g PAm: 0.02 MBSA: 0.02 ABS	Hydroxyl, carboxyl, amide, and carbonyl	229
Hyd/CB	Nanocomposite	1.0 g CMC: 0.1 g KPS: X g Hyd: X g CB	Amine, sulphonic, hydroxyl, amide, carboxyl, and carbonyl	230
PAm/B/CN	Physical mixing	2.0 g bentonite:20 g Am: 40 mg MBA: X g g-C_3N_4	**	233

X g unkowm amount, ** Not Detected.

–$CONH_2$ and –COOH groups and approved by broadening and shifting in FTIR stretching bands. Moreover, ion exchange mechanisms play significant roles in partially hydrolyzed PAm hydrogels systems through reversible interactions between $–COO^-$ groups and dissolved ionic species in solution, improving adsorption performance and recyclability. Additionally, π–π stacking become significant interactions may occur in composite hydrogels incorporating carbon-based nanomaterials (e.g., GO or CNTs) further enhancing the adsorption affinity of aromatic dyes. Overall, the mechanisms of adsorption processes in PAm-based hydrogels systems are governed by a synergistic interplay of these mechanisms, functional group density, and solution conditions. Where chelation governing metal ions adsorption performance and electrostatic interactions controlling the adsorption affinity of dyes, as consistently supported by FTIR, XPS, and Zeta potential analyses in previously reported PAm-based systems [12,16,45,51,60–63].

4. Challenges and future perspectives of fabrication and applications of polyacrylamide-based hydrogels in water treatment

Although hydrogel-based adsorbents have demonstrated promising performance and significant potential in wastewater treatment, PAm-based hydrogels limitations should be discussed and evaluated in comparison with other hydrogel-based materials systems. Compared with natural-polymer-based hydrogels, PAm-based hydrogels are widely recognized for their tunable swelling behavior, pronounced hydrophilicity, controllable crosslinking density, highly tunable network structure, and higher structural uniformity which collectively contribute to efficient pollutant removal. On the other hand, in comparison with advanced hydrogel systems such as double-network, nanocomposite, or supramolecular hydrogels, conventional PAm-based materials often exhibit inferior mechanical stability, particularly under repeated reusability, and limited resistance to cyclic deformation, particularly under harsh physicochemical conditions (e.g., wide pH variations, high ionic strength). In contrast, double-network or nanocomposite hydrogels reported in the literature generally exhibit resistance to deformation and superior mechanical strength. The major challenges, along with prospective future directions to address them, are outlined below.

4.1. Mechanical and structural limitations

Conventional PAm-based hydrogel materials show insufficient mechanical strength, particularly under certain conditions, which are typical of continuous flow water/wastewater treatment processes, such

Table 9
Comparative Performance of Pure PAm Hydrogels and other investigated composite hydrogels systems 18–68,85–92.

System	Adsorption Capacity	Mechanical Strength	Swelling Behavior	Reusability	Key Performance Driver	References
Pure PAm hydrogel	Moderate	Moderate (flexible network)	High	Moderate	Amide groups (–$CONH_2$), 3D network	[97,98,155,158]
GO/PAm hydrogel	High	Improved	Controlled/ moderate	Improved	π–π interaction, oxygen groups, surface area	[106,142,145,147,176,196,198,207, 211,220,222,225,231]
Cellulose (TOCNF)/PAm	Moderate–high	High	High–very high	Good	Hydrogen bonding, nanofiber reinforcement	[105,117–119,185,186]
Metal oxide/PAm	High	Moderate–high	Moderate	High	Coordination, electrostatic interaction	[137,138,140,163,168,170,182,183, 194,202,204,214,225,228]
DN/IPN PAm hydrogel	Moderate–high	Very high	Controlled	High	Interpenetrating network	[85–92,149,162,209]
Post-modified PAm	High	Moderate	Tunable	Good	Increased charge density (–COO^-, –NH_2)	[59–68,102]

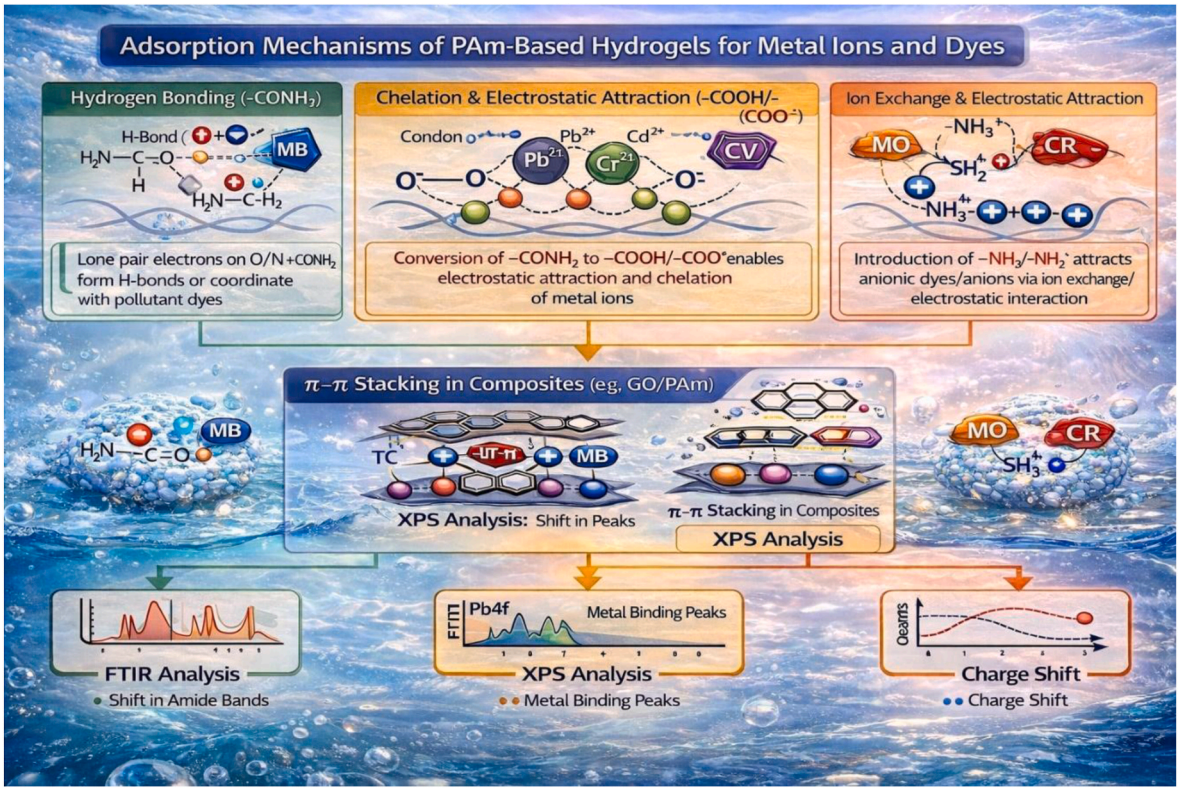

Scheme 8. The most common adsorption mechanisms of PAm-based hydrogels for heavy metal ions and dyes.

as high pressure, agitation, high flow, as well as repeated swelling–deswelling cycles. Such limitations lead to loss of structural integrity during use, fragmentation, deformation, and reduced adsorption efficiency. To overcome such challenges, further work is needed to improve durability underflow and mechanical stress by incorporating promising nanoparticles and other suitable materials. Also, adjusting the density, selecting a suitable crosslinker, and controlling rehydration/ dehydration can improve strength, toughness, robustness, and elasticity.

4.2. Selectivity limitations

Real wastewater/water contains various species of pollutants such as metal ions, dyes, and other species, which can compete with the active sites, leading to a significant reduction in sorption ability and selectivity. This is a major limitation of PAm-based hydrogels, which often exhibit non-specific removal behavior. Therefore, many of the fabricated PAm-based materials require modification with specific functional groups (depending on the type of pollutant), or the synthesis of hybrid PAm-based materials, or the embedding of selective sorbents within hydrogels.

4.3. Reusability and regeneration challenges

Due to the presence of various species of contaminants and species in the wastewater/water systems, the competition for active adsorption sites of various types of PAm-based hydrogel materials accelerated capacity decline. Most of these active sites in hydrogel remain saturated and lose their capacity to adsorb pollutants after a certain number of reusability and regeneration cycles. To overcome these challenges and extend their lifespans, the fabricated PAm-based hydrogels must be modified with suitable pre- and post-treatment units.

4.4. Environmental risks

One of the most critical challenges limiting the application of polyacrylamide-based hydrogels in water treatment technologies,

especially for potable water and environmentally sensitive systems, is the potential release of toxic species. In particular, residual acrylamide monomers from fabrication processes, as well as monomers or degradation by-products released during operation or disposal, are neurotoxic and pose a serious threat to ecosystems and public health. Therefore, many recommendations should be taken into account to control all of these environmental risks, such as the fabrication of hydrogels within suitable supporting materials to eliminate the leaching hazard, minimizing free acrylamide monomers during fabrication and purification processes, in addition to developing standardized protocols and regulatory frameworks governing the safe disposal and sustainable recovery of such hazardous polymeric materials.

Another critical environmental risk associated with the synthesis and applications of PAm–based hydrogel materials is the potential leaching of embedded nanoparticles. The release of nanoparticles from these systems poses substantial concerns in environmental, biomedical, and water-treatment applications, as it may compromise material safety, functionality, and regulatory acceptance. The risks arising from nanoparticle leaching can be systematically classified into environmental, human health, performance-related, and regulatory categories.

To overcome these challenges, several strategies have been investigated, including covalent or ionic immobilization of nanoparticles onto the PAm backbone via appropriate surface functionalization, as well as in situ nanoparticle generation within the hydrogel network to enhance physical confinement. Additional approaches involve surface modification and optimization of cross-linking density to limit excessive swelling and reduce leaching propensity. Finally, comprehensive leaching and aging studies conducted under realistic operational conditions are essential to ensure long-term stability, safety, and regulatory compliance of PAm-based nanocomposite hydrogels.

From a regulatory perspective, the ongoing tightening of legislation governing the discharge of nanomaterials into water bodies and the environment may significantly constrain the commercial implementation of nanocomposite hydrogels. Public and regulatory apprehension regarding “nano-pollution” further limits their adoption, particularly in high-sensitivity applications such as potable water treatment and biomedical devices. Moreover, the end-of-life disposal or gradual degradation of nanoparticle-containing hydrogels may trigger unintended and uncontrolled nanoparticle release, thereby amplifying potential ecological and toxicological impacts.

4.5. Production and scalability gap challenge

Scaling up the synthesis of PAm-based hydrogel materials from laboratory to industrial scale for water treatment remains a significant economic challenge, owing to higher fabrication costs and the need for specialized equipment. Therefore, scaling the preparation processes of uniform, high-performance PAm-based hydrogels from bench to industrial volumes remains challenging, owing to manufacturing complexity, quality control, and the prohibitive costs without process innovation. To overcome this important challenge, hydrogels can be fabricated in various shapes, such as granules, beads, or monoliths, depending on their applications. Developing energy-efficient, scalable preparation strategies suitable for large-scale industrial manufacturing processes, and integrating the prepared hydrogels into hybrid treatment systems combining different processes, is also important. Furthermore, most published works rely on model pollutant systems, underscoring the need for studies that employ real wastewater matrices and continuous-flow treatment processes.

To address and avoid all these challenges and disadvantges, future research related to fabrication and applications of PAm-based hydrogel materials should focus on the following targeted optimization strategies, such as.

- developing and investigating greener fabrication strategies of PAm-based hydrogel materials and minimizing residual acrylamide contents through inclusive purification protocols.
- improving the adsorption capacity and performance with maintain regeneration and recycability efficiencies of PAm-based hydrogel materials by introducing new functional groups and/or hybrid components.
- reducing the environmental risks of PAm-based hydrogels without compromising their performance by integrating and modifying PAm networks with biodegradable or partially bio-based components.
- enhancing mechanical strength and reusability performance of PAm-based hydrogels through designing reinforced or double-network structures and incorporating nanofillers.

Overall, while PAm-based hydrogels offer notable advantages and remain highly promising hydrogel-based materials due to their adsorption performance and structural versatility, their practical deployment requires targeted advancements addressing mechanical durability, long-term reusability, their future development should focus on overcoming their mitigating environmental risks, reusability, mechanical stability limitations to translate these promising hydrogels from lab-scale works to sustainable real-world water treatment approaches.

In summary, PAm-based hydrogels facing different challenges which can be systematically reorganized into three categories, including intrinsic network, composite-induced, and engineering applications limitations, as shown in Scheme 9, Therefore, proposed solutions are required to bridge the gaps between laboratory performance and large-scale water treatment applications. Accordingly, the proposed solution includes network system optimization (crosslink density control, DN/IPN architectures, and dynamic crosslinking), improved composite design (filler functionalization, in situ incorporation, and enhanced interfacial compatibility), and process-level strategies (scalable fabrication, structured forms, and continuous-flow operation).

5. Conclusions

Generally, this review article provides a comprehensive overview of the fabrication and applications of polyacrylamide-based hydrogels for the elimination of heavy metal ions and dye molecules from aquatic systems. Polyacrylamide-based hydrogels offer a promising class of adsorbents for the effective adsorption of heavy metal ions and dyes from contaminated water, owing to their high swelling capacity, adjustable network structure, and abundance of functional groups. The recently reviewed works demonstrate that the fabrication of a polyacrylamide-based hydrogel network architecture and the incorporation of functional materials, biopolymers, inorganic fillers, and nanomaterials have markedly improved mechanical stability, sorption performance, and reusability, in addition to demonstrating superior removal efficiencies through synergistic interactions between polyacrylamide chains and embedded functional materials.

Despite these advances, challenges such as mechanical and structural, selectivity, reusability and regeneration, environmental risks, and production and scalability continue to limit large-scale application. Moreover, most studies remain limited to laboratory-scale investigations, underscoring the need for pilot-scale testing and real-world wastewater evaluations. Future research should prioritize green fabrication strategies, designing multifunctional hydrogel materials to enhance selectivity toward targeted pollutants, improving recyclability, and comprehensively assessing the life-cycle and environmental risks associated with polyacrylamide-based hydrogels that leach from fabrication processes, as well as residual monomers or degradation by-products released during operation or disposal. Addressing these limitations will facilitate the transition of polyacrylamide-based hydrogel materials from lab-scale research to industrial scale, providing sustainable solutions for water treatment and environmental remediation. Overall, continued innovation in the fabrication and functionalization of

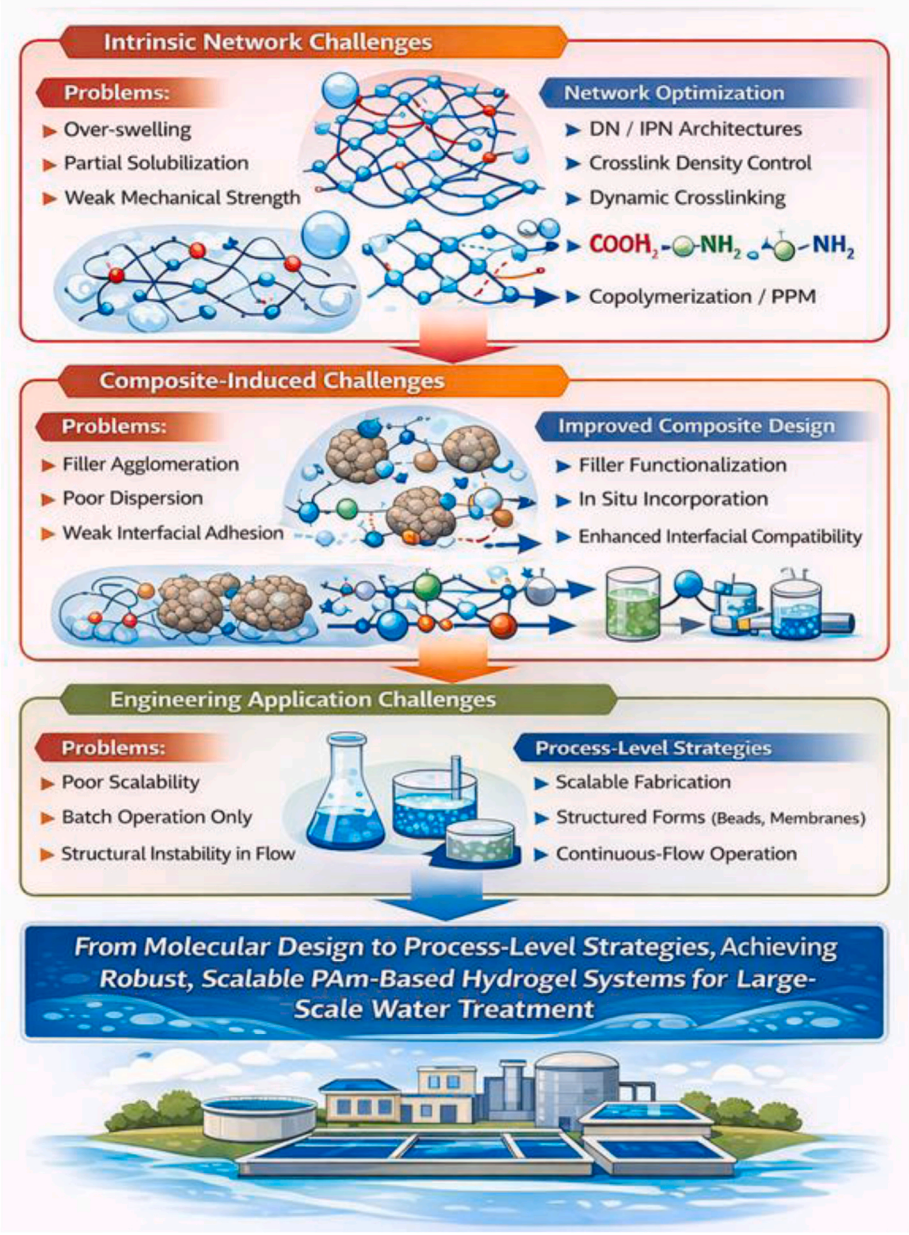

Scheme 9. Challenges and solutions for PAm-based hydrogel systems from fabrication to application scale.

polyacrylamide-based hydrogel materials is expected to play a vital role in advancing sustainable and efficient water treatment technologies.

CRediT authorship contribution statement

AbdElAziz A. Nayl: Conceptualization, Data curation, Formal analysis, Investigation, Software, Supervision, Writing – original draft. **Ismail M. Ahmed:** Conceptualization, Formal analysis, Resources, Writing – original draft. **Sultan A. Alsahli:** Conceptualization, Data curation, Formal analysis, Software. **Wael A.A. Arafa:** Conceptualization, Data curation, Resources, Software. **Abdullah A. AlShammari:** Data curation, Resources, Software. **Ahmed Hamad Alanazi:** Data curation, Formal analysis, Resources, Software. **Meshari D. Alanazi:** Data curation, Formal analysis, Resources, Software. **Mohammed Ezzeldien:** Data curation, Formal analysis, Resources, Software. **Stefan Bräse:** Conceptualization, Data curation, Investigation, Project administration, Software, Supervision, Writing – review & editing. **Ahmed I. Abd-Elhamid:** Conceptualization, Data curation, Formal analysis, Software, Writing – original draft.

Declaration of competing interest

The authors declare that they have no known competing financial interests or personal relationships that could have appeared to influence the work reported in this paper.

Acknowledgments

This work was funded by the Deanship of Graduate Studies and Scientific Research at Jouf University under grant No. (DGSSR-2025-FC-01037).

The authors acknowledge support from the KIT-Publication Fund of the Karlsruhe Institute of Technology.

Appendix A. Supplementary data

Supplementary data to this article can be found online at https://doi.org/10.1016/j.polymertesting.2026.109234.

List of Acronyms and Full Names (Alphabetical)

AA	Acrylic Acid
AAm	Acrylamide
AEBI	2-Aminoethylbenzimidazole
AK	Acid khaki
Alg	Alginate
AM	Acrylamide
AR	Acid red
APAm	Anionic Polyacrylamide
ARGET ATRP	Activators Regenerated by Electron Transfer Atom Transfer Radical Polymerization
ATRP	Atom Transfer Radical Polymerization
BB	Brilliant blue
CAA	Citric Acid–Acrylamide
κC	kappa-carrageenan
CF	Carbon Fiber
CMC	Carboxymethyl Cellulose
CNF/CNC	Cellulose nanofibers/Cellulose nanocrystals
CNTs	Carbon Nanotubes
CPAm	Cationic Polyacrylamide
CR	Congo red
CRP	Controlled/Living Radical Polymerization
CTS	Chitosan
CV	Crystal violet
DMAPAm	N, N-Dimethylaminopropylacrylamide
DTPA	Diethylenetriaminepentaacetic Acid
EDC	*1-Ethyl-3-(3-dimethylaminopropyl)*carbodiimide
EDTA	Ethylenediaminetetraacetic Acid
FB	Fast blue
Fe_3O_4	Magnetite
GG	Guar Gum
GO	Graphene Oxide
rGO	Reduced graphene oxide
HG	Hydrogel
HL	Halloysite
HPAm	Hydrolyzed Polyacrylamide
HPAmF	Hydrolyzed Polyacrylamide Fiber
LDH	Layered double hydroxide
MA	Methacrylic Acid
MB	Methylene Blue
MG	Malachite green
MHNT	Magnetic Halloysite Nanotubes
MO	Methyl orange
MOFs	Metal–Organic Frameworks
MRI	Magnetic Resonance Imaging
MV	Methyl Violet
MWCNTs	Multi-Walled Carbon Nanotubes
NIPAm	N-Isopropylacrylamide
NHS	N-Hydroxysuccinimide
NR	Neutral red
OP	Orange Peel
PAm	Polyacrylamide
PAA	Poly(acrylic acid)
PET-ATRP	Photoinduced Electron Transfer Atom Transfer Radical Polymerization
PET-RAFT	Photoinduced Electron Transfer Reversible Addition–Fragmentation Chain Transfer
PEI	Polyethyleneimine
PPM	Post-Polymer Modification
RAFT	Reversible Addition–Fragmentation Chain Transfer
RH	Rice Husk
RhB	Rhodamine B
SA	Sodium Alginate
SH	Thiol
TA	Tannic Acid
TiO_2	Titanium Dioxide
TOCNF	TEMPO-Oxidized Cellulose Nanofibers
UV	Ultraviolet
XO	Xylenol orange
ZIF	Zeolitic Imidazolate Framework

Data availability

No data was used for the research described in the article.

References

[1] S.J. Peighambardoust, H. Safarzadeh, Swelling behavior study of poly (methacrylic acid-co-acrylamide) nano-composite hydrogel adsorbents containing different nanoparticles, Desalination Water Treat. 298 (2023) 44–52, https://doi.org/10.5004/dwt.2023.29610.

[2] M. Zeeshan, T. Javed, C. Kumari, et al., Investigating the interactions between dyes and porous/composite materials: a comprehensive study, Sustainable Chemistry and Environment 9 (2025) 100217, https://doi.org/10.1016/j.scenv.2025.100217.

[3] O.F. Ccoyo, A.M. Lechuga-Chacon, R.L. Aranzábal-Carrasco, et al., Preparation of nanocomposite hydrogel based on Fe_3O_4-TMSPM/poly(HEMA-PEG6MA-IA) for the removal of methylene blue dye from aqueous solution, Results Chem. 12 (2024) 101888, https://doi.org/10.1016/j.rechem.2024.101888.

[4] M.A. Saad, E.R. Sadik, B.M. Eldakiky, et al., Recent developments in the application of hydrogels as draw agents in the forward osmosis desalination process, Adv. Compos. Hybrid Mater. 8 (2025) 309, https://doi.org/10.1007/s42114-025-01385-z.

[5] K.M. Sharifi, A. Poursattar Marjani, P. Gozali Balkanloo, Enhanced dye removal using montmorillonite modified with graphene quantum dots in sustainable salep nanocomposite hydrogell, Sci. Rep. 14 (2024) 7011, https://doi.org/10.1038/s41598-024-57729-0.

[6] P. Maijan, K. Junlapong, J. Arayaphan, et al., Synthesis and characterization of highly elastic superabsorbent natural rubber/polyacrylamide hydrogel, Polym. Degrad. Stabil. 186 (2021) 109499, https://doi.org/10.1016/j.polymdegradstab.2021.109499.

[7] H. Wang, G. Qu, X. Liu, et al., Hydrogel materials in agriculture: a review, J. Environ. Chem. Eng. 13 (2025) 116385, https://doi.org/10.1016/j.jece.2025.116385.

[8] Y. Guo, J. Bae, Z. Fang, et al., Hydrogels and hydrogel-derived materials for energy and water sustainability, Chem. Rev. 120 (2020) 7642–7707, https://doi.org/10.1021/acs.chemrev.0c00345.

[9] Y.C. Wu, H.M. Wang, L.L. Yuan, et al., Lignin-based functional hydrogels: an eco-friendly bulk material, ACS Sustain. Chem. Eng. 12 (2024) 17952–17976, https://doi.org/10.1021/acssuschemeng.4c06064.

[10] C. Xiong, Y. Chen, Y. Xu, et al., A review of complications of polyacrylamide hydrogel injection, Chinese Journal of Plastic and Reconstructive Surgery 5 (2023) 86–95, https://doi.org/10.1016/j.cjprs.2022.11.003.

[11] X. Song, N.N. Mensah, Y. Wen, et al., β-Cyclodextrin–polyacrylamide hydrogel for removal of organic micropollutants from water, Molecules 26 (2021) 5031, https://doi.org/10.3390/molecules26165031.

[12] G. Martínez, M. Castellano-Pozo, M. Merinero de los Santos, et al., Biodegradable polyacrylamide-based hydrogels with unique bactericidal and osteoinductive properties to improve the clinical success of porous titanium implants, Prog. Org. Coating 210 (2026) 109704, https://doi.org/10.1016/j.porgcoat.2025.109704.

[13] A. Beteta, L. Nurmi, L. Rosati, et al., Polymer chemical structure and its impact on EOR performance. Proceedings of the SPE Improved Oil Recovery Conference, 2020, https://doi.org/10.2118/200441-MS. SPE-200441-MS.

[14] N. Karimzadeh-Dehkordi, S. Shojaei, A. Asefnejad, et al., The effect of three types of cross-linked hydrogels and volume fraction of polyacrylamide on the swelling and thermal behavior using molecular dynamics simulation, J. Mater. Res. Technol. 24 (2023) 4627–4638, https://doi.org/10.1016/j.jmrt.2023.04.102.

[15] L. Tang, D. Zhao, B. Wang, et al., Adsorption and in vitro controlled–release properties of a soybean cellulose nanocrystal/polyacrylamide–based hydrogel as a carrier for different polyphenols, Food Chem. 479 (2025) 143843, https://doi.org/10.1016/j.foodchem.2025.143843.

[16] M.H. Mohamed, M.E. Mohyaldinn, Polyacrylamide-based solutions: a comprehensive review on nanomaterial integration, supramolecular design, and sustainable approaches for integrated reservoir management, Polymers 17 (2025) 2202, https://doi.org/10.3390/polym17162202.

[17] S. Awasthi, J.K. Gaur, M.S. Bobji, et al., Nanoparticle-reinforced polyacrylamide hydrogel composites for clinical applications: a review, J. Mater. Sci. 57 (2022) 8041–8063, https://doi.org/10.1007/s10853-022-07146-3.

[18] H. Hameed, S. Faheem, A.C. Paiva-Santos, et al., A comprehensive review of hydrogel-based drug delivery systems: classification, properties, recent trends,

and applications, AAPS PharmSciTech 25 (2024) 64, https://doi.org/10.1208/s12249-024-02786-x.
[19] G. Sennakesavan, M. Mostakhdemin, L.K. Dkhar, et al., Acrylic acid/acrylamide based hydrogels and its properties - a review, Polym. Degrad. Stabil. 180 (2020) 109308, https://doi.org/10.1016/j.polymdegradstab.2020.109308.
[20] Y. Wu, S. Li, G. Chen, Hydrogels as water and nutrient reservoirs in agricultural soil: a comprehensive review of classification, performance, and economic advantages, Environ. Dev. Sustain. 26 (2024) 24653–24685, https://doi.org/10.1007/s10668-023-03706-y.
[21] H. Du, S. Shi, W. Liu, et al., Processing and modification of hydrogel and its application in emerging contaminant adsorption and in catalyst immobilization: a review, Environ. Sci. Pollut. Control Ser. 27 (2020) 12967–12994, https://doi.org/10.1007/s11356-020-08096-6.
[22] Y. Yang, Q. Zhu, X. Peng, et al., Hydrogels for the removal of the methylene blue dye from wastewater: a review, Environ. Chem. Lett. 20 (2022) 2665–2685, https://doi.org/10.1007/s10311-022-01414-z.
[23] A.E. Segneanu, L.E. Bejenaru, C. Bejenaru, et al., Advancements in hydrogels: a comprehensive review of natural and synthetic innovations for biomedical applications, Polymers 17 (2025) 2026, https://doi.org/10.3390/polym17152026.
[24] E. Olaret, B. Bălănucă, J. Ghitman, et al., Reinforcement of nanostructured polyacrylamide hydrogels through the generation of secondary physical network using the nanoparticles' functional groups, Polym. Test. 132 (2024) 108380, https://doi.org/10.1016/j.polymertesting.2024.108380.
[25] P. Lu, D. Ruan, M. Huang, et al., Harnessing the potential of hydrogels for advanced therapeutic applications: current achievements and future directions, Signal Transduct. Targeted Ther. 9 (2024) 166, https://doi.org/10.1038/s41392-024-01852-x.
[26] A. Kumar, S. Pandey, K. Kumar, Hydrogels: classification, cross-linking methods, characteristics, and current trends in biomedical applications, Polym. Bull. 83 (2026) 49, https://doi.org/10.1007/s00289-025-06053-2.
[27] B.G. Soliman, A.K. Nguyen, J.J. Gooding, et al., Advancing synthetic hydrogels through nature-inspired materials chemistry, Adv. Mater. 36 (2024) e2404235, https://doi.org/10.1002/adma.202404235.
[28] S. Pruksawan, J.E.T. Loh, K.H.Z. Chong, et al., Tough, self-healing, and weldable hydrogels via thermal engineering of optimized multi-scale structures, Commun. Mater. 6 (2025) 103, https://doi.org/10.1038/s43246-025-00818-y.
[29] V. Manimaran, R.P. Nivetha, T. Tamilanban, et al., Nanogels as novel drug nanocarriers for CNS drug delivery, Front. Mol. Biosci. 10 (2023) 1232109, https://doi.org/10.3389/fmolb.2023.1232109.
[30] S.A. Jaseem, P. Rahmani, T. Sakorikar, et al., Liquid metals as initiators of free-radical polymerization of hydrogels: a perspective, Adv. Funct. Mater. 36 (2026) e14024, https://doi.org/10.1002/adfm.202514024.
[31] R. Guerrero-Santos, E. Saldívar-Guerra, I. Zapata-González, J. Bonilla-Cruz, E. Vivaldo-Lima, Free-radical polymerization, in: E. Saldívar-Guerra, E. Vivaldo-Lima (Eds.), Polymer Science, Engineering, and Sustainability, 2025, https://doi.org/10.1002/9781119820123.ch3.
[32] C. Zuo, P. Liu, J. Du, X. Chen, X. Zhang, R. Zhao, B. Wen, J. Zhao, Polymer nano-network topological fluid via trifunctional nano-grafting and multifunctional free radical capture groups strategy for ultra-high temperature and deep reservoir stimulation, Chem. Eng. J. 528 (2026) 172297, https://doi.org/10.1016/j.cej.2025.172297.
[33] M. Roa-Luna, G. de losSantos Villarreal, R. Torres-Lubián, E. Saldívar-Guerra, Recent applications of reversible deactivation radical polymerization techniques in nanotechnology and bio-nanoscience, J. Appl. Polym. Sci. 143 (2026) e58095, https://doi.org/10.1002/app.58095.
[34] S. Shanmugam, J.T. Xu, C. Boyer, Photoinduced electron transfer–reversible addition–fragmentation chain transfer (PET-RAFT) polymerization of vinyl acetate and N-Vinylpyrrolidinone: kinetic and oxygen tolerance study, Macromolecules 47 (2014) 4930–4942, https://doi.org/10.1021/ma500842u.
[35] X. Jiang, M. Xi, L. Bai, et al., Surface-initiated PET-ATRP and mussel-inspired chemistry for surface engineering of MWCNTs and application in self-healing nanocomposite hydrogels, Mater. Sci. Eng., C 109 (2020) 110553, https://doi.org/10.1016/j.msec.2019.110553.
[36] W. Zhao, C. Li, J. Chang, et al., Advances and prospects of RAFT polymerization-derived nanomaterials in MRI-assisted biomedical applications, Prog. Polym. Sci. 146 (2023) 101739, https://doi.org/10.1016/j.progpolymsci.2023.101739.
[37] Y. Choi, H.Y. Koh, J.Y. Han, et al., Synthesis of hydrogel-based microgels and nanogels toward therapeutic and biomedical applications, Appl. Sci. 15 (2025) 1368, https://doi.org/10.3390/app15031368.
[38] L.A. Beneditt-Jimenez, I. Cruz-Cruz, N.A. Ulloa-Castillo, et al., Step-by-Step analysis of a copper-mediated surface-initiated atom-transfer radical polymerization process for polyacrylamide brush synthesis through infrared spectroscopy and contact angle measurements, Polymers 17 (2025) 1835, https://doi.org/10.3390/polym17131835.
[39] B. Wu, E. Feng, Y. Liao, et al., Brush-modified hydrogels: preparation, properties, and applications, Chem. Mater. 34 (2022) 6210–6231, https://doi.org/10.1021/acs.chemmater.2c01666.
[40] K. Matyjaszewski, Future directions for atom transfer radical polymerizations, Chem. Mater. 36 (2024) 1775–1778, https://doi.org/10.1021/acs.chemmater.3c03213.
[41] S. Dworakowska, F. Lorandi, A. Gorczynski, et al., Toward green atom transfer radical polymerization: current status and future challenges, Adv. Sci. 9 (2022) 2106076, https://doi.org/10.1002/advs.202106076.
[42] K. Wang, J. Qiu, W. Huang, et al., Preparation of crosslinked lignin-polyacrylamide hydrogel with high resistance to temperature and salinity, Int. J. Biol. Macromol. 296 (2025) 139730, https://doi.org/10.1016/j.ijbiomac.2025.139730.
[43] C. Peng, S. Gou, Q. Wu, et al., Modified acrylamide copolymers based on β-cyclodextrin and twin-tail structures for enhanced oil recovery through host–guest interactions, New J. Chem. 43 (2019) 5363–5371, https://doi.org/10.1039/C8NJ06432F.
[44] H. Omidian, R.L. Wilson, Enhancing hydrogels with quantum dots, J. Compos. Sci. 8 (2024) 203, https://doi.org/10.3390/jcs8060203.
[45] M. Moghadam, A. Dalvand, E. Arkan, et al., Modified polyacrylamide nanofiber membrane for efficient nitrate removal from landfill leachate, Sci. Rep. 15 (2025) 20826, https://doi.org/10.1038/s41598-025-05093-y.
[46] J. Li, M. Long, F. Xu, et al., Microneedles self-implanting Astragalus polysaccharides-hybridized composite hydrogel combined with minoxidil to enhance in situ anti-androgenetic alopecia, Drug Deliv. Transl. Res. (2026), https://doi.org/10.1007/s13346-026-02053-5.
[47] S.F. Umashankar, M.S. Narayanasamy, A comprehensive review of nanogel-based drug delivery systems, Cureus 16 (2024) e68633, https://doi.org/10.7759/cureus.68633.
[48] T. Sandu, A.L. Chiriac, A. Zaharia, et al., New trends in preparation and use of hydrogels for water treatment, Gels 11 (2025) 238, https://doi.org/10.3390/gels11040238.
[49] G. Sharma, B. Thakur, M. Naushad, et al., Applications of nanocomposite hydrogels for biomedical engineering and environmental protection, Environ. Chem. Lett. 16 (2018) 113–146, https://doi.org/10.1007/s10311-017-0671-x.
[50] A.M. Farahani, R.Z. Moghadam, M. Marandi, Electrospinning of nanofibers and the functional potential of starch: a comprehensive review, Discover Nano 21 (2026) 24, https://doi.org/10.1186/s11671-026-04434-8.
[51] W.M. Seleka, E. Makhado, Synthesis and characterization of polyacrylamide–graphene oxide hydrogel nanocomposite for dye removal, Int. J. Biol. Macromol. 305 (2025) 141015, https://doi.org/10.1016/j.ijbiomac.2025.141015.
[52] I. lebkiri, B. Abbou, A. El Amri, et al., Investigation of polyacrylamide as potential adsorbent for efficient heavy metal removal: insights into the swelling mechanism, adsorption isotherms, and kinetics, Euro-Mediterr J Environ Integr 10 (2025) 2213–2230, https://doi.org/10.1007/s41207-025-00787-1.
[53] J. Ke, B. Han, W. Wang, et al., Three-dimensional electrospun nanofiber scaffolds: fabrication methods and biomedical applications, Macromol. Biosci. 26 (2026) e00573, https://doi.org/10.1002/mabi.202500573.
[54] H. Mazi, K. Erbalci, Adsorption of methylene blue from wastewater using poly (acrylamide-co-itaconic acid-co-stearyl methacrylate) hydrogels, Polymer 335 (2025) 128837, https://doi.org/10.1016/j.polymer.2025.128837.
[55] X. Yin, T. Ke, H. Zhu, P. Xu, H. Wang, Efficient removal of heavy metals from aqueous solution using licorice residue-based hydrogel adsorbent, Gels 6 (2023) 559, https://doi.org/10.3390/gels9070559.
[56] M.A. Ludeña, F.d.L. Meza, R.I. Huamán, A.M. Lechuga, A.C. Valderrama, Preparation and characterization of Fe_3O_4/Poly(HEMA-co-IA) magnetic hydrogels for removal of methylene blue from aqueous solution, Gels 10 (2024) 15, https://doi.org/10.3390/gels10010015.
[57] H. Hosseinzadeha, N. Khoshnood, Removal of cationic dyes by poly(AA-co-AMPS)/montmorillonite nanocomposite hydrogel, Desalination Water Treat. 57 (2016) 6372–6383, https://doi.org/10.1080/19443994.2015.1008052.
[58] L. Zhang, H. Li, G. Wang, S. Li, Synthesis and characterization of chitosan/polyacrylamide hydrogel grafted poly(N-methylaniline) for methyl red removal, Int. J. Biol. Macromol. 187 (2021) 240–250, https://doi.org/10.1016/j.ijbiomac.2021.07.124.
[59] A. Das, A. Babu, S. Chakraborty, et al., Poly(N-isopropylacrylamide) and its copolymers: a review on recent advances in the areas of sensing and biosensing, Adv. Funct. Mater. 34 (2024) 2402432, https://doi.org/10.1002/adfm.202402432.
[60] Y. Song, S. Zhou, H. Li, et al., Controllable synthesis of cellulose/methylene bisacrylamide aerogels for enhanced adsorption performance, J. Appl. Polym. Sci. 138 (2021) e50204, https://doi.org/10.1002/app.50204.
[61] Y. Pan, M. Ouchi, Post-polymerization modification enabling library synthesis of highly isotactic polyacrylamides carrying different pendant groups, Commun. Chem. 8 (2025) 259, https://doi.org/10.1038/s42004-025-01663-3.
[62] Ali M. El Shafey, M.K. Abdel-Latif, H.M. Abd El-Salam, The facile synthesis of poly (acrylate/acrylamide) titanium dioxide nanocomposite for groundwater ammonia removal, Desalination Water Treat. 212 (2021) 61–70, https://doi.org/10.5004/dwt.2021.26637.
[63] Y. Wang, Y. Lu, H. Zhong, et al., Efficient adsorption and utilisation of methylene blue by NaOH-Modified nanocellulose–polyacrylamide interpenetrating network gels, Gels 11 (2025) 252, https://doi.org/10.3390/gels11040252.
[64] R.A. Ramli, W. Abd El-Fattah, M. Sillanpää, A. Guesmi, N. Ben Hamadi, Polysaccharide-based biodegradable hydrogel adsorbents for sustainable water treatment: functional enhancements and environmental sustainability – a critical review, Int. J. Biol. Macromol. 351 (2026) 151028, https://doi.org/10.1016/j.ijbiomac.2026.151028.
[65] V. Penkavova, A. Spalova, J. Tihon, Polyacrylamide hydrogel-based nanocomposites containing graphene, kaolin or laponite: physico-mechanical characterization and adsorption properties, Mater. Today 34 (2023) 105150, https://doi.org/10.1016/j.mtcomm.2022.105150.
[66] I.K. Abdel Maksoud, I.K. Bassioni, G. Nady, et al., Radiation synthesis and chemical modifications of p(AAm-co-AAc) hydrogel for improving their adsorptive removal of metal ions from polluted water, Sci. Rep. 13 (2023) 21879, https://doi.org/10.1038/s41598-023-49009-0.

[67] F. Palazon, C.M. Benavides, D. Léonard, et al., Carbodiimide/NHS derivatization of COOH-terminated SAMs: activation or byproduct formation? Langmuir 30 (2014) 4545–4550, https://doi.org/10.1021/la5004269.

[68] S. Keleştemur, M. Altunbek, M. Culha, Influence of EDC/NHS coupling chemistry on stability and cytotoxicity of ZnO nanoparticles modified with proteins, Appl. Surf. Sci. 403 (2017) 455–463, https://doi.org/10.1016/j.apsusc.2017.01.235.

[69] L. Taiariol, C. Chaix, C. Farre, et al., Click and bioorthogonal chemistry: the future of active targeting of nanoparticles for nanomedicines? Chem. Rev. 122 (2022) 340–384, https://doi.org/10.1021/acs.chemrev.1c00484.

[70] L. Alsaka, L. Alsaka, A. Altaee, et al., A review of hydrogel application in wastewater purification, Separations 12 (12) (2025) 51, https://doi.org/10.3390/separations12020051, 2.

[71] A.K. Agrahari, S. Rajkhowa, S.K. Singh, et al., Growing impact of bioorthogonal click chemistry in cell surface glycan labeling, Curr. Org. Chem. 29 (2025) 495–517, https://doi.org/10.2174/0113852728326779240911055902.

[72] X. Zou, H. Zhang, T. Chen, et al., Preparation and characterization of polyacrylamide/sodium alginate microspheres and its adsorption of MB dye, Colloids Surf. A Physicochem. Eng. Asp. 567 (2019) 184–192, https://doi.org/10.1016/j.colsurfa.2018.12.019.

[73] G. Bayramoglu, M. Kılıc, I. Acıkgoz-Erkaya, et al., Preparation of hydrogel adsorbents with functional sulfone groups for removal of cationic dyes from aqueous solution, J. Polym. Res. 32 (2025) 242, https://doi.org/10.1007/s10965-025-04466-1.

[74] H.S. Alkhaldi, M. Baata, F. Alhajri, et al., Recent progress in the preparation and environmental applications of functionalized adsorbent hydrogel: a review, RSC Adv. 16 (2026) 7287–7336, https://doi.org/10.1039/d5ra07905e.

[75] H. Li, J. Zhong, C. Bi, et al., ROS-responsive robust hydrogels based on thiol-ene click chemistry for enhancing the healing of infected wounds, Bioeng. Transl. Med. (2026) e70143, https://doi.org/10.1002/btm2.70143.

[76] B. Jia, X. Zhao, X. Wan, et al., Biofunctional and interface-engineered hydrogels for advanced tissue engineering, Adv. Healthcare Mater. 14 (2025) 2502146, https://doi.org/10.1002/adhm.202502146.

[77] L. Zou, Y. Li, S. Feng, Z. Wang, H. Xiao, S. Chen, Y. Wang, L. He, X. Mao, Innovations and applications of composite hydrogels: from polymer-based systems to metal-ion-doped and functional nanomaterial-enhanced architectures, Small 21 (2025) 2503147, https://doi.org/10.1002/smll.202503147.

[78] E. Oläreț, Ș.I. Voicu, R. Oprea, F. Miculescu, L. Butac, I.-C. Stancu, A. Serafim, Nanostructured polyacrylamide hydrogels with improved mechanical properties and antimicrobial behavior, Polymers 4 (2022) 2320, https://doi.org/10.3390/polym14122320.

[79] Q. Yang, Y. Zhang, Z. Yu, K. Lv, Y. Ye, J. Zhou, N. Lin, Mechanical enhancements and structural simulation of reactive poly(ethylene glycol) and cellulose nanocrystals to polyacrylamide hydrogels, Int. J. Biol. Macromol. 321 (2025) 146494, https://doi.org/10.1016/j.ijbiomac.2025.146494.

[80] E. Olaret, B. Balanuca, J. Ghitman, I.-C. Stancu, A. Serafim, Reinforcement of nanostructured polyacrylamide hydrogels through the generation of secondary physical network using the nanoparticles' functional groups, Polym. Test. 132 (2024) 108380, https://doi.org/10.1016/j.jwpe.2021.102412.

[81] F. Seidi, W. Zhao, H. Xiao, Y. Jin, C. Zhao, PLayer-by-Layer assembly for surface tethering of thin-hydrogel films: design strategies and applications, Chem. Rec. 2020 (2020) 857–881, https://doi.org/10.1002/tcr.202000007.

[82] H. Chen, R. Feng, T. Xia, Z. Wen, Q. Li, X. Qiu, B. Huang, Y. Li, Progress in surface modification of titanium implants by hydrogel coatings, Gels 9 (2023) 423, https://doi.org/10.3390/gels9050423.

[83] H. Chen, X. Nie, Q. Hu, X. Ma, J. Li, C. Gao, Coating modification techniques for medical catheters: from methods to applications, BME Horiz 4 (2026) 202539, https://doi.org/10.70401/bmeh.2026.0020.

[84] X. Chen, H. Yan, C. Bao, Q. Zhu, Z. Liu, Y. Wen, Z. Li, T. Zhang, Q. Lin, Fabrication and evaluation of homogeneous alginate/polyacrylamide–chitosan–gelatin composite hydrogel scaffolds based on the interpenetrating networks for tissue engineering, Polym. Eng. Sci. 62 (2022) 116, https://doi.org/10.1002/pen.25838.

[85] L. Hanyková, J. Šťastná, I. Krakovský, Influence of composition and network formation sequence on the responsive behavior of double-network hydrogels, Gels 12 (2026) 260, https://doi.org/10.3390/gels12030260.

[86] M. Ma, K. Lu, R. Han, Q. Luo, X. Li, C. Meng, L. Yang, Z. Zhang, Carrageenan/polyacrylamide semi-interpenetrating network bio-hydrogel for high-efficiency uranium capture, Process Saf. Environ. Prot. 201 (2025) 107430, https://doi.org/10.1016/j.psep.2025.107430.

[87] G. Liu, Q. Ma, X. Zhang, Agar-polyacrylamide dual network hydrogel-carbon nanotube composites with long-term stability for high efficient solar water purification, Compos. Commun. 53 (2025) 102248, https://doi.org/10.1016/j.coco.2025.102248.

[88] R.K. Kumar, H. Dugga, P.K. Samantara, Emerging macromolecular approaches to pore engineering and interfacial control using interpenetrating polymer networks: recent developments, Macromol. Rapid Commun. 47 (2026) e00627, https://doi.org/10.1002/marc.202500627.

[89] S. Sun, G. Zhang, X. Li, T. Li, M. Fu, Q. Han, H. He, X. Tang, C. Zhang, PEG-engineered semi-interpenetrating network hydrogel with superior deformability and robustness for ultra-sensitive pressure sensing, J. Colloid Interface Sci. 698 (2025) 138019, https://doi.org/10.1016/j.jcis.2025.138019.

[90] Y. Feng, G. Xu, S. Liu, Z. Wu, B. Chen, C. Lu, C. Lu, Dual-Cross-linking semi-interpenetrating network ionogels with ultra-stretchability and harsh environment tolerance for high-performance wearable sensing, Ind. Eng. Chem. Res. 65 (2026) 7014–7024, https://doi.org/10.1021/acs.iecr.5c04820.

[91] G.K. Gokul, S. Parathakkatt, Rheo-mechanical characterisation of polyol-modified polyacrylamide-gellan gum interpenetrating network organohydrogels, J. Polym. Environ. 34 (2026) 53, https://doi.org/10.1007/s10924-026-03785-8.

[92] X. Liu, Y. Deng, P. Wang, et al., Improved tough and conductive polyacrylamide/sodium alginate dual-network hydrogel by ionic liquid for flexible capacitor and multifunctional sensor, J. Polym. Res. 32 (2025) 306, https://doi.org/10.1007/s10965-025-04534-6.

[93] F. Ccoyo Ore, F.d.L.M. López, A.C. Valderrama Negrón, M.A. Ludeña Huaman, Fe_3O_4/Poly(acrylic acid) composite hydrogel for the removal of methylene blue and crystal violet from aqueous media, Chemistry 7 (2025) 156, https://doi.org/10.3390/chemistry7050156.

[94] V. Losetty, S.K. Lakkaboyana, H.Y. Chappidi, et al., Transformative applications of polymer-based metal oxide nanocomposites in medicine, industry, and environmental remediation: a review, J. Inorg. Organomet. Polym. 36 (2026) 64–96, https://doi.org/10.1007/s10904-025-03707-6.

[95] Z. Zhang, Y. Lu, S. Gao, S. Wu, Sustainable and efficient wastewater treatment using cellulose-based hydrogels: a review of heavy metal, dye, and micropollutant removal applications, Separations 12 (2025) 72, https://doi.org/10.3390/separations12030072.

[96] K.G. Dev, M. Pal, Challenges and future perspectives of hydrogels in wastewater treatment, in: S. Bardhan, M.P. Shah (Eds.), Applications of Hydrogels in Modern Wastewater Treatment. Advances in Wastewater Research, Springer, Singapore, 2026, https://doi.org/10.1007/978-981-95-1598-1_15.

[97] I. lebkiri, B. Abbou, A. El Amri, et al., Investigation of polyacrylamide as potential adsorbent for efficient heavy metal removal: insights into the swelling mechanism, adsorption isotherms, and kinetics, Euro-Mediterr J Environ Integr 10 (2025) 2213–2230, https://doi.org/10.1007/s41207-025-00787-1.

[98] I. Lebkiri, B. Abbou, L. Kadiri, A. Ouass, A. Elamri, H. Ouaddari, et al., Equilibrium, kinetic data, and adsorption mechanism for lead adsorption onto polyacrylamide hydrogel, JOTCSA 8 (3) (2021) 731–748, https://doi.org/10.18596/jotcsa.912479.

[99] Siti Nurul Ain Md Jamil, Mastura Khairuddin and rusli daik preparation of acrylonitrile/acrylamide copolymer beads via a redox method and their adsorption properties after chemical modification, E-Polymers 15 (1) (2015) 45–54.

[100] X. Chen, Y. Liu, H. Wang, Polyacrylamide/graphene oxide hydrogels as efficient adsorbents for wastewater treatment: mechanism and performance evaluation, J. Mol. Liq. 343 (2021) 117382, https://doi.org/10.1016/j.molliq.2021.117382.

[101] E. Aljamal, A.A. Al-Massaedh, F. Khalili, et al., Investigations on the equilibrium, kinetics and thermodynamics of anionic polyacrylamide-based monolith adsorption of uranium (VI) from aqueous solution, Jordan J. Chem. 19 (2024) 49–64, https://doi.org/10.34041/jjc.2024.19.49.

[102] A.A. Al-Massaedh, F.I. Khalili, et al., Removal of heavy metal ions from aqueous solution by anionic polyacrylamide-based monolith: equilibrium, kinetic and thermodynamicstudies, Desalination Water Treat. 228 (2021) 297–311, https://doi.org/10.5004/dwt.2021.27339.

[103] K. Fujimoto, B.A. Omondi, S. Kawano, et al., Ionized acrylamide-based copolymer/terpolymer hydrogels for recovery of positive and negative heavy metal ions, PLoS One 19 (2024) e0298047, https://doi.org/10.1371/journal.pone.0298047.

[104] Z. Wang, Q. Yang, X. Zhao, et al., Facile fabrication of a low-cost alginate-polyacrylamide composite aerogel for the highly efficient removal of lead ions, Appl. Sci. 9 (2019) 4754, https://doi.org/10.3390/app9224754.

[105] Y. Chen, X. Liu, R. Zhou, et al., Sodium alginate/cellulose nanofiber/polyacrylamide composite hydrogel microspheres for efficient removal of heavy metal from water, Chem. Select 10 (2025) e202405988, https://doi.org/10.1002/slct.202405988.

[106] H. Jiang, Y. Yang, Z. Lin, et al., Preparation of a novel bio-adsorbent of sodium alginate grafted polyacrylamide/graphene oxide hydrogel for the adsorption of heavy metal ion, Sci. Total Environ. 744 (2020) 140653, https://doi.org/10.1016/j.scitotenv.2020.140653.

[107] M. Alizadeh, S.J. Peighambardoust, R. Foroutan, et al., Efficacious adsorption of divalent nickel ions over sodium alginate-g-poly(acrylamide)/hydrolyzed Luffa cylindrica-$CoFe_2O_4$ bionanocomposite hydrogel, Int. J. Biol. Macromol. 254 (2024) 127750, https://doi.org/10.1016/j.ijbiomac.2023.127750.

[108] H. Wang, M. Huang, L. Li, et al., Highly efficient copper ions removal by sodium alginate/sodium humate@Polyacrylamide: adsorption behavior and removal mechanism, Water, Air, Soil Pollut. 235 (2024) 250, https://doi.org/10.1007/s11270-024-07046-z.

[109] C.B. Godiya, X. Cheng, D. Li, et al., Carboxymethyl cellulose/polyacrylamide composite hydrogel for cascaded treatment/reuse of heavy metal ions in wastewater, J. Hazard. Mater. 364 (2019) 28–38, https://doi.org/10.1016/j.jhazmat.2018.09.076.

[110] J. Ma, G. Zhou, L. Chu, et al., Efficient removal of heavy metal ions with an EDTA functionalized chitosan/polyacrylamide double network hydrogel, ACS Sustain. Chem. Eng. 5 (2017) 843–851, https://doi.org/10.1021/acssuschemeng.6b02181.

[111] S. Pavithra, G. Thandapani, S. Sugashini, et al., Batch adsorption studies on surface tailored chitosan/orange peel hydrogel composite for the removal of Cr (VI) and Cu(II) ions from synthetic wastewater, Chemosphere 271 (2021) 129415, https://doi.org/10.1016/j.chemosphere.2020.129415.

[112] Y. He, S. Gou, L. Zhou, et al., Amidoxime-functionalized polyacrylamide-modified chitosan containing imidazoline groups for effective removal of Cu^{2+} and Ni^{2+}, Carbohydr. Polym. 252 (2021) 117160 https://doi.org/10.1016/j.carbpol.2020.117160.

[113] Q. Alshamusi, K. Hameed, A. Taher, et al., Efficiency of chitosan-grafted poly (Carboxymethyl Cellulose-Co-Acrylamide) Nano Hydrogel for cadmium (II) removal: Batch adsorption study, J. Nanostruct. 14 (2024) 1122–1133, https://doi.org/10.22052/JNS.2024.04.013.

[114] M.A. Habila, Z.A. AlOthman, A.M. El-Toni, et al., One-step carbon coating and polyacrylamide functionalization of Fe_3O_4 nanoparticles for enhancing magnetic adsorptive-remediation of heavy metals, Molecules 22 (2017) 2074, https://doi.org/10.3390/molecules22122074.

[115] M. Keshawy, R.S. Kamal, A.E. Abdelhamid, et al., Novel green sustainable hydrogel composites based on guar gum and algal species for wastewater remediation, Int. J. Environ. Sci. Technol. 22 (2025) 8895–8918, https://doi.org/10.1007/s13762-024-06159-6.

[116] M. Zhao, Z. Gong, L. Wang, et al., High-efficiency heavy metal adsorption in complex systems via FeS-modified poly(acrylamide-co-2-acrylamido-2-methylpropane sulfonic acid)-g-carboxymethylcellulose-Ca(II) hydrogel, J. Environ. Chem. Eng. 13 (2025) 118327, https://doi.org/10.1016/j.jece.2025.118327.

[117] L. Mo, S. Zhang, F. Qi, et al., Highly stable cellulose nanofiber/polyacrylamide aerogel via in-situ physical/chemical double crosslinking for highly efficient Cu (II) ions removal, Int. J. Biol. Macromol. 209 (2022) 1922–1932, https://doi.org/10.1016/j.ijbiomac.2022.04.167.

[118] Y. Zhang, X. Zhao, W. Yang, et al., Enhancement of mechanical property and absorption capability of hydrophobically associated polyacrylamide hydrogels by adding cellulose nanofiber, Mater. Res. Express 7 (2020) 015319, https://doi.org/10.1088/2053-1591/ab6373.

[119] Y. Pei, M. Li, W. Li, et al., Cr(VI) removal by cellulose-based composite adsorbent with a double-network structure, Colloids Surf., A 625 (2021) 126963, https://doi.org/10.1016/j.colsurfa.2021.126963.

[120] X. Yin, H. Zhu, T. Ke, et al., Preparation of hydrogels based Radix isatidis residue grafted with acrylic acid and acrylamide for the removal of heavy metals, Water 14 (2022) 3811, https://doi.org/10.3390/w14233811.

[121] Z.M. Şenol, Polyacrylamide@Tangerine peel composite: a novel adsorbent for efficient removal of Pb^{2+} ions from water, Cumhuriyet Sci. J. 45 (2024) 322–330, https://doi.org/10.17776/csj.1452166.

[122] A.E. Samuel, O.O. Olotu, I.C. Nwankwo, et al., Utilization of polyacrylamide grafted brewer spent grain (BSG) for sorption of Cd^{2+}, Cu^{2+} and Pb^{2+} ions in aqueous solution, Int. J. Eng. Trends Technol. 43 (2017) 47–52, https://doi.org/10.14445/22315381/IJETT-V43P208.

[123] Z.S. Keskin, Efficient adsorption of Pb(II) ions using novel adsorbent polyacrylamide/coffee ground composite: isotherm, kinetic and thermodynamic studies, Polym. Bull. 81 (2024) 8425–8446, https://doi.org/10.1007/s00289-023-05111-x.

[124] K. Moreno-Sader, A. García-Padilla, A. Realpe, et al., Removal of heavy metal water pollutants (Co^{2+} and Ni^{2+}) using polyacrylamide/sodium montmorillonite (PAM/Na-MMT) nanocomposites, ACS Omega 4 (2019) 10834–10844, https://doi.org/10.1021/acsomega.9b00981.

[125] N. Nuryanthi, A.R. Syahputra, O. Oktaviani, et al., Preparation of Zeolite-g-Polyacrylamide using radiation induced grafting and its adsorption isotherms study on several heavy metal ions, Macromol. Symp. 391 (2020) 1900139, https://doi.org/10.1002/masy.201900139.

[126] Y. Hui, Q. Huan, Y. Hu, et al., Permeability and adsorption mechanisms of surfactant and polymer modified bentonite in Pb(II) and Cr(VI) contaminated groundwater, Sep. Purif. Technol. 366 (2025) 132774, https://doi.org/10.1016/j.seppur.2025.132774.

[127] A.E. Baradaran Mahdavi, E. Panahpour, R.J. Kalbasi, et al., Investigation of adsorption activity of poly (acrylamide–styrene)/bentonite nanocomposite for efficient removal of manganese ions from aqueous solution, Desalination Water Treat. 210 (2021) 316–329, https://doi.org/10.5004/dwt.2021.26505.

[128] Z.M. Şenol, Z.S. Keskin, A. Özer, et al., Application of kaolinite-based composite as an adsorbent for removal of uranyl ions from aqueous solution: kinetics and equilibrium study, J. Radioanal. Nucl. Chem. 331 (2022) 403–414, https://doi.org/10.1007/s10967-021-08070-7.

[129] E.L.M. Amutenya, F. Zhou, J. Liu, et al., Preparation of humic acid-bentonite polymer composite: a heavy metal ion adsorbent, Heliyon 8 (2022) e09720, https://doi.org/10.1016/j.heliyon.2022.e09720.

[130] J. Li, Y. Zheng, X. Feng, et al., Adsorption removal of Ni(II) and phenol from aqueous solution by modified attapulgite and its composite hydrogel, Environ. Technol. 42 (2021) 2413–2427, https://doi.org/10.1080/09593330.2019.1703821.

[131] A. Vahedi, M. Rahmani, Z. Rahmani, et al., Application of polymer-sepiolite composites for adsorption of Cu(II) and Ni(II) from aqueous solution: equilibrium and kinetic studies, E-Polymers 18 (2018) 217–228, https://doi.org/10.1515/epoly-2017-0170.

[132] A. Sharma, P.P. Pande, P. Khare, et al., A study of polyacrylamide-pumice composite for fast removal of copper ions from aqueous solutions: Synthesis, kinetics and thermodynamics, Iran. J. Chem. Chem. Eng. 42 (2023) 1758–1774, https://doi.org/10.30492/ijcce.2022.551167.5262.

[133] S. Gu, L. Wang, X. Mao, et al., Selective adsorption of Pb(II) from aqueous solution by triethylenetetramine-grafted polyacrylamide/vermiculite, Materials 11 (2018) 514, https://doi.org/10.3390/ma11040514.

[134] X. Hu, X. Luo, G. Xiao, et al., Low-cost novel silica@polyacrylamide composites: fabrication, characterization, and adsorption behavior for cadmium ion in aqueous solution, Adsorption 26 (2020) 1051–1062, https://doi.org/10.1007/s10450-020-00225-4.

[135] H.B. Garud, S.A. Jadhav, S.P. Jadhav, et al., Synthesis and testing of polyacrylamide-grafted waste sand derived composite adsorbent for water purification, Polym. Adv. Technol. 34 (2023) 1757–1768, https://doi.org/10.1002/pat.6009.

[136] M. Ma, Y. Li, D. Wang, et al., Highly efficient and sustainable polyacrylic acid-polyacrylamide double-network hydrogels prepared by cross-linking of waste residues for heavy metals ions removal, J. Environ. Chem. Eng. 12 (2024) 114294, https://doi.org/10.1016/j.jece.2024.114294.

[137] E. Ebrahimpour, A. Kazemi, Mercury(II) and lead(II) ions removal using a novel thiol-rich hydrogel adsorbent; PHPAm/Fe_3O_4@SiO_2-SH polymer nanocompositel, Environ. Sci. Pollut. Res. 30 (2023) 13605–13623, https://doi.org/10.1007/s11356-022-23055-z.

[138] M. Keshawy, A.R. Mahmoud, M.E.S. Abdel-Raouf, Polystyrene-based magnetic hydrogels for elimination of some toxic metal cations from aqueous solutions, Environ. Sci. Pollut. Res. 27 (2020) 26982–26997, https://doi.org/10.1007/s11356-020-08340-z.

[139] S.F. Abo-Zahra, I.M. Abdelmonem, T.E. Siyam, et al., Radiation synthesis of polyacrylamide/functionalized multiwalled carbon nanotubes composites for the adsorption of Cu(II) metal ions from aqueous solution, Polym. Bull. 79 (2022) 4395–4415, https://doi.org/10.1007/s00289-021-03726-6.

[140] F. Zhao, C. Su, W. Yang, et al., In-situ growth of UiO-66-NH_2 onto polyacrylamide-grafted nonwoven fabric for highly efficient Pb(II) removal, Appl. Surf. Sci. 527 (2020) 146862, https://doi.org/10.1016/j.apsusc.2020.146862.

[141] X. Zhu, Z. Wang, J. Ren, et al., Graphene/polyacrylamide interpenetrating structure hydrogels for wastewater treatment, Adv. Compos. Hybrid Mater. 6 (2023) 169, https://doi.org/10.1007/s42114-023-00731-3.

[142] S. Zheng, S. Li, X. Luo, et al., Photothermal composite polyamidoxime-graphene oxide/polyacrylamide hydrogel for efficient and selective uranium extraction from seawater, Desalination 593 (2025) 118238, https://doi.org/10.1016/j.desal.2024.118238.

[143] S. Azizi, H. Shaki, M.S. Shafeeyan, et al., Chitosan-polyethylene oxide nanofiber/polyacrylamide-co-acrylic acid hydrogel nanocomposite: a copper ion adsorbent of aqueous solutions, Inorg. Chem. Commun. 159 (2024) 111682, https://doi.org/10.1016/j.inoche.2023.111682.

[144] F. Yu, W. Song, Z. Wu, et al., Cationic polyacrylamide aerogel intercalated molybdenum disulfide for enhanced removal of Cr(VI) and organic contaminants, Sep. Purif. Technol. 294 (2022) 121188, https://doi.org/10.1016/j.seppur.2022.121188.

[145] P. Sittipranee, Q. Liang, X. Zhou, et al., Fabrication of Zn-MOF-74/polyacrylamide coated with reduced graphene oxide (Zn-MOF-74/rGO/PAM) for As(III) removal, Physica E 125 (2021) 114377, https://doi.org/10.1016/j.physe.2020.114377.

[146] H.-Y. Niu, J.-C. Li, J.-S. Li, et al., Preparation, properties and applications of porous hydrogels containing thiol groups for heavy metal removal, J. Environ. Chem. Eng. 11 (2023) 110983, https://doi.org/10.1016/j.jece.2023.110983.

[147] R. Ahmad, K. Ansari, M.O. Ejaz, Enhanced sequestration of heavy metals from aqueous solution on polyacrylamide grafted with cell@Fe_3O_4 nanocomposite, Emerg. Mater. 5 (2022) 1517–1531, https://doi.org/10.1007/s42247-021-00338-8.

[148] M.M. Sajeevan, A. Thayyullathil, C.M. Naseera, Preparation of Fe-Loaded polyacrylamide grafted shellac for the removal of cadmium (II) ions from aqueous solution, Int. J. Creat. Res. Thoughts 6 (2018) 2320–2882.

[149] K. Ji, R. Li, H. Zhou, et al., Synthesis and characterization of calamus-based polyacrylamide hydrogel for heavy metal adsorption, Polym. Bull. 82 (2025) 9125–9147, https://doi.org/10.1007/s00289-025-05878-1.

[150] A.M. Elbarbary, S.E.A. Sharaf El-Deen, E.M. Abu Elgoud, et al., Radiation fabrication of hybrid activated carbon and functionalized terpolymer hydrogel for sorption of Eu(III) and Sm(III) ions, Radiochim. Acta 111 (2023) 439–457, https://doi.org/10.1515/ract-2023-0127.

[151] O. Sökmen, N. Çankaya, et al., Remediation of toxic Cu(II) using acrylamide-based hydrogels, Adv. Clin. Toxicol. 8 (2023) 000278, https://doi.org/10.23880/act-16000278J.

[152] F. Laila, W. Yulianti, I. Resmeiliana, et al., Adsorption of Cd(II) using polyacrylamide/rice husk hydrogel, E3S Web Conf. 454 (2023) 02022, https://doi.org/10.1051/e3sconf/202345402022.

[153] O. Oktaviani, A.L. Yunus, N. Nuryanthi, et al., Selectivity study of heavy metal ions adsorption onto zeolite-g-polyacrylamide, AIP Conf. Proc. 2381 (2021) 020052, https://doi.org/10.1063/5.0066633.

[154] N. Kumar, R. Gusain, S. Pandey, et al., Hydrogel nanocomposite adsorbents and photocatalysts for sustainable water purification, Adv. Mater. Interfac. 10 (2023) 2201375, https://doi.org/10.1002/admi.202201375.

[155] M.R. Krishnan, E.H. Alsharaeh, Rapid and effective absorption of dye molecules from their low-concentrated water solutions by organically cross-linked polyacrylamide-hexagonal boron nitride nanocomposite and polyacrylamide hydrogels, Colloids Surf. C 3 (2025) 100055, https://doi.org/10.1016/j.colsuc.2025.100055.

[156] A. Padhan, V. Singh, Reusable underwater superoleophobic polyacrylamide membranes for effective oil-water separation and dye removal, ChemistrySelect 9 (2024) e202304653, https://doi.org/10.1002/slct.202304653.

[157] P. Kongseng, P. Amornpitoksuk, S. Chantarak, Development of multifunctional hydrogel composite based on poly(vinyl alcohol-g-acrylamide) for removal and photocatalytic degradation of organic dyes, React. Funct. Polym. 172 (2022) 105207, https://doi.org/10.1016/j.reactfunctpolym.2022.105207.

[158] I. Lebkiri, B. Abbou, L. Kadiri, et al., Swelling properties and basic dye adsorption studies of polyacrylamide hydrogel, desal, Water Treat. 233 (2021) 361–376, https://doi.org/10.5004/dwt.2021.27530.

[159] S.Y. Karimi, S. Marofi, M.A. Zare, Fabricating pentaazatetraethylene modified sulfonated polyacrylamide for dye adsorption from aqueous media: isotherms and

kinetics models, Environ. Sci. Pollut. Res. 31 (2024) 25849–25866, https://doi.org/10.1007/s11356-024-32590-w.
[160] J.M.C. da Feira, J.M. Klein, M.M.C. Forte, et al., Ultrasound-assisted synthesis of polyacrylamide-grafted sodium alginate and its application in dye removal, Polímeros 28 (2018) 139–146, https://doi.org/10.1590/0104-1428.11316.
[161] O. İsmail, Ö.G. Kocabay, Absorption and adsorption studies of polyacrylamide/sodium alginate hydrogels, Colloid Polym. Sci. 299 (2021) 783–796, https://doi.org/10.1007/s00396-020-04796-0.
[162] Y. Yue, X. Wang, J. Han, et al., Effects of nanocellulose on sodium alginate/polyacrylamide hydrogel: mechanical properties and adsorption-desorption capacities, Carbohydr. Polym. 206 (2019) 289–301, https://doi.org/10.1016/j.carbpol.2018.10.105.
[163] S. Li, Y. Liang, Q. Li, et al., Easily recyclable magnetic polyacrylamide/sodium alginate/Fe_3O_4@ZIF-8 hydrogel beads for effective removal of Congo red, J. Polym. Res. 31 (2024) 359, https://doi.org/10.1007/s10965-024-04195-x.
[164] L. Zhu, C. Guan, B. Zhou, et al., Adsorption of dyes onto sodium alginate graft Poly(Acrylic Acid-co-2-Acrylamide-2-Methyl propane sulfonic Acid)/Kaolin hydrogel composite, Polym. Polym. Compos. 25 (2017) 627–634, https://doi.org/10.1177/096739111702500808.
[165] A. Massrour, S.J. Peighambardoust, M. Foroughi, et al., Crystal violet removal by sodium alginate-g-polyacrylamide/hydroxyapatite/Cu-Fe LDH nanocomposite, Environ. Technol. Innov. 38 (2025) 104149, https://doi.org/10.1016/j.eti.2025.104149.
[166] Y. Zhao, B. Li, Preparation and superstrong adsorption of a novel La(III)-crosslinked alginate/modified diatomite macroparticle composite for anionic dye removal from aqueous solutions, Gels 8 (2022) 810, https://doi.org/10.3390/gels8120810.
[167] W.A.A. Sadik, A.G.M. El-Demerdash, H.A. Gabre, et al., Effective removal of malachite green dye by eco-friendly pectin-grafted poly(acrylamide-co-sodium acrylate) hydrogel from aqueous solutions, Polym. Bull. 82 (2025) 281–311, https://doi.org/10.1007/s00289-024-05502-8.
[168] S.J. Peighambardoust, B. Fakhiminajafi, P. Mohammadzadeh Pakdel, et al., Simultaneous elimination of cationic dyes from water media by carboxymethyl cellulose-graft-poly(acrylamide)/magnetic biochar nanocomposite hydrogel adsorbent, Environ. Res. 273 (2025) 121150, https://doi.org/10.1016/j.envres.2025.121150.
[169] S.J. Peighambardoust, M.M. Azari, P.M. Pakdel, et al., Carboxymethyl cellulose-grafted poly(acrylamide)/magnetic biochar nanocomposite hydrogel for efficient elimination of methylene blue, Biomass Convers. Biorefinery 15 (2025) 15193–15209, https://doi.org/10.1007/s13399-024-06180-2.
[170] S.J. Peighambardoust, S. Rezaei-Aghdam, J. Sakhaei Niroumand, et al., Efficient methylene blue elimination from water media by nanocomposite adsorbent-based carboxymethyl cellulose-grafted poly(acrylamide)/magnetic biochar decorated with ZIF-67, RSC Adv. 15 (2025) 32407–32423, https://doi.org/10.1039/D5RA03796D.
[171] F. Veghari Atigh, H. Shaki, Cost-effective removal of methylene blue dye from wastewater using polyacrylamide/sodium carboxymethyl cellulose/magnetic halloysite nanotube hydrogel, Int. J. Environ. Sci. Technol. 22 (2025) 9849–9876, https://doi.org/10.1007/s13762-025-06461-x.
[172] A.M. Aljeboree, H.H. Ghazi, S.A. Hussein, et al., Facile fabrication of a low-cost carboxymethyl cellulose–polyacrylamide composite for the highly efficient removal of cationic dye: optimization, kinetic and reusability, J. Iran. Chem. Soc. 22 (2025) 91–111, https://doi.org/10.1007/s13738-024-03132-5.
[173] H. Zhao, Z.-X. Liang, Z.-Z. Gao, Facile preparation of floatable carboxymethyl cellulose-based composite hydrogel for efficient removal of organic dyes, Colloid Interface Sci. Commun. 49 (2022) 100637, https://doi.org/10.1016/j.colcom.2022.100637.
[174] A. Pourjavadi, Z. Bassampour, H. Ghasemzadeh, et al., Porous Carrageenan-g-polyacrylamide/bentonite superabsorbent composites: swelling and dye adsorption behavior, J. Polym. Res. 23 (2016) 60, https://doi.org/10.1007/s10965-016-0955-z.
[175] S.M. Qasim, Z.T. Al-Khateeb, F.A. Jabbar, et al., Adsorptive and reactivation potential of clay based superabsorbent kappa (κ)-carrageenan-graft-poly (acrylic acid-co-acrylamide)/kaolin composite for malachite green dye: Linear and non-linear modeling, J. Mol. Struct. 1348 (2025) 143448, https://doi.org/10.1016/j.molstruc.2025.143448.
[176] X. Liu, K. Jing, S. Peng, et al., Facile preparation of graphene oxide-based composite aerogel to efficiently adsorb methylene blue, Colloids Surf., A 681 (2024) 132754, https://doi.org/10.1016/j.colsurfa.2023.132754.
[177] I.R. Patel, S.R. Patel, B.V. Patel, et al., Removal of anionic/cationic dyes by chitosan poly(acrylamide-co-crotonic acid)/Fe_3O_4 composite hydrogel: kinetics, isotherm and removal mechanism, Compos. Interfaces 3 (2026) 775–795, https://doi.org/10.1080/09276440.2025.2551989.
[178] A.U. Awode, S.E. Elaigwu, A.A. Oladipo, et al., Removal of methylene blue dye from aqueous solution using trichlorovinylsilane chitosan-g-polyacrylamide hydrogel, JOTCSA 10 (2023) 1009–1018, https://doi.org/10.18596/jotcsa.1292604.
[179] M.T. AlSamman, J. Sánchez, Chitosan- and alginate-based hydrogels for the adsorption of anionic and cationic dyes from water, Polymers 14 (2022) 1498, https://doi.org/10.3390/polym14081498.
[180] X. Lin, Z. Liu, R. Chen, et al., A multifunctional polyacrylamide/chitosan hydrogel for dyes adsorption and metal ions detection in water, Int. J. Biol. Macromol. 246 (2023) 125613, https://doi.org/10.1016/j.ijbiomac.2023.125613.
[181] P. Najafi, M. Zabihi, M. Faghihi, Remarkable adsorption of anionic dye on the supported magnetic and non-magnetic polymeric nanocomposites including chitosan/polyacrylamide and chitosan/polylactic acid, Water, Air, Soil Pollut. 235 (2024) 366, https://doi.org/10.1007/s11270-024-07165-7.
[182] E. Binaeian, S. Babaee Zadvarzi, D. Yuan, Anionic dye uptake via composite using chitosan–polyacrylamide hydrogel as matrix containing TiO_2 nanoparticles; comprehensive adsorption studies, Int. J. Biol. Macromol. 162 (2020) 150–162, https://doi.org/10.1016/j.ijbiomac.2020.06.158.
[183] N.S. Mazari Moghaddam, T.J. Al-Musawi, F.S. Arghavan, et al., Effective removal of Sirius yellow K-CF dye by adsorption process onto chitosan-polyacrylamide composite loaded with ZnO nanoparticles, Int. J. Environ. Anal. Chem. 103 (2023) 8782–8798, https://doi.org/10.1080/03067319.2021.1998470.
[184] G. Kaur, S.K. Tank, Smart hydrogel system based on Jhingan gum for enhanced crystal violet dye sequestration: synthesis, characterization, and environmental application, Polym. Bull. 83 (2026) 62, https://doi.org/10.1007/s00289-025-06094-7.
[185] Y. Wang, Y. Lu, H. Zhong, et al., Efficient adsorption and utilization of methylene blue by NaOH-modified nanocellulose–polyacrylamide interpenetrating network gels, Gels 11 (2025) 252, https://doi.org/10.3390/gels11040252.
[186] Y. Deng, Z. Li, R. Wang, et al., Cellulose nanocrystal and polymer composite microspheres for methylene blue adsorption, Polymers 17 (2025) 1205, https://doi.org/10.3390/polym17091205.
[187] A. Sharma, P.P. Pande, P. Khare, et al., Synthesis and application of polyacrylamide/cellulose gel/fuller's earth composite for removal of methylene blue from water, Iran. J. Chem. Chem. Eng. 41 (2022) 3660–3674, https://doi.org/10.30492/ijcce.2022.533829.4828.
[188] Y.-W. Tai, P. Khamwongsa, X.-T. Chen, et al., Bacterial cellulose and keratin reinforced PAM hydrogels for advanced dye removal: insights from batch and QCM analyses, Int. J. Biol. Macromol. 308 (2025) 142458, https://doi.org/10.1016/j.ijbiomac.2025.142458.
[189] N. Hu, D. Chen, Q. Guan, et al., Preparation of hemicellulose-based hydrogels from biomass refining industrial effluent for effective removal of methylene blue dye, Environ. Technol. 43 (2022) 489–499, https://doi.org/10.1080/09593330.2020.1795930.
[190] N.N. Xia, Q. Wu, S.L. Bi, Ultra-efficient removal of heavy-metal ions and dyes using a novel cellulose-based three-dimensional network, Cellulose 31 (2024) 3747–3761, https://doi.org/10.1007/s10570-024-05817-9.
[191] I.A. Khan, F. Haq, A.I. Osman, et al., Starch-grafted polyacrylic acid copolymer with acrylamide: an advanced adsorbent for Victoria Green B dye removal and environmental remediation, J. Polym. Environ. 32 (2024) 4589–4612, https://doi.org/10.1007/s10924-024-03265-x.
[192] H. Al-Aidy, E. Amdeha, Green adsorbents based on polyacrylic acid-acrylamide grafted starch hydrogels: the new approach for enhanced adsorption of malachite green dye from aqueous solution, Int. J. Environ. Anal. Chem. 101 (2020) 2796–2816, https://doi.org/10.1080/03067319.2020.1711896.
[193] F. Zamani-Babgohari, A. Irannejad, M. Kalantari Pour, et al., Synthesis of carboxymethyl starch co (polyacrylamide/polyacrylic acid) hydrogel for removing methylene blue dye from aqueous solution, Int. J. Biol. Macromol. 269 (2024) 132053, https://doi.org/10.1016/j.ijbiomac.2024.132053.
[194] P. Kongseng, P. Amornpitoksuk, S. Chantarak, ZnO/cassava starch-based hydrogel composite for effective treatment of dye-contaminated wastewater, Macromol. Mater. Eng. 308 (2023) 2200481, https://doi.org/10.1002/mame.202200481.
[195] K. Chen, Y. Li, M. Wang, et al., Removal of methylene blue dye from aqueous solutions by pullulan polysaccharide/polyacrylamide/activated carbon complex hydrogel adsorption, ACS Omega 8 (2023) 857–867, https://doi.org/10.1021/acsomega.2c06205.
[196] K. Chen, Y. Li, M. Wang, et al., Removal of methylene blue from wastewater using a ternary composite hydrogel system: Pullulan polysaccharides grafted with polyacrylamide and decorated with graphene oxide, J. Polym. Environ. 30 (2022) 4605–4618, https://doi.org/10.1007/s10924-022-02506-1.
[197] Z. Kadhum, A. Aljeboree, M. Said, et al., High-efficient adsorbent based on modified guar gum/acrylic acid micro/nano surface, acrylamide for removal of methyl violet dye from aqueous solution, J. Nanostruct. 15 (2025) 621–630, https://doi.org/10.22052/JNS.2025.02.022.
[198] W.M. Seleka, E. Makhado, Synthesis and characterization of xanthan gum/acrylic acid/acrylamide modified with graphene oxide hydrogel nanocomposite for removal of methylene blue from aqueous solution, Int. J. Biol. Macromol. 305 (2025) 141015, https://doi.org/10.1016/j.ijbiomac.2025.141015.
[199] G. Sharma, A. Kumar, M. Naushad, et al., Fabrication and characterization of Gum arabic-cl-poly(acrylamide) nanohydrogel for effective adsorption of crystal violet dye, Carbohydr. Polym. 202 (2018) 444–453, https://doi.org/10.1016/j.carbpol.2018.09.004.
[200] N. Kumar, H. Mittal, V. Parashar, et al., Efficient removal of rhodamine 6G dye from aqueous solution using nickel sulphide incorporated polyacrylamide grafted gum karaya bionanocomposite hydrogel, RSC Adv. 6 (2016) 21929–21939, https://doi.org/10.1039/C5RA24299A.
[201] S. Khan, N.U. Rahman, S. Alam, et al., Removal of basic fuchsin from aqueous solution using polyacrylamide and gellan gum-based hydrogels, Chem. Pap. 78 (2024) 3569–3587, https://doi.org/10.1007/s11696-024-03329-1.
[202] E.S. Agorku, A. Kangmennaa, B.Y. Danu, et al., Core-shell V_2O_5-gum ghatti grafted poly(acrylamide-co-methacrylic acid) adsorbent for removal of methylene blue dye in water: kinetic, equilibrium and thermodynamic studies, Sustain. Times 5 (2025) 100069, https://doi.org/10.1016/j.nxsust.2024.100069.
[203] E.A. Fadl, W.A.A. Sadik, A.G. ElDemerdash, et al., Microwave-assisted synthesis and characterization of Xanthan gum-grafted polyacrylamide hydrogel for the removal of acid red 8 dye from aqueous solutions, Sci. Rep. 15 (2025) 32425, https://doi.org/10.1038/s41598-025-14539-2.

[204] Y. Hu, C. Hou, J. An, et al., Fe_3O_4-doped silk fibroin-polyacrylamide hydrogel for selective and highly efficient absorption of cationic dyes pollution in water, Nanotechnology 33 (2022) 265601, https://doi.org/10.1088/1361-6528/ac5f9b.
[205] S.J. Peighambardoust, Z. Imani, M. Foroughi, et al., Effectiveness of polyacrylamide-g-gelatin/ACL/Mg-Fe LDH composite hydrogel as an eliminator of crystal violet dye, Environ. Res. 258 (2024) 119428, https://doi.org/10.1016/j.envres.2024.119428.
[206] Z. Zhao, L. Li, G.S. Geleta, et al., Polyacrylamide-phytic acid-polydopamine conducting porous hydrogel for efficient removal of water-soluble dyes, Sci. Rep. 7 (2017) 7878, https://doi.org/10.1038/s41598-017-08220-6.
[207] N.A. Ahmed, M.F. Elshahawy, R.D. Mohammed, et al., Removal of Astrazon red dye from wastewater using eggshell/graphene oxide embedded in (gum acacia/acrylamide) hydrogel nanocomposites synthesized by gamma irradiation, J. Inorg. Organomet. Polym. 33 (2023) 3617–3637, https://doi.org/10.1007/s10904-023-02775-w.
[208] S.J. Peighambardoust, H.F. Karimzadeh, P.P. Mohammadzadeh, et al., Decontamination of methylene blue from aqueous media using alginate-bonded polyacrylamide/carbon black nanocomposite hydrogel, Polym. Adv. Technol. 35 (2024) e6336, https://doi.org/10.1002/pat.6336.
[209] A. Rahmatpour, P. Soleimani, A. Mirkani, et al., Eco-friendly poly(vinyl alcohol)/partially hydrolyzed polyacrylamide/graphene oxide semi-IPN nanocomposite hydrogel as a reusable and efficient adsorbent of cationic dye methylene blue from water, React. Funct. Polym. 175 (2022) 105290, https://doi.org/10.1016/j.reactfunctpolym.2022.105290.
[210] A. Nair, Y.K. Kumawat, S. Choudhary, et al., Malachite green dye adsorption from wastewater using pine gum-based hydrogel: kinetic and thermodynamic studies, J. Mol. Struct. 1295 (2024) 136671, https://doi.org/10.1016/j.molstruc.2023.136671.
[211] X. Liu, K. Jing, S. Peng, et al., Mild preparation of amino-functionalized graphene oxide-based recyclable aerogel to efficiently adsorb methyl orange, J. Mater. Sci. 58 (2023) 15336–15351, https://doi.org/10.1007/s10853-023-08982-7.
[212] J. Yang, K. Wang, Z. Lv, et al., Facile preparation and dye adsorption performance of poly(n-isopropylacrylamide-co-acrylic acid)/molybdenum disulfide composite hydrogels, ACS Omega 6 (2021) 28285–28296, https://doi.org/10.1021/acsomega.1c04433.
[213] Q. Lv, Y. Shen, Y. Qiu, et al., Poly(acrylic acid)/poly(acrylamide) hydrogel adsorbent for removing methylene blue, J. Appl. Polym. Sci. 2020 (2020) e49322, https://doi.org/10.1002/app.49322.
[214] S. Inphonlek, C. Ruksakulpiwat, Y. Ruksakulpiwat, The effect of silver nanoparticles/titanium dioxide in poly(acrylic acid-co-acrylamide)-modified, deproteinized, natural rubber composites on dye removal, Polymers 16 (2024) 92, https://doi.org/10.3390/polym16010092.
[215] S.J. Peighambardoust, O. Aghamohammadi-Bavil, R. Foroutan, N. Arsalani, Removal of malachite green using carboxymethyl cellulose-g-polyacrylamide/montmorillonite nanocomposite hydrogel, Int. J. Biol. Macromol. 159 (2020) 1122–1131, https://doi.org/10.1016/j.ijbiomac.2020.05.093.
[216] S. Khan, N.U. Rahman, S. Alam, et al., Synthesis of poly(GG-co-AAm-co-MAA), a terpolymer hydrogel for the removal of methyl violet and fuchsin basic dyes from aqueous solution, ACS Omega 9 (2024) 7692–7704, https://doi.org/10.1021/acsomega.3c07118.
[217] A.H. Idan, O.H. Salah, Z.H.A. Alzahraa, et al., Powdered highly porous hydrogel nanocomposite prepared from acrylamide-acrylic acid treated by activated carbon for brilliant blue dye removal, Adv. J. Chem. A (7) (2024) 607–616, https://doi.org/10.48309/ajca.2024.456222.1519.
[218] K. Didehban, M. Hayasi, F. Kermajani, Removal of anionic dyes from aqueous solutions using polyacrylamide and polyacrylic acid hydrogels, Kor. J. Chem. Eng. 34 (2017) 1177–1186, https://doi.org/10.1007/s11814-017-0010-8.
[219] Y. Yildirim, H. Yilmaz, G A. K., et al., New copolymer of acrylamide with allyl methacrylate and its capacity for the removal of azo dyes, Polímeros 25 (2015) 137–145, https://doi.org/10.1590/0104-1428.1615.
[220] N. Sarkar, G. Sahoo, S.K. Swain, Nanoclay sandwiched reduced graphene oxide filled macroporous polyacrylamide-agar hybrid hydrogel as an adsorbent for dye decontamination, Nano-Struct. Nano-Objects 23 (2020) 100507, https://doi.org/10.1016/j.nanoso.2020.100507.
[221] H. Mittal, A. Al Alili, S.M. Alhassan, et al., High efficiency removal of methylene blue dye using κ-carrageenan-poly(acrylamide-co-methacrylic acid)/AQSOA-Z05 zeolite hydrogel composites, Cellulose 27 (2020) 8269–8285, https://doi.org/10.1007/s10570-020-03365-6.
[222] S. Ma, H. Bai, R. Jin, et al., Synthesis and characterization of magnetic Fe_3O_4/PAAm/LMSH nanocomposite hydrogel, Mater. Sci. Forum 848 (2016) 49–56. https://doi.org/10.4028/www.scientific.net/MSF.848.49.
[223] M. Bilgiç, S. Şimşek, Z.M. Şenol, Removal of methylene blue dye from aqueous solution using pure talc and polyacrylamide-talc composite: isotherms, kinetic and thermodynamic studies, Polym. Bull. 80 (2023) 11049–11067, https://doi.org/10.1007/s00289-022-04602-7.
[224] H. Safarzadeh, S.J. Peighambardoust, S.H. Mousavi, et al., Adsorption ability evaluation of poly(methacrylic acid-co-acrylamide)/cloisite 30B nanocomposite hydrogel as a new adsorbent for cationic dye removal, Environ. Res. 212 (2022) 113349, https://doi.org/10.1016/j.envres.2022.113349.
[225] A. Rahmatpour, B. Shoghinia, A.H. Alizadeh, A self-assembling hydrogel nanocomposite based on xanthan gum modified with SiO_2 NPs and HPAM for improved adsorption of crystal violet cationic dye from aqueous solution, Carbohydr. Polym. 330 (2024) 121819, https://doi.org/10.1016/j.carbpol.2024.121819.
[226] F. Chen, R. Wang, H. Chen, et al., Preparation of polyacrylamide/MXene hydrogels as highly-efficient electro-adsorbents for methylene blue removal, Polym. Plast. Technol. Mater. 60 (2021) 1568–1584, https://doi.org/10.1080/25740881.2021.1921207.
[227] D.Ş. Arslan, H. Ertap, Z.M. Şenol, et al., Preparation of polyacrylamide titanium dioxide hybrid nanocomposite by direct polymerization and its applicability in removing crystal violet from aqueous solution, J. Polym. Environ. 32 (2024) 573–587, https://doi.org/10.1007/s10924-023-03004-8.
[228] A.M. Khalil, S. Kamel, M.S. Mohy-Eldin, Photocatalytic degradation of Congo red dye using innovative cerium titanate nanorods embedded in a cellulose-based hydrogel, Sci. Rep. 16 (2026) 12476, https://doi.org/10.1038/s41598-026-43425-8.
[229] M. Kousar, M. Almas, S. Kamal, et al., High adsorption performance of pH-responsive graphene oxide/polyacrylamide hydrogels for the removal of drimarene brilliant blue, desal, Water Treat. 252 (2022) 371–380, https://doi.org/10.5004/dwt.2022.28168.
[230] S. Peighambardoust, E. Ghergherehchi, P. Mohammadzadeh, et al., Facile removal of methylene blue using carboxymethyl cellulose grafted polyacrylamide/carbon black nanocomposite hydrogel, J. Polym. Environ. 31 (2023) 939–953, https://doi.org/10.1007/s10924-022-02660-6.
[231] T. Silveira, V. Caliman, G.G. Silva, Hydrogels based on polyacrylamide and functionalized carbon nanomaterials for adsorption of a cationic dye, J. Polym. Environ. 30 (2022) 5339–5351, https://doi.org/10.1007/s10924-022-02624-w.
[232] M. Inala, N. Erduran, M. Gökgöz, The dye adsorption and antibacterial properties of composite polyacrylamide cryogels modified with ZnO, J. Ind. Eng. Chem. 98 (2021) 200–210, https://doi.org/10.1016/j.jiec.2021.04.001.
[233] Q. Hao, T. Chen, R. Wang, et al., A separation-free polyacrylamide/bentonite/graphitic carbon nitride hydrogel with excellent performance in water treatment, J. Clean. Prod. 197 (2018) 1222–1230, https://doi.org/10.1016/j.jclepro.2018.06.289.